Targeted delivery of long-acting SNARE-inactivating protease into inflammatory cells and sensory neurons for the treatment of chronic pain

The thesis submitted for the degree

of

Doctor of Philosophy

By

Minhong Tang B.Sc., M.Sc.

Supervised by

Dr. Jiafu Wang

School of Biotechnology

Dublin City University

Ireland

September 2018

Declaration

I hereby certify that this material, which I now submit for assessment on the programme of study leading to the award of Doctor of Philosophy, is entirely my own work, and that I have exercised reasonable care to ensure that the work is original, and does not to the best of my knowledge breach any law of copyright, and has not been taken from the work of others save and to the extent that such work has been cited and acknowledged within the text of my work.

Signed: Minhong Tang ID No: 14212828

Date:

Acknowledgement

I would like to give a great thank to my supervisor Dr. Jiafu Wang who provided this PhD study opportunity through his career development award from Science Foundation Ireland and guided me to carry on this research project. His profound knowledge, great experience and insightful comments influence me very much. All these become my wealth for my Ph.D. study and research career in the future. I deeply appreciate for his poignant suggestions, elaborated review and corrections during preparation of this thesis. In addition, I would like to thank my independent supervisor Dr Ciarán Ó'Fágáin [Ciarán Fagan] who gave me many supervisions in past four years, especially in preparing transfer examination. I also would like to acknowledge Science Foundation Ireland for providing me financial support.

I want to thank Dr. Kim Orange who assisted with revising and making useful comments on this thesis. I am also grateful to all ICNT numbers for valuable discussion, good advices and kindly supporting.

I am also thankful to my dear friend Dr Jianghui Meng who takes good care and love to me. Your care and love do not let me feel alone and lonely at all. The gloomy mood is also far from me quickly under your encouragement and assistance.

Finally, I would like to thank my dear mum and dad who share my laughing, crying, joy and anger with me every day. When I was in trouble, they always encourage and aid me to overcome it again and again. Without you, I cannot complete this work. Thank you for understanding and forgiving me I do not spend enough time staying with you. I will try my best to accompany you in the future.

Publications

1. Jiafu Wang, Jianghui Meng, Marc Nugent, Minhong Tang and J. Oliver Dolly (2017). "Neuronal entry and high neurotoxicity of botulinum neurotoxin A require its N-terminal binding sub-domain." Sci Rep **7**: 44474.

2. Karl Syson, Clare E. M. Stevenson, Farzana Miah, J. Elaine Barclay, Minhong Tang, Andrii Gorelik, Abdul M. Rashid, David M. Lawson and Stephen Bornemann (2016). "Ligand-bound Structures and Site-directed Mutagenesis Identify the Acceptor and Secondary Binding Sites of Streptomyces coelicolor Maltosyltransferase GlgE." J Biol Chem **291**(41): 21531-21540.

3. Minhong Tang and Jiafu Wang."Novel secretion inhibitors of cytokines/neuropeptides targeted to macrophages or sensory neurons with potential for relieving chronic pain. Submitted to Scientific Reports (under revision).

Table of Contents

List of figures

Chapter 1

Chapter 2

Chapter3

Chapter4

Chapter5

Figure 5.7. Effect of /D-SP conjugate on VAMP1 cleavage in cultured DRGs.

List of tables

Chapter2

Abbreviations

AEX, anion-exchange chromatography

A-MuLV, Abselon Leukemia Virus

APS, ammonium persulfate

Ara-C, cytosine-β-D-arabinofuranoside

BK, bradykinin

BoNT/A, B, C1, D, E, F, and G, Botulinum neurotoxins

BOTOX, botulinum toxin A-haemagglutinin complex

BSA, bovine serum albumin

CE, cauda equine

CFA, complete Freund's adjuvant

CGRP, calcitonin gene related peptide

COX, cyclooxygenase

CRLR, calcitonin receptor-like receptor

DAPI, 4',6-diamidino-2-phenylindole

/D-Atsttrin, BoNT/DΔH_C –Atsttrin

DB, Dragon's blood

DC, di-chain form

/D-CGRP$_{8-37}$, BoNT /DΔH_C-CGRP$_{8-37}$

DD, death domain

DMEM, Dulbecco's Modified Eagle's Medium

DMEM/F12, Dulbecco's Modified Eagle's Medium/Nutrient Mixture F-12 Ham

/DΔH_C-CS, BoNT/DΔH_C-LPETG

/DIL-1β, BoNT/DΔH_C-IL-1β

DIV, day in vitro

DPBS, Dulbecco's Phosphate Buffered Saline

DR, dorsal root;

/DRA, BoNT/DΔH_C-IL-1RA

DRG, dorsal root ganglia

DTT, dithiothreitol

ECL, enhanced chemiluminescence

EIA, enzyme immunoassay

ELISA, enzyme-linked immunosorbent assay

FBS, fetal bovine serum

FLS, fibroblast-like synoviocytes

FT, flow through

GEP, granulin epithelin precursor

GMP, good manufacture production

H_C, binding domain

H_{CC}, C terminal binding sub-domain

$H_{CN,}$ N terminal binding sub-domain

HFLS, human fibroblast-like synoviocytes

H_N, translocation domain

H_N-TL, translocation domain-targeted ligand

HK, high k^+ (60 mM)

HPC-1, Anti-Syntaxin-1

HRP, Horseradish Peroxidase

IFNγ, interferon gamma

IL-1, interleukin-1

IL-1RA, IL-1 receptor antagonist

IL-1RI, IL-1 type1 receptor

IL- 1RII, IL-1 type 2 receptor

IL-1β, interleukin-1β

IL-6, interleukin-6

IL-6R, IL-6 receptor

IL-10, interleukin-10

IMAC, immobilized metal affinity chromatography

IRAK, IL-1 receptor-activated protein kinase

JAKs, Janus kinases

JNK, c-Jun N-terminal kinase

LC, light-chain

LDS, lithium dodecyl sulfate

LK, low k^+ (3.5 mM)

LPS, lipopolysaccharides

MAPK, mitogen-activated protein kinase

MIA, monosodium iodoacetate

MMPs, metalloproteinases

Mr, molecular mass

mTNF, membrane TNF

MYD88, myeloid differentiation response gene 88

NFκB, nuclear factor kappa B

NGF, nerve growth factor

NK cells, natural killer cells

NK, neurokinin

NSAIDs, nonsteroidal anti-inflammatory drugs

NSB, non-specific binding

NTNH, non-haemagglutinin

OA, osteoarthritis

P, pedicles

PAR-2, protease activated receptor-2

PCDGF, PC-cell-derived growth factor

PEPI, proepithelin

PGRN, progranulin

PMSF, phenylmethylsulfonyl fluoride

p38 MAPK, p38 mitogen activated protein kinase

RA, rheumatoid arthritis

RAMP, receptor activity modifying protein

RAW cells, the murine macrophage cell line (RAW 264.7)

RCP, receptor component protein

Sbr, synaptic vesicle protein synaptobrevin

SC, single-chain

SNAP-23, protein synaptosomal-associated protein of 23k

SNAP-25, protein synaptosomal-associated protein of 25k

SNARE, N-ethylmaleimide sensitive factor attachment receptor

SNI model, spared nerve injury models

SP, substance P

sTNF, soluble TNF

SV2, synaptic vesicle protein 2

SW982 human synovial sarcoma cell line

Syt I, synaptotagmin I

Syx, syntaxin

TACE, TNF-α-converting enzyme

TGF-β, transforming growth factor-β

TMB, 3,3',5,5'-tetramethylbenzidine

TNF-α, tumour necrosis factor-α

TNFR, tumour necrosis factor receptor

TRAF, tumor necrosis factor-associated factor

TrkA, tropomyosin receptor kinase A

TRPV1, transient receptor potential cation channel subfamily V member 1

Trx-His_6-IL-1β, Trx-His_6-Gly_5-IL-1β

VAMP, vesicle-associated membrane protein

WB, western blotting

WHO, World Health Organization

Abstract

Chronic pain, including arthritis, poses a substantial economic and social burden on society. A major unmet need exists for effective, long-lasting and non-addictive safe analgesics. Treatment of chronic pain could be revolutionized by targeted delivery of long-acting secretion blocker into inflammatory cells and/or sensory neurons to inhibit the release of pro-inflammatory cytokines and pain neuropeptides. In this thesis, we selected the interleukin-1 receptor (IL-1R), TNF receptor (TNFR) and CGRP (calcitonin gene related peptide) receptor as specific targets for selective delivery of long-lasting botulinum neurotoxin type D (BoNT/D) protease into immune cells and/or peripheral sensory (but not motor) neurons to cleave SNAREs(N-ethylmaleimide sensitive factor attachment receptors). The latter are essential for the release of cytokines and pain-peptides which play pivotal roles in the pathogenesis of arthritis. To achieve this goal, the receptor binding domain of BoNT/D is replaced recombinantly with an IL-1R targeting ligand [IL-1β (agonist), IL-1 receptor antagonist (IL-1RA)] or an TNFR receptor antagonist (Atsttrin) to yield three novel retargeted BoNT/D based therapeutics (/DIL-1β, /DRA and /D-Atsttrin). These proteins were successfully expressed in *E. coli* and purified using affinity chromatography with retention of biological activities of their targeting ligands. Not surprisingly, these ligands successfully delivered the BoNT/D protease into cultured immune cells (macrophages) resulting in cleavage of vesicle associated membrane protein 3 (VAMP-3) and inhibition of two important cytokines release (TNF-α and IL-6), much more potently than the non-ligand control protein. Moreover, these therapeutic candidates also entered into cultured dorsal root ganglion neurons, cleaved VAMP-1 and inhibited substance P peptide release, unlike the non-ligand control protein. Thus, for the first time, we have successfully engineered dual-targeting BoNT-derived secretion blockers. Furthermore, we also developed a novel effective delivery strategy using sortase to site-specifically ligate BoNT/D core-therapeutic to CGRP receptor antagonist ($CGRP_{8-37}$) with

ability to inhibit substance P release. Inhibiting the release of pro-inflammatory cytokines and/or pain-peptides by engineered novel biotherapeutics highlights their potential for the treatment of chronic inflammatory pain.

Chapter 1: Introduction

1.1 Pain

Pain is commonly described as any unpleasant or uncomfortable feeling; however, this does not mean that it is a homogeneous sensory entity (Woolf, 2002). Pain is a complex sensory and emotional experience which is associated with existing or imminent damage to the body (Marchand et al., 2005) .

1.1.1 Pain pathway

Physiological pain transduction is a widespread and sophisticated pathway, involving basic biological events which occur at different levels of the nervous system (Fig.1.1) (Cheryl L. Stucky, 2001). First of all, the sensation of pain is initially transmitted to the primary afferent nociceptors which are evoked by painful stimuli such as heat, cold, inflammation or tissue damage (Cheryl L. Stucky, 2001). Nociceptors are specialized primary sensory neurons which can be divided into A-fibre nociceptors and C-fibre nociceptors. A-fibre nociceptors contain lightly myelinated axons which mediate the fast pain sensation and C-fibre nociceptors contain unmyelinated axons, mediating the slower pain stimuli (Dubin and Patapoutian, 2010). This input is then transferred from the dorsal root ganglion (DRG) to the spinal cord and up fibre tracts which terminate in the supraspinal structures, including the medulla, midbrain, and thalamus (Cheryl L. Stucky, 2001).

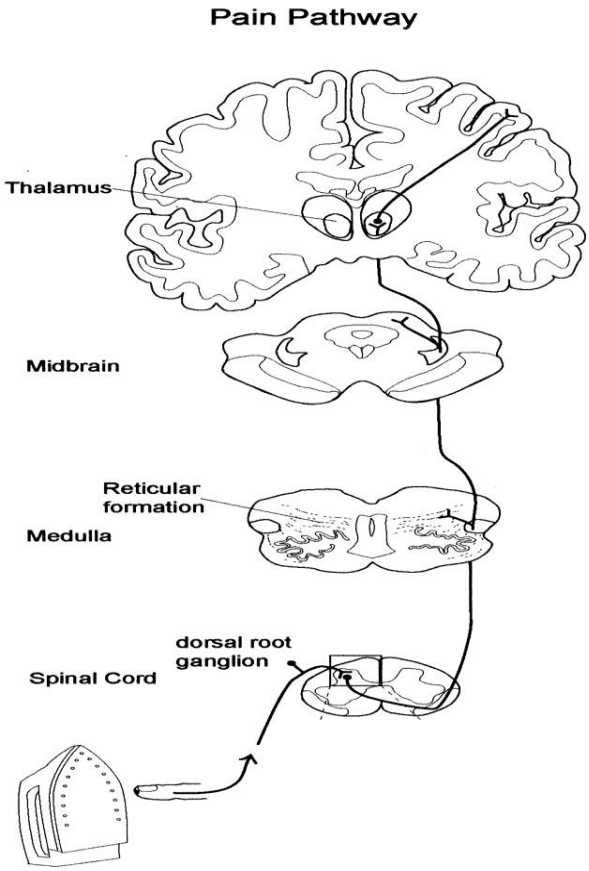

Figure 1.1. Pain transduction pathway.

Painful stimuli activate primary afferent nociceptors. The signals transmitted from the peripheral to the thalamus across the spinal cord, midbrain connection and cause central pain sensation(Cheryl L. Stucky, 2001).

1.1.2 Types of pain

The pain pathway described above can rapidly respond to dangerous or damaging stimuli to provide an early warning to protect the body from these injuries and aid the preservation of homeostasis. Adaptive sensations conferred by acute pain are caused by noxious stimuli acting on a specialized high-threshold sensory system, the nociceptive system. Therefore, acute pain is also named nociceptive pain (Figure 1.2 A) (Woolf, 2002). Once these

adaptive sensations have mediated information regarding preventable tissue damage, the nociceptive pain is revoked as well. If the pain persists more than six months, which extends far beyond the time expected for healing to be complete (normally 3-6 months) or shifted to a disease processes in which healing does not happen, it is defined as chronic pain (O'Callaghan and Miller, 2010). Chronic pain can be further divided into chronic inflammatory or neuropathic pain, according to different underlying pain mechanisms. Once tissue damage or inflammation has occurred, inflammatory mediators such as tumour necrosis factor (TNF), interleukin-1 (IL-1), interleukin-6 (IL-6) and others are released from inflammatory cells such as macrophages and mast cells. The release of these inflammatory mediators directly activates nociceptors, triggering long-lasting spontaneous pain and hypersensitivity (Figure 1.2 B). Neuropathic pain is elicited by injury or a lesion of the central and peripheral nervous system, resulting in hypersensitivity as a result of lower thresholds (hyperalgesia), the painful perception of innocuous stimuli (allodynia) and spontaneous pain (Figure 1.2 C) (Kidd and Urban, 2001).

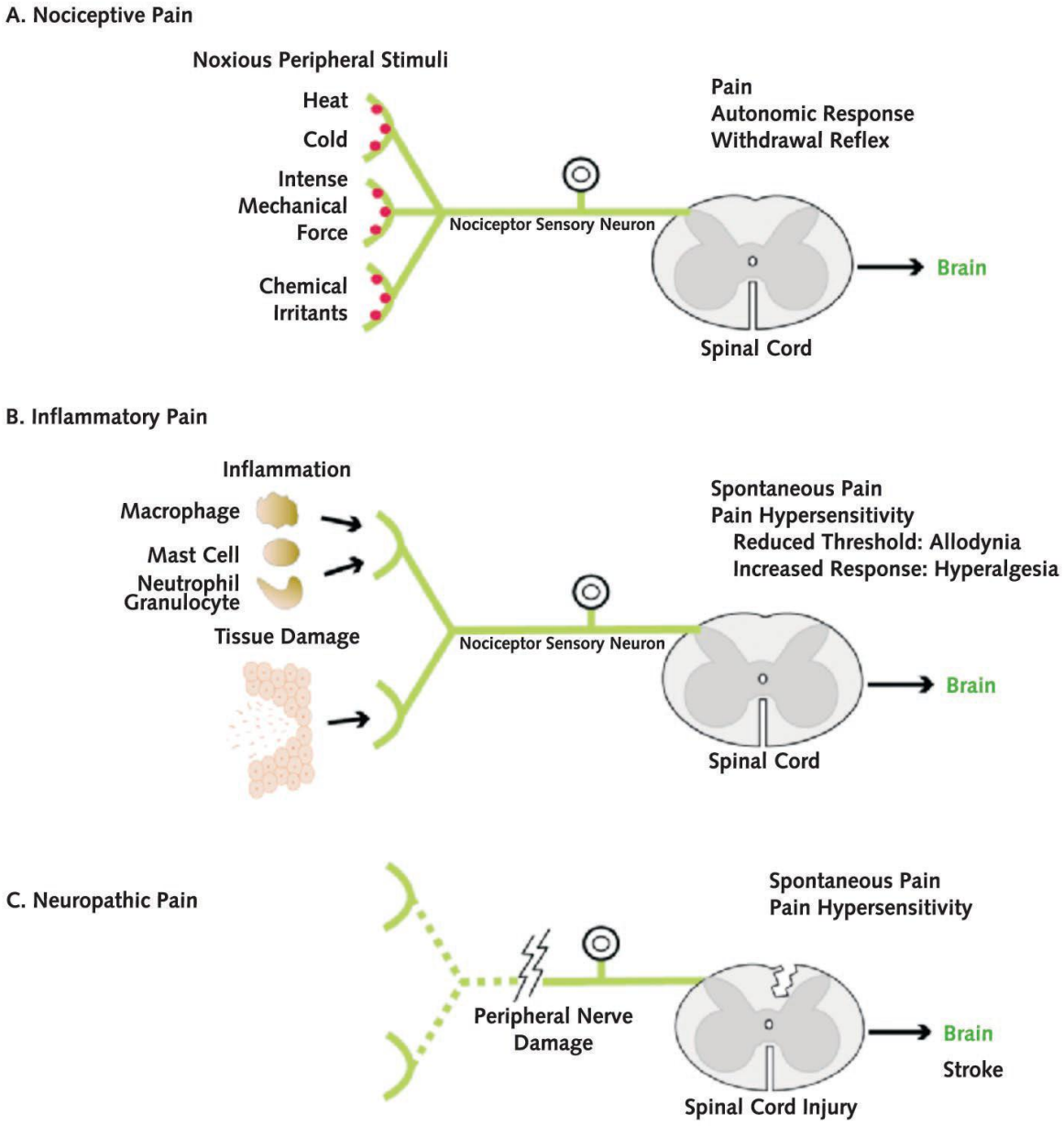

Figure1.2. Three types of pain: nociceptive, inflammatory and neuropathic pain. A. nociceptive pain is evoked by painful stimuli such as heat, cold and chemical irritants. After the painful stimuli are removed, nociceptive pain is also withdrawn. B. Inflammation condition and tissue damage induce immune cells (e.g. macrophages, mast cells, neutrophil granulocyte etc.) to release TNF-α, IL-6 and other inflammatory cytokines and chemokines. These directly activate the primary nociceptors and eventually cause long-lasting spontaneous pain and hypersensitivity. C. Neuropathic pain is induced by damage to the

peripheral or central nerve, resulting in hypersensitivity and spontaneous pain (Woolf et al., 2004).

1.2 Chronic pain

Even today, chronic pain is still a major medical challenge, with a high number of people suffering from persistent pain worldwide. Their daily activities, social and working lives are seriously affected. It is estimated that about 20% of the European adult population have chronic pain symptoms (Brennan et al., 2007). According to a report by The Irish Health Organisation, chronic pain affects at least 30% of the Irish population (Condon, 2010). Estimates from the World Health Organization (WHO) in 2005 state that nearly 10% of men and 18% of women aged >60 years suffer from osteoarthritis; 0.3-1% of the general population suffer from rheumatoid arthritis, which is more prevalent among women (Phillips, 2009). A recently survey in Ireland, found around 68% of the Irish people over 18 years old have a back pain symptoms once a week (Sherry, 2018). Breivik and his colleagues found that most chronic pain patients had not received any effective pain treatment and 40% of them manage their pain in an inadequate way (Breivik et al., 2006). The extent of chronic pain problems not only debilitates individuals, but economics as a whole. In Ireland, one third of the costs of health services results from chronic pain, an estimated €2.5 billion euro per year (Condon, 2010). In American, NHS reported at least $16 million was spent for the treatment of low back pain (Frymoyer, 1988). In addition, people with chronic pain illness maybe absent from work due to the pain, therefore, their levels of productivity are reduced and at the same time, the risk of leaving the labour market is increased. It has been estimated, that worldwide, hundreds of billions of pounds are lost in the social economic domain, due to the loss of production, resulting from the number of people on sick leave due to chronic pain (CARE, 2006).

1.2.1 Pathogenesis of chronic inflammatory and neuropathic pain

According to Scholz and Woolf (2004), pathogenesis of inflammatory pain is associated with inflammatory and immune mechanisms, both in the periphery and the central nervous system. When tissue is damaged, inflammatory response is triggered and then immune cells are activated, many related inflammatory mediators are produced and secreted. These inflammatory mediators directly stimulate a neuroimmune response and can sensitise primary afferent neurones to trigger long-lasting spontaneous pain and hypersensitivity. Likewise, long-lasting inflammation may cause damage to neurons and produce neuropathic pain.

1.2.1.1 Non neuron cells and secreted inflammatory cytokines

Several inflammatory cells are involved in the pathogenesis of chronic pain, such as mast cells and macrophages. In addition, after tissue damage or nerve injury, these inflammatory cells are activated to produce or secrete many mediators, including cytokines, chemokines, histamines, leukotriene B4, various proteases, nerve growth factor, and prostaglandins (Marchand et al., 2005). These mediators play an important role in activating neurons and inducing sensitisation.

1.2.1.1.1 Mast cells

Mast cells were first given a description in Ehrlichs 1878 doctoral thesis and overtime it became extensively investigated by researchers (Amin, 2012). Mast cells are round or oval shape granulated immune cells; they are found in the skin and all mucosal tissues such as respiratory, urogenital, and gastrointestinal tract, which are involved in homeostasis and the pathogenesis of several disease conditions (Lorentz et al., 2015). Mast cells are derived from hematopoietic stem cells in the bone marrow; however, newly produced mast cells leave the bone marrow in an immature condition, migrate into circulating peripheral blood, settle in various tissue types and upon stimulation become mature mast cells. Mast cells not only play a vital role in the pathophysiology of immediate-type allergic reactions; they also contribute to chronic inflammatory pain and auto-immune diseases (Lorentz et al.,

2015). Mast cells normally interact with epithelial cells, vascular endothelial cells, vascular and smooth muscle cells, fibroblasts and peripheral nerves (Olsson, 1968). After stimulation due to chronic inflammation or nerve lesion, these mast cells are activated and degranulated at the site of tissue damage or nerve injury (Olsson, 1968, Zuo et al., 2003). Activation and degranulation of mast cells rapidly release several mediators, including histamine, heparin, serotonin, chemotactic factors and various proteases, such as tryptase and chymase many of which are capable of sensitising or activating neurons (Graziottin et al., 2014). Released histamine interacts with histamine receptors expressed on endothelial cells to recruit a wide range of neutrophils and macrophages to the inflammatory site (Yamaki et al., 1998). Both of these cell types play an important role in inflammatory and neuropathic pain (Liu et al., 2000, Perkins and Tracey, 2000). Histamine also can directly evoke visceral nociceptors to elicit chronic pain. Tryptase is a trypsin-like serine protease and that is only secreted by mast cells. This is one of the most commonly used mast cell mediators as it is released by degranulation. Tryptase binds to the protease activated receptor-2 (PAR-2) on primary sensory neurons to induce inflammatory hyperalgesia (Kawabata et al., 2001, Vergnolle et al., 2001). In addition, activated mast cells may also secret many secondary mediators by inconspicuous degranulation, such as serotonin (Theoharides and Cochrane, 2004). It can directly act on the nociceptor to trigger inflammatory hyperalgesia (Sommer and Kress, 2004).

1.2.1.1.2 Macrophage

Macrophages are a type of white blood cell and play an important role in the immune system (van den Berg et al., 2001). Macrophages are derived from haematopoietic precursor cells and then released into peripheral blood where they occupy a variety of roles which are dependent on the position of stimulation as this leads to the different specialized subpopulations (van den Berg et al., 2001). They play a vital role in homeostasis as well as immune regulation during various pathological conditions such as infection and inflammation (van den Berg et al., 2001). After tissue damage or infection, nerve injury or lesion, macrophages located in skin and around nerves, are activated. These activated macrophages will phagocytose injured or dead tissue and the dead Schwann cells or

axotomized axons (Bruck, 1997). The function of phagocytosis is regulated by a range of macrophage surface receptors, including scavenger receptors, lectins, complement receptors and Fc-receptor (Bendszus and Stoll, 2003). In the peripheral nerve, these macrophages also play an important role in removing cellular debris which is an essential step for regeneration of peripheral nerves (Correale and Villa, 2004). In addition, activated macrophages also infiltrate into DRGs from damaged peripheral nerves and release excitatory agents which produce ectopic activity and elicit neuropathic pain (Hu and McLachlan, 2002). In 2000, Liu and colleagues confirmed that macrophages contribute to neuropathic hyperalgesia revealed by depletion of macrophages in nerve-injured rats (Liu et al., 2000). Furthermore, another important function of a macrophage is to release a wide range of inflammatory mediators which can lead to chronic pain. These include reactive oxygen species, nitric oxide, and cytokines such as TNF (Sommer et al., 1998b), IL-1β, IL-6, IL-10 and transforming growth factor (TGF) β (Sommer and Kress, 2004). Macrophages also secrete prostaglandins which can be subdivided into prostaglandin E2 and I2 (Nathan, 1987). An increase in prostaglandins causes activation of primary afferents which directly triggers hyperalgesia, leading to chronic pain (Nathan, 1987).

1.2.1.1.3 Fibroblast-like synoviocytes (FLS)

Fibroblast-like synoviocytes (FLS) present in the joint synovium (Chang et al., 2010). It plays a critical role in cartilage and bone damage, due to the joint synovium inflammation by increasing inflammatory cytokines release (Bartok and Firestein, 2010). Inside joints, there is a barrier between the joint cavity and the fibrous joint capsule (Chang et al., 2010). This barrier is the joint synovium which involves two different layers: lining and sublining layers. FLS is located in the lining layer (Chang et al., 2010). The lining layer of synovium normally makes up of one to three layers of FLS and macrophages and covers at the top of sublining layer (Noss and Brenner, 2008). However, after being affected by joints related disease, such as rheumatoid arthritis (RA), the joint synovium becomes hyperplastic to form a pannus tissue with 10-20 cells depth (Bartok and Firestein, 2010). With accumulation of the pannus tissue, articular cartilage and bone are gradually covered by the pannus tissue and finally destructed (Bartok and Firestein, 2010). FLS is a major

contributor in the cartilage and bone damage. The RA is a long-lasting autoimmune joint related disorder which associates with joint synovium inflammation (Noss and Brenner, 2008). FLS produces and secretes many pro-inflammatory cytokines, such as IL-1, IL-6 and TNF-α, chemokines and proteases in response to inflammation. FLS and macrophages stored in the lining layer of joint synovium are then activated to grow massively and FLS also promotes the infiltration of T and B cells into joint synovium (Fox et al., 2010). All of these over growing cells contribute to the formation of pannus tissue. The formed pannus tissue can gradually create cloaks at the surface of cartilage and bone to destroy cartilage and bone (Bartok and Firestein, 2010).

1.2.1.2 Cytokines

Cytokines are small proteins; they are important mediators of interactions between cells within short distances (Thacker et al., 2007). Several cytokines are pro-inflammatory including TNF, IL-6 and IL-1β. It is well known that these pro-inflammatory cytokines play a crucial role in eliciting pain and hyperalgesia (Sommer and Kress, 2004). These pro-inflammatory cytokines are synthesized and released by a variety of immune cells, such as mast cells and macrophages. They synergistically induce the production of one another and contribute to both neuropathic and inflammatory pain by two main mechanisms. Firstly, they directly act on primary afferent neurons to trigger chronic pain and secondly, they induce signalling transduction and then, indirectly act on nociceptors in secondary neuron cells which are described in above (Thacker et al., 2007).

1.2.1.2.1 TNF-α and TNF receptor (TNFR) antagonists

TNF-α is the main cytokine to elicit inflammation to lead to chronic inflammatory diseases such as ankylosing spondylitis and Crohn's Disease (Clark, 2007). TNF was first discovered in 1975 due to its tumour cytotoxicity; it can induce necrosis of tumours *in vitro* (Clark, 2007). TNF is a 26k transmembrane protein and is the archetype of the TNF superfamily (Clark, 2007). It is produced not only by activated macrophages, but also by a diverse array of other cells, including activated NK and T cells, mast cells, endothelial

cells and fibroblast cells. After body or nerve infection or damage, upregulation of TNF is triggered. Membrane TNF (mTNF) is directly activated and the extracellular domain of TNF is cleaved into a soluble TNF (sTNF) by a metalloprotease, TNF-α-converting enzyme (TACE) found in blood plasma (Black et al., 1997). Soluble TNF is a 17k functional trimeric soluble cytokine. TNF-α mainly interacts with two types of transmembrane receptors which are named TNFR1 (also known as p55-R) and TNFR2 (also known as p75-R) (Locksley et al., 2001). TNFR1 constitutively expressed in most tissues is a cell membrane receptor with molecular weights of 55k. TNFR2 is a 75k cell membrane receptor. Some cells, such as immune cells and endothelia cells, predominantly express TNFR2 (Idriss and Naismith, 2000). Cytokines, especially interferons, play an important role in regulating expression levels of these TNFR proteins. TNFR1 contains a cytoplasmic death domain (DD) which mediates signalling pathways for cell death, whereas TNFR2 does not (Bremer, 2013). However, TNFR2 can keep the balance between transduction of inflammatory and cell death signalling via TNFR1 (Figure 1.3) (Bremer, 2013). Activation of either receptor leads to activation of nuclear factor kappa B (NFκB) signalling via phosphorylation of p38 mitogen activated protein kinase (p38 MAPK) resulting in translocation of NFκB to the nucleus where they bind to DNA to promote transcription of several genes such as COX-2, inducible nitric oxide synthase, TNF, IL-1β and IL-6 (Micheau and Tschopp, 2003, Schafers et al., 2003b).

It is worth noting that TNF can act on both of the TNF receptors 1 and 2 (Figure 1.3) (Bremer, 2013, Sommer et al., 1998a). Whereas, sTNF can only bind to TNFR1 to elicit the signalling pathway modulated by TNFR1 (Figure 1.3) (Bremer, 2013). Finally, the activated signalling pathways result in faster allodynia and increased spontaneous pain behaviour (Schafers et al., 2003a).

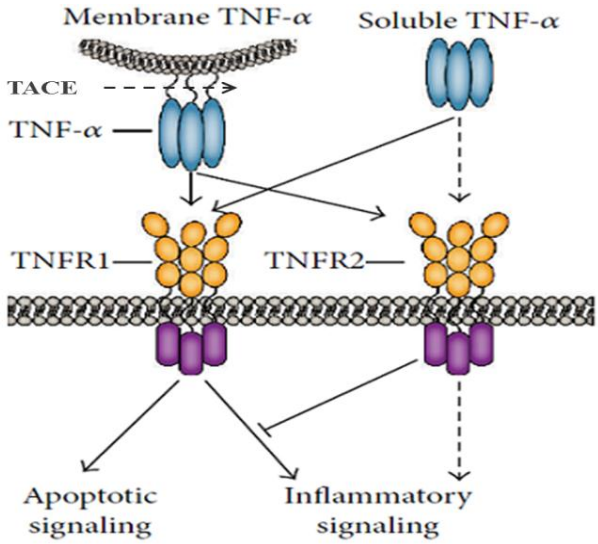

Figure 1.3. TNF-α mediated signaling. This picture shows that mTNF can act on both of the TNF receptors (TNFR1 and TNFR2) to activate signalling pathways associated with TNF receptors, including apoptotic and inflammatory signalling. However, soluble TNF can only bind to TNFR1 to elicit signalling pathways induced by TNFR1. TNFR2 plays a role in regulating the balance between inflammatory and cell death signalling, triggered by TNFR1 (Bremer, 2013).

The growth factor progranulin (PGRN) also called granulin epithelin precursor (GEP), PC-cell-derived growth factor (PCDGF), proepithelin (PEPI), and acrogranin is a growth factor (Liu, 2011). It has seven-and-a-half repeats of a cysteine-rich motif ($CX_{5-6}CX_5CCX_8CCX_6CCXDX_2HCCPX_4CX_{5-6}C$) in the order P-G-F-B-A-C-D-E, where A-G are full repeats and P is the half-motif (Hrabal et al., 1996). PGRN is expressed in epithelial cells, immune cells, some human cancer cells, chondrocytes and neurons (Bateman and Bennett, 2009, Feng et al., 2010). PGRN plays a critical role in anti-inflammation and immune regulation (Tang et al., 2011). In 2011, Tang et al. reported PGRN internalised into cells via directly binding to surface TNFR. A protein named Atsttrin (an antagonist of TNF/TNFR Signalling via targeting to TNF receptors) was then engineered by combining three TNFR-interacting fragments (Tang et al., 2011). Atsttrin binds to TNFR without activation of intracellular TNF-α signalling pathway, unlike TNF-α (Tang et al., 2011). Research results from Tang et al. demostrated that after injection with Atsttrin to mice with induced arthritis, their symptoms of inflammation were reduced

which correlated with inhibiting TNF-α function by competing TNF-α binding and antagonising its intracellular signalling. This finding shows the protential of Atsttrin for anti-inflammatory treatment.

1.2.1.2 .2 IL-6

IL-6 is a pro-inflammatory cytokine and anti-inflammatory myokine (a cytokine produced in muscle) which not only contributes to stimulating an immune response during various pathological conditions such as infection and inflammation, but also regulation of metabolic, regenerative, and homeostatic processes (Scheller et al., 2011). IL-6 is secreted by many different types of cells, such as mast cells, macrophages, lymphocytes etc. (Moalem and Tracey, 2006). Human IL-6 is a glycosylated 21–28k protein, including 212 amino acids which are encoded by the human IL-6 gene (Scheller et al., 2011). The structure of IL-6 is a typical four-helix bundle structure, including four long α-helices (A, B, C, D) assembled to create an up-up down-down topology (Scheller et al., 2011). The IL-6 receptor (IL-6R) and gp130 are of the two main receptors which interact with IL-6. The IL-6R is a glycosylated cell-surface type I protein with molecular weight of 80k (Scheller et al., 2011). Gp130 which is also known as CD130 is a 130-150k glycosylated transmembrane type I protein (Scheller et al., 2011). Upon upregulation of IL-6, IL-6 binds to its receptors IL-6R and gp130 to form a complex. The receptors are then activated and transduce two main signaling pathways, including Janus kinases (JAKs)-STAT factors pathway and the JAK-SHP-2 mediated mitogen-activated protein kinase (MAPK) pathway to trigger infection and inflammatory response (Figure 1.4) (Tanaka et al., 2014, De Jongh et al., 2003, Grothe et al., 2000). In addition, levels of IL-6 are also increased in the DRG and spinal cord upon nerve jury (Lee et al., 2004).

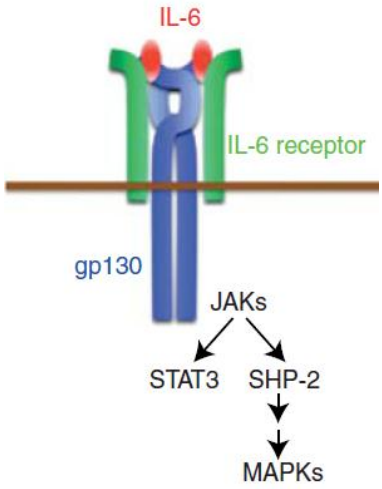

Figure 1.4. The schematic of IL-6 receptor system. IL-6 binds to transmembrane IL-6R and gp130 to form a complex activation of JAKs and STAT factors pathway and the JAK-SHP-2 eventually leading to activation of MAPKs (Tanaka et al., 2014).

1.2.1.2 .3 IL-1β and IL-1RA

IL-1β is a pro-inflammatory cytokine and plays a key role in chronic inflammation, such as rheumatoid arthritis and neuropathic pain (Ren and Torres, 2009). It is released not only by immune cells, including activated macrophage and mast cells, but also by other cell types, such as endothelial cells, fibroblasts and synoviocytes. IL-1β is a 17.5k protein encoded by the IL-1β gene. IL-1 type1 receptor (IL-1RI) and IL-1 type 2 receptor (IL- 1RII) are two types of IL-1 receptors. However, IL-1β can only bind to IL-1RI to transduce signaling and cannot induce any signaling via binding to IL- 1RII (Dinarello, 1999). After binding with IL-1RI, the IL-1RAcP (IL-1 receptor associate protein) co-receptor is recruited to form a trimeric complex (Figure 1.5) (Wang et al., 2010). This trimeric complex quickly assembles myeloid differentiation response gene 88 (MYD88) which is an intracellular signaling protein to recruit tumor necrosis factor-associated factor (TRAF) 6 via phosphorylation of IL-1 receptor-activated protein kinase (IRAK) 1, 2 and 4 (Weber et al., 2010). Therefore, IL-1 signaling pathways are stimulated to produce inflammation by the activation of c-Jun N-terminal kinase (JNK), MAPKs p38 and transcription factors κB (NFκB) (Weber et al., 2010). During inflammation and pain, pro-IL-1β is converted to

IL-1β by Caspase-1; this upregulation of IL-1β is known to enhance pain. IL-1β not only indirectly acts on nociceptors, but also directly acts on nociceptors. From Fukuoka and colleagues' research findings, IL-1β promotes the release of calcitonin gene related peptide (CGRP) from nociceptors (Fukuoka et al., 1994, Sommer and Kress, 2004). Many research groups have also demonstrated that the level of IL-1β is increased in sciatic nerve, dorsal root ganglia (DRG) and spinal cord injury (Ferreira et al., 1988, Follenfant et al., 1989). In addition, Ferreira and colleagues also found that IL-1β triggers hyperalgesia when it is injected into the peripheral rat paw. By neutralizing antibodies to the IL-1 receptor, neuropathic pain relief can be achieved in nerve damage mice (Sommer et al., 1999, Schafers et al., 2001). In contrast to IL-1β, IL-1RA is an IL-1 receptor antagonist, belonging to the IL-1 family as well (Arend, 1991). It also binds to interleukin-1 receptors, however, after binding, internalization and transduction of signaling pathways are not undergone and induced (David J. Dripps, 1991). Therefore, inflammatory response is not activated and inflammatory effects are then blocked. It is a natural inhibitor and recombinant IL-1RA is currently used as a therapeutic for treatment of rheumatoid arthritis (Waugh and Perry, 2005).

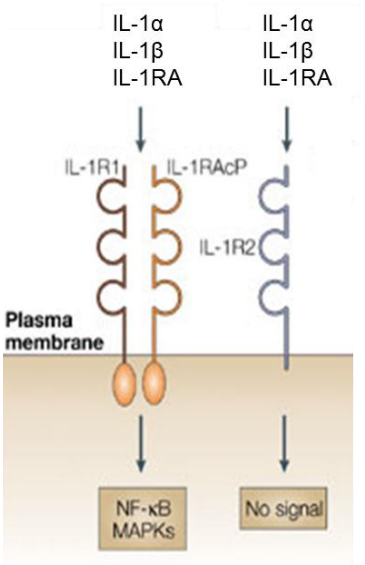

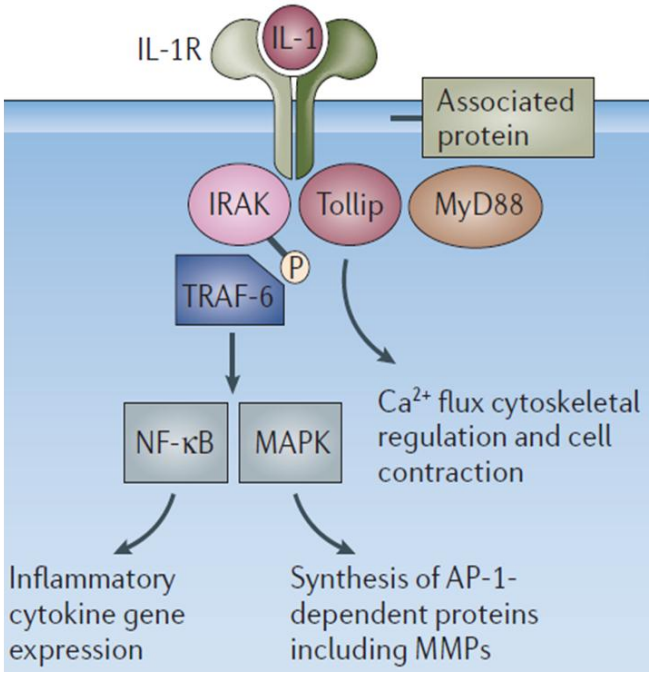

Figure 1.5. The schematic of IL-1 receptor pathway. IL-1 receptor agonists (IL-1α and β) bind to IL-R1 and recruit IL-1RAcP to form a complex. Binding to receptors triggers intracellular signalling pathways, including NF- κB and MAPK, resulting in increased inflammatory cytokine gene expression and synthesis of AP-1-dependent proteins including MMPs. IL-1RA, which is an IL-1 receptor antagonist, binds to IL-R1, but, after binding, no signalling pathway is transduced. They also bind to IL-1R2; however, no signal is triggered.

1.2.1.3 Peripheral sensory neurons and pain peptides

Many different types of sensory nerves participate in the perception of pain (Woolf et al., 2004). For example, activation of the dorsal root ganglion neurons occurs in both chronic inflammatory and neuropathic pain (Brennan et al., 2007).

1.2.1.3.1 Dorsal root ganglion neurons (DRGs)

A DRG contains a cluster of sensory (afferent) neuron cell bodies and is located in a posterior root of a spinal nerve. Figure 1.6 shows the structure of a DRG and its surroundings (Sapunar et al., 2012). These sensory neurons are pseudounipolar and run an axon-like program (Sapunar et al., 2012). Sensory information is carried from one branch, which extends toward the periphery, to another branch heading toward the grey matter of the spinal cord. The DRG transfers these sensory signals from the peripheral nervous system to the central nervous system (brain) across the spinal cord (Sapunar et al., 2012). Following nerve inflammation or damage, these neurons are activated allowing nociceptive signal to be conveyed from the periphery to central nervous system by DRGs leading to the sensation of pain. In addition, DRGs play an important role in neuropathic pain induction by alternating gene/protein expression (Sapunar et al., 2012). After peripheral nerve injury, upregulated expression of proteins such as bradykinin (BK) B1 and capsaicin transient receptor potential cation channel subfamily V member 1 (TRPV1) receptors is triggered to promote hyperalgesia as well as downregulation of protein expression, including

bradykinin (BK) B2 and substance P receptors, which contribute to pain transmission (Sapunar et al., 2012). A variety of sensory neuronal peptides are also synthesised and secreted, including substance P and CGRP, to enhance pain sensation after peripheral nerve injury.

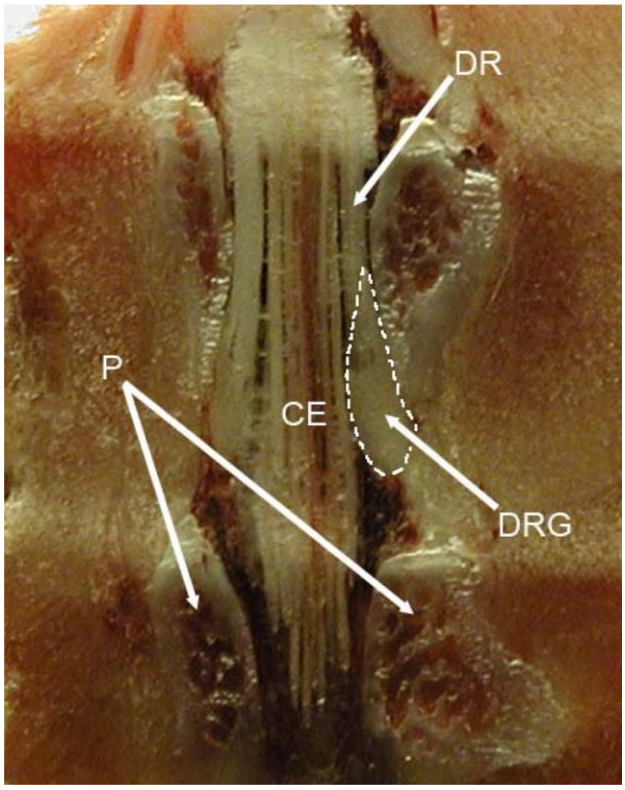

Figure 1.6. Image of the rat L5 DRG and its surroundings (Sapunar et al., 2012). Abbreviations: DRG, dorsal root ganglion; DR, dorsal root, CE, cauda equine; P, pedicles (Sapunar et al., 2012).

1.2.1.3.2 Substance P (SP)

SP is a pain peptide and a sensory neuronal transmitter which is involved in pain transmission (Besson, 1999). It is secreted from primary sensory neurons located at the peripheral (O'Connor et al., 2004). Following peripheral inflammation, the release of SP is

increased to induce inflammatory and neuropathic pain. In addition, SP degranulates mast cells evoking the release of histamine and simultaneously stimulates the release of cytokines from mast cells and macrophages (Harrison and Geppetti, 2001, Kulka et al., 2008). SP is a member of the tachykinin neuropeptide family and contains 11 amino acids, thus, it is also called undecapeptide (Harrison and Geppetti, 2001). The structure of SP is H-Arg^{1}-Pro^{2}-Lys^{3}-Pro^{4}-Gln^{5}-Gln^{6}-Phe^{7}-Phe^{8}-Gly^{9}-Leu^{10}-Met^{11}-NH_2 (RPKPQQFFGLM) (Figure 1.7) (Harrison and Geppetti, 2001). It is encoded by the pre-protachykinin-A (PPT-A) gene. PPT-A gene is produced by duplication of a common ancestral gene (Lazarczyk et al., 2007). SP mainly interacts with tachykinin (neurokinin: NK) receptors, which belongs to rhodopsin-like coupled G-proteins family, involving seven extra and intracellular loops linked hydrophobic transmembrane domains (Lazarczyk et al., 2007) . Tachykinin receptors include three different types of receptors, NK_1, NK_2 and NK_3 (Pennefather et al., 2004). They interact with SP, neurokinin A, and neurokinin B (Pennefather et al., 2004). SP not only acts on NK_1 receptors, but also binds to NK_2 and NK_3 receptors in several tissue types. Some NK_1 receptor antagonists have been previously developed for treatment of pain related diseases. For example, CP 99994 which is a NK_1 receptor antagonist displayed the ability to decrease pain after dental extraction operations at a dose which does not produce side effects (Dionne et al., 1998).

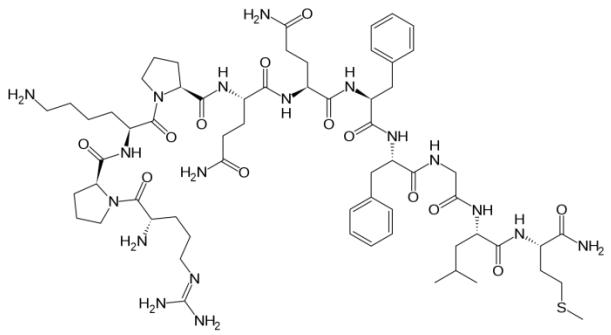

Figure 1.7. Chemical structure of substance P.

1.2.1.3.3 CGRP

CGRP is a neuropeptide that plays a critical role in pain transmission and neurogenic inflammatory pain such as migraine (Durham, 2006). CGRP is derived from both the peripheral and central neural system (Ji, 2004). However, when the function of CGRP is associated with the transmission of pain, CGRP is mainly released from DRGs (Durham, 2006). CGRP belongs to the calcitonin family of peptides and there are two isoforms of CGRP, α-CGRP (or CGRP I) and β-CGRP (or CGRP II). They have very similar biological activities; however, they are encoded by different genes. The α-CGRP is a 37 amino acid peptide encoded by the alternative splicing of the CGRP gene in chromosome 11 (Benemei et al., 2009). The β-CGRP is also a 37 amino acid peptide, but compared to α-CGRP, it has three different amino acids in humans and one in rats. It is encoded by a separate CGRP gene with high homology (Benemei et al., 2009). α-CGRP and β-CGRP are CGRP receptor agonists. They interact with CGRP receptors to transduce CGRP signalling pathways. $CGRP_{8-37}$ includes 30 amino acids, missing 7 amino acids at the beginning compared with CGRP. $CGRP_{8-37}$, is a CGRP receptor antagonist which binds to CGRP receptors without the activation of signalling pathways. CGRP acts on two major types of CGRP receptors, the CGRP1 and 2 receptors (Yu et al., 2009). The cloned calcitonin receptor-like receptor (CRLR) from human and rat, is a seven transmembrane domain G-protein-coupled orphan receptor which can identify and interact with the receptor activity modifying protein (RAMP) to become active allow to CGRP binding (Figure 1.8) (Yu et al., 2009). There are three different types of RAMPs; RAMP1, RAMP2 and RAMP3. It is known that the association of RAMP1 with CRLR preferentially expresses a functional CGRP receptor (Buhlmann et al., 1999).

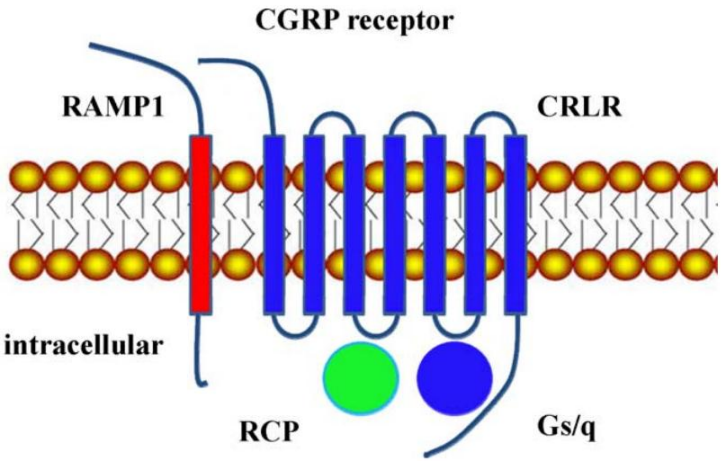

Figure 1.8. Functional CGRP receptor containing CRLR, RAMP1 and RCP. CRLR is a seven transmembrane domain G-protein-coupled orphan receptor. RAMP1 is a 148-amino acid peptide with a single-transmembrane domain receptor component protein (RCP). CGRP receptor component protein, transduce G-protein-coupled signal at receptors for CGRP (Yu et al., 2009).

During headache related diseases attacks, the release of CGRP and pro-inflammatory mediators is triggered. These mediators further elevate CGRP synthesis and release by activation of MAPK signalling pathways (see earlier TNFα section) (Durham, 2006). It has been demonstrated that several specific CGRP inhibitors based antimigraine compounds, such as ergot derivatives and triptans, can attenuate the release of sensory neuropeptides from trigeminal neurons in an animal model (Durham, 2006).

1.3 Chronic pain conventional treatment

Currently, three main types of medicine are widely used to treat chronic pain, including nonsteroidal anti-inflammatory drugs (NSAIDs), opioids and an adjuvant such as antidepressants and anticonvulsants.

1.3.1 Nonsteroidal anti-inflammatory drugs (NSAIDs)

Nonsteroidal anti-inflammatory drugs (NSAIDs) are a class of drugs used to relieve chronic pain or treat fever and inflammatory diseases (Rao and Knaus, 2008). Aspirin, ibuprofen, ketoprofen, and naproxen are the most popular drugs in this class (Jones, 2001). NSAIDs act by inhibiting the activity of cyclooxygenase-1 (COX-1) and 2 (COX-2), and thereby, decrease the level of synthesis of prostaglandins and thromboxanes. The blockade of signalling pathway of COX provides the anti-inflammatory, analgesic and antipyretic effects as COX plays a key role in pain and inflammation (Rao and Knaus, 2008). However, continued use/long term administration or over doses of these drugs can lead to ulcers and increase the risk for heart attack as well as kidney and liver related diseases (Barkin et al., 2005).

1.3.2 Opioids

Several opioid drugs have the ability of controlling chronic pain and therefore are used as therapeutics; these include codeine, morphine, oxycodone and other opioid medications (Barkin et al., 2005). These opioid drugs act by binding to opioid receptors which are widely distributed in both the central and peripheral nervous system and play an important role in pain regulation (Vallejo et al., 2004). However, these opioids are avoided by doctors due to the addictive side effects (Benyamin et al., 2008). In addition, the half-lives of most opioids are short; therefore, the frequency of administration or the amount per dose needs to be increased to achieve the desired effects (Scimeca et al., 2000). The balance between risk and benefit should be seriously concerned before choosing opioids as a painkiller.

1.3.3 Adjuvants

As I mentioned at the beginning of the introduction, pain is commonly described as any unpleasant or uncomfortable feeling. Therefore, chronic pain patients are susceptible to anxiety and depression. Thus, several anti-depression drugs approved by the FDA are also used as part of treatment of chronic pain, including amitriptyline (Elavil), imipramine

(Tofranil) and clomipramine (Anafranil), desipramine (Norpramin), doxepin (Sinequan), nortriptyline (Pamelor), venlafaxine (Effexor) and duloxetine (Cymbalta). In addition, many anticonvulsants drugs, such as gabapentin (Neurontin), pregabalin (Lyrica), and lamotrigine (Lamictal) are also prescribed by doctors to help chronic pain patients to alleviate their chronic pain symptoms (Haldeman, 2012). These drugs seem to be just as effective at treating chronic pain as depression and convulsions; however, they have several undesirable side effects including dry mouth, sedation, urinary retention, unstable gait (ataxia), sedation, liver related disease and in extreme cases death (Haldeman, 2012).

1.3.4 Botulinum neurotoxins (BoNTs) as analgesic

A pressing unmet need exists for persistently-acting and non-addictive medication for chronic pain, due to its major healthcare/economic burdens. Toward this end, botulinum neurotoxins have been proposed to have significant potential as local treatments for chronic pain with its long lasting action, lack of non-addictive features.

BoNTs are commonly applied as therapeutics to treat a wide range of overactive disorders by controlling overactive muscles (voluntary and involuntary) or glands innervated by such neurons (Ney and Joseph, 2007). However, during the treatment, some patients find that it not only controls overactive disorders effectively, but also helps them alleviate their concomitant pain symptoms (Binder et al., 2000). BoNTs are therefore considered as therapeutics for chronic pain and in 2010, BOTOX® (a BoNT complex) was approved by the FDA to treat chronic migraines (Oh and Chung, 2015).

In 1817, a German physician called Justinus Kerner first described a paralytic condition caused by consumption of poisoned food, this food-borne paralysis was then named "botulism" (Masuyer et al., 2014). BoNTs are the most potent neurotoxins known to date, they cause flaccid neuromuscular paralysis. BoNTs are produced by *Clostridum botulinum*, a gram-positive, anaerobic, spore-forming and rod-shaped bacterium (Wang et al., 2011). There are 7 identified serotypes of BoNT which are named A-G (/A - /G) in the order of their discovery chronology (Wang et al., 2011). Only serotypes A, B, E, and F are capable

of causing human botulism, whereas, serotypes C and D are responsible for animal and avian botulism (Masuyer et al., 2014). BoNT serotype A has been the most widely studied and successfully used serotype for therapeutic purposes to date, due to its long-lasting effect (Davletov et al., 2005; Foran et al., 2003; Jankovic, 2004).

BoNTs usually form large protein complexes with several non-toxic proteins called haemagglutinins as well as a non-toxic non-haemagglutinin (NTNH) protein (Masuyer et al., 2014). During the digestion of BoNT contaminant food, these associated non-toxic proteins play an important role in protecting and stabilizing the toxin in the low pH of the stomach and intestine which contains several intestinal proteases (Masuyer et al., 2014). In the small intestine, the toxin attaches and crosses the small intestinal wall to migrate into the bloodstream and cause botulism (Masuyer et al., 2014).

1.3.4.1 Mechanism of botulinum neurotoxin

These potent neurotoxins act by inhibiting the release of acetylcholine at the neuromuscular junction which has been proven by blocking synaptic transmission at peripheral cholinergic nerve endings (Dolly et al., 2009). Each BoNT serotype is expressed as an approximately 150k single-chain protein (Binz et al., 2010). It is encoded by an approximately 3.9 kb gene (Masuyer et al., 2014). Later on, this single-chain (SC) toxin is cleaved by clostridial or host endogenous proteases to activated di-chain form (DC) (Binz et al., 2010).

The 3D crystal structures of BoNT/A, /B and /E have been identified (Figure 1.9) (Lacy et al., 1998).The structure of botulinum neurotoxin involves three individual functional domains: an N-terminal catalytic domain (a zinc dependent endopeptidase light-chain, LC), a translocation domain (H_N) which contributes to the translocation of BoNT LC into the neuronal cytosol, and a binding domain (H_C) responsible for receptor binding, each approximately 50k (Wang et al., 2008). The binding domain is subdivided into two subdomains: C terminal binding sub-domain (H_{CC}) and N terminal binding sub-domain (H_{CN}) (Masuyer et al., 2014).

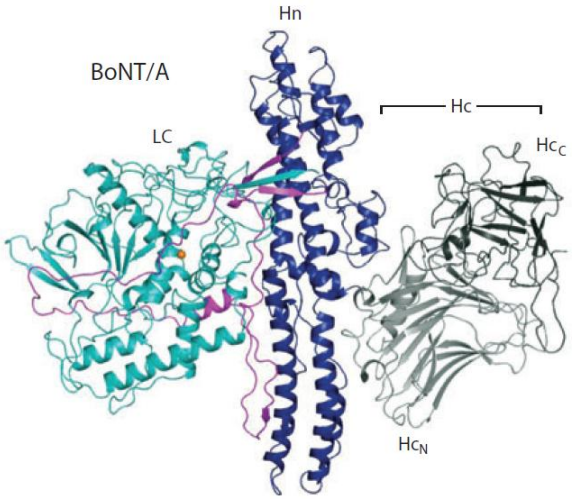

Figure 1.9. The crystal structure of BoNT/A (PDB 3BTA) (Lacy et al., 1998). In BoNT/A ribbon diagram, LC, Hn, and belt are labeled with cyan, dark blue and pink, respectively. H_C is labeled with gray (H_{CN} and H_{CC} highlighted with light and dark gray). An orange sphere is represented Zinc ion (Masuyer et al., 2014).

BoNTs bind specifically to ecto-acceptors on cholinergic nerve endings (Masuyer et al., 2014, Dolly et al., 2011, Dolly et al., 2009). This evokes endocytosis of ecto-acceptors leading to internalization of BoNTs into vesicles where the translocation of LC is triggered allowing BoNT LC to cross the endosomal membranes and move into the cytosol of the neuron (Binz et al., 2010). After translocation of the BoNT LC into the neuronal cytosol, the LC selectively cleaves its target soluble NSF (N-ethylmaleimide sensitive factor) attachment receptor (SNARE) protein and inhibits vesicle fusion and neurotransmitter release (Figure 1.10) (Masuyer et al., 2014).

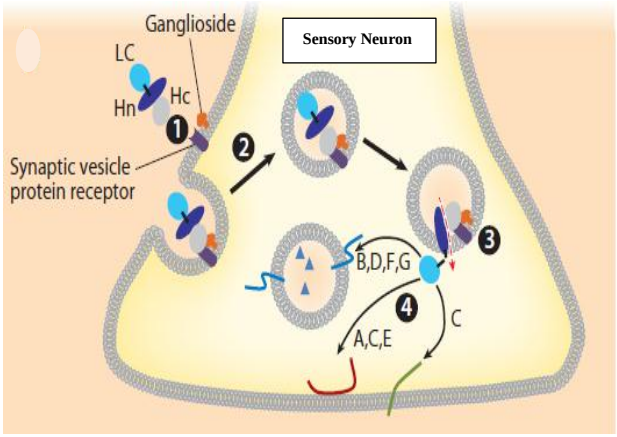

Figure 1.10. Schematic of action of BoNTs. (1) BoNTs bind to specific ecto-accceptors on the neuron and trigger endocytosis (2). (3) The acidic environment in the limited membranes component induces formation of channels for translocation of LC. (4) LC is separated from H_C by the reducing cytoplasmic environment and cleaves SNAREs. (Masuyer et al., 2014).

BoNT/A, /D, /E, and /F have been reported to bind to synaptic vesicle protein 2 (SV2) which is a high-affinity membrane glycoprotein acceptor (Peng et al., 2011, Meng et al., 2009, Fu et al., 2009, Boddul et al., 2014). BoNT/B and /G bind to Synaptotagmin I (Syt I) and/or II (Syt II) receptors (Peng et al., 2011, Jin et al., 2006). After binding, BoNTs are endocytosed to allow the translocation of their LC into the cytosol where it cleaves one or two SNARE proteins (Meng and Wang, 2015). Peripheral membrane protein synaptosomal-associated protein of 25k (SNAP-25) is cleaved by BoNT/A /C and /E, albeit at distinct sites. BoNT/B, /D, /F and /G cleave synaptic vesicle protein synaptobrevin (Sbr) [also known as vesicle-associated membrane protein (VAMP)] isoforms I, II and III (Meng and Wang, 2015). In addition, the plasma membrane protein syntaxin (Syx) is cleaved by BoNT/C1 (Meng and Wang, 2015).

During neuronal exocytosis, syntaxin and synaptobrevin are found attached to the cell and synaptic vesicle membranes, by their C-terminal domains, respectively (Carr and Munson, 2007). However, SNAP-25 is anchored in the plasma membrane via several cysteine-linked palmitoyl chains (Carr and Munson, 2007). The SNARE complex is a four-α-helix

bundle (Figure 1.11) (Masuyer et al., 2014). One α-helix is contributed by syntaxin and another synaptobrevin (VAMP), whereas two α-helices are contributed by SNAP-25 (Masuyer et al., 2014). Additionally, Meng and colleagues have proved that SNAREs mediate cytokine and pain peptide release from inflammatory cells and sensory neurons (Meng et al., 2007, Boddul et al., 2014). Therefore, truncation of SNARE proteins by BoNTs before the formation of SNARE complex, blocks cytokine and pain peptides release potentially leading to the relief of chronic pain.

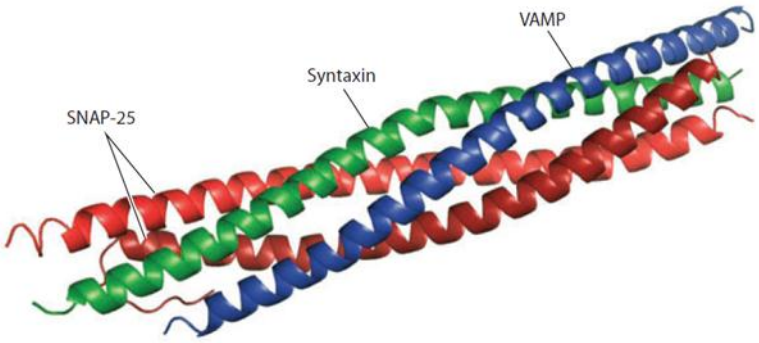

Figure 1.11. The crystal structure of SNARE complex. This ribbon diagram shows the SNARE complex is a four-α-helix bundle (Masuyer et al., 2014).

1.4 Aims and objectives

The aim of my project is to create and investigate new therapeutics, based on Botulinum neurotoxin with potential targeting ligands, as dual targeting anti-inflammatory and/or anti-nociceptive agents. Therefore, the acceptor binding domain of BoNT/D could be either replaced recombinantly with an interleukin receptor targeting ligand IL-1β or IL-1RA or a TNF receptor targeting ligand Atsttrin. We also exploited the sortase-mediated protein ligation technique to make functional targeted BoNT based fusion proteins by stitching BoNT protease to the cell-specific targeting ligand IL-1β or CGRP receptor antagonist $CGRP_{8-37}$. All therapeutics should meet the criteria of a desirable anti-nociceptive: ability to bind and enter immune cells and/or sensory neurons, cleave SNAREs and block the evoked release of cytokines and pain peptides.

To assess the anti-nociceptive potential of these therapeutics their ability to cleave SNARE proteins and block cytokine release in inflammatory cells (macrophages) and sensory (but not motor) neurons (rat DRGs) will be investigated, the results of which will be discussed herein. In macrophages, VAMP-3 has been previously reported to be involved in the release of pro-inflammatory cytokines such as TNF-α and IL-6. Therefore by cleaving VAMP-3 the proposed therapeutics should in turn prevent the release of this key inflammatory cytokines, making VAMP-3 cleavage and cytokine release key indicators of therapeutic efficacy. Likewise in sensory neurons VAMP-1 is known to be involved in the release of pain peptides, such as SP and CGRP, making these mediators suitable readouts.

The overall objective of this project is to engineer dual targeting novel therapeutics which can target both immune cells and sensory neurons, blocking their respective mediator release and therefore blocking pain transmission and hopefully treating chronic pain.

Chapter 2: Materials and Methods

2.1 Materials

2.1.1 Reagents for cloning, protein expression, purification and nicking

Restriction enzymes and Enterokinase were bought from New England Biolabs (Dublin, Ireland). Thrombin enzyme and vectors were ordered from Merck/Millipore (Cork, Ireland). All chemicals which were used in protein purification were supplied by Sigma Aldrich (Arklow, Ireland). Talon cobalt resin was bought from Clontech Laboratories, Inc. (Mountain View, USA). Resource Q and PD-10 columns were ordered from GE Healthcare (Dublin, Ireland). Gene synthesis and DNA sequencing were serviced by Eurofins Genomics (Ebersberg, Germany).

2.1.2 Reagents for sortase A mediated chemical conjugation reaction

Rat Gly_3-$CGRP_{8-37}$ and Gly_3-substance P peptides with C-terminal amide modification were synthesized by LifeTein, LLC (New Jersey, USA). Zeba Spin Desalting Columns were supplied by Life Technologies Ltd (Paisley, UK). pET30b-7M SrtA encoding hepta-mutant *Staphylococcus aureus* sortase A was a gift from Hidde Ploegh (Addgene plasmid # 51141).

2.1.3 Reagents for cell culture

Dulbecco's modified Eagle's Medium (DMEM), Dulbecco's modified Eagle's Medium/Nutrient Mixture F-12 Ham (DME/F12), RPMI 1640 medium with sodium bicarbonate and L-glutamine, fetal bovine serum (FBS), Dulbecco's Phosphate Buffered Saline without $CaCl_2$ and $MgCl_2$ (DPBS), Trypsin EDTA, penicillin/ streptomycin, Cytosine-β-D-arabinofuranoside (Ara-C), poly-L-lysine and laminin were bought from Sigma Aldrich (Arklow, Ireland). Human synoviocytes growth medium was supplied by tebu-bio (local distributor of Cell Applications, Inc) (Peterborough, UK). Mouse nerve growth factor (NGF-2.5S) was ordered from Alomone Labs (Jerusalem, Israel). B-27

Supplement and Collagenase I were supplied by Life Technologies Ltd (Paisley, UK). Dispase II was bought from Roche Products Ltd. (Dublin, Ireland).

2.1.4 Cell lines

RAW 264.7 cell line murine macrophage and Human fibroblast-like synoviocytes (HFLS) were obtained from Sigma Aldrich (Arklow, Ireland) and Cell Applications, Inc., respectively. A human synovial sarcoma cell line (SW982) was supplied by American Tissue Culture Collection (Teddington, UK).

2.1.5 Antibodies

Table 1. List of antibodies used in the project

Primary antibodies	Catalogue numbers	Vendor	Dilution factor for Western blotting or immune-fluorescent staining
SNAP-23	Cat. No. 111 202	Synaptic Systems	1:1000
Syntaxin I	Cat. No. S0664	Sigma	1:2000
VAMP I	Cat. No. 104 002	Synaptic Systems	1:1000
VAMP I/II/III	Cat. No. 104 102	Synaptic Systems	1:1000
IL1 Receptor I	Cat. No.ab106278	Abcam	1:500
IL-6	Cat. No.ab6672	Abcam	1:500
Substance P (staining)	Cat. No. ab14184	Abcam	1:500
TNF Receptor I	Cat. No. ab19139	Abcam	1:500
CGRP	Cat. No. C 8198	Sigma	1:10,000
Substance P (WB)	Cat. No. BML-SA 1270	Enzo	1:2500
6x-His Tag	Cat. No. MA1-21315-BTIN	Bio-Sciences	1:500
alpha-Tubulin	Cat. No.T5168	Sigma	1:4000

Secondary antibodies conjugated to horseradish peroxidase or fluorescently-labelled were supplied by Jackson Immuno-Research (Suffolk, UK) and Bio-Sciences (Dun Laoghaire, Ireland), respectively..

2.1.6 Enzyme-linked immunosorbent assay (ELISA) assay reagents

Mouse IL-6 and TNF-α and human IL-6 Duo-set ELISA kits were bought from R&D Systems Eire (Abingdon, UK). Substance P enzyme immunoassay (EIA) kit from Cayman Chemical was supplied by Bertin Bioreagent (York, UK). . 3,3',5,5'-tetramethylbenzidine (TMB, ELISA substrate), MaxiSorp™ 96 well plates, lipopolysaccharides (LPS) and interferon gamma (IFNγ) were purchased from Sigma Aldrich (Arklow, Ireland) and R&D Systems Eire supplied human IL-1β.

2.1.7 Other reagents

Bradford protein assay kit was provided by Bio-Rad (Dublin, Ireland). All chemicals which were used for making SDS-PAGE gels were bought from Sigma Aldrich (Arklow, Ireland). Enhanced chemiluminescence (ECL) developing reagents were purchased from GE's healthcare (Dublin.Ireland) or Merck/Millipore (Cork, Ireland). Precast 12% Bis-Tris gels, Click-iT® EdU microplate assay kitand alamar blue reagent were bought from Bio-Sciences (Dun Laoghaire, Ireland). Any reagent not specified was ordered from Sigma Aldrich (Arklow, Ireland). Antifade reagent, containing (4',6-diamidino-2-phenylindole) DAPI was supplied by Bio-Sciences (Dun Laoghaire, Ireland).

2.1.8 Animals

Sprague Dawley rat pups were bred in Bio Resources Unit, Dublin City University (DCU).

All of the procedures which carried on living animals have been permitted by the Dublin City University Research Ethics Committee were carried out under licenses granted from the Health Products Regulatory Authority under Directive 2010/63/EU and the European Union (Protection of Animals Used for Scientific Purposes) Regulations 2012 (S.I. No. 543 of 2012).

2.2 Methods

2.2.1 Plasmid construction

BoNT/DΔH_C-IL-1β, BoNT/DΔH_C-IL-1RA, BoNT/DΔH_C-Atsttrin and BoNT/DΔH_C genes were cloned into an *E. coli* expression vector (pET-29a) between NdeI and XhoI sites. A short nucleotide encoding a non-structural linker 2x (Gly_4Ser), LPETG and a thrombin recognition sequence was cloned into the Sal I and Xho I sites of the BoNT/DΔH_C plasmid to yield a construct encoding BoNT/DΔH_C-CS. Synthetic gene encoding Trx-His_6-Gly_5-IL-1β was cloned into the pET32b vector immediately after the enterokinase recognition site. These constructs were designed and cloned by Dr. Jiafu Wang. Clones of them were screened by restriction enzyme digestion analysis using NdeI, XhoI and SacI. Finally all inserted genes were confirmed by DNA sequencing by Eurofins MWG Operon Company.

2.2.2 Protein Expression and Purification

E. coli strain BL21 (DE3) was transformed with the construct for BoNT/DΔH_C-IL-1β, BoNT/DΔH_C-IL-1RA, BoNT/DΔH_C-Atsttrin, BoNT/DΔH_C, BoNT/DΔH_C-CS, Trx-His_6-Gly_5-IL-1β, or sortase A following a heat-shock protocol published on Methods in Enzymology by Hanahan and his colleagues (Hanahan et al., 1991). A starter culture was established by inoculating LB medium with a single colony and culturing overnight at 37℃ and shaking at 220 rpm. The starter culture was then transferred into autoinduction medium (1000 fold dilution) and grown at 37℃ for 6-8 h with shaking (220 rpm), followed by 22℃ overnight (Zhou et al., 1995, Lawrence et al., 2007). The following day, cells were harvested by centrifugation at 4424 g for 30 mins. The cell pellets were then resuspended and lysed in lysis buffer (145 mM NaCl, 20 mM HEPES, pH 8, 1 mM PMSF with lysozyme to a final concentration of 2 mg/ml). Lysates were rotating on a roller at 4℃ for 1 h, followed by two repeated freeze-thaw cycles. Recombinant proteins were purified by immobilized metal affinity chromatography (IMAC), using equilibrated Talon cobalt-super

flow resin. First, the lysate was incubated with the resin for 1 h at 4°C, to allow binding, then the lysate and resin mix was added to an empty column and any unbound proteins allowed to flow through. After washing the resin with washing buffer (145 mM NaCl, 20 mM HEPES, 5 mM imidazole, pH 8), any bound proteins were eluted by adding 500 mM imidazole to the wash buffer. Finally, eluted fractions were combined and desalted into toxin storage buffer (20 mM Hepes, 145 mM NaCl, pH 7.4) using PD-10 columns. Successful purification of recombinant target proteins were confirmed by running samples from the various stages on 10% hand-made Tris-glycine SDS-PAGE gels (Table 2). They were run at 130 volts using Tris-Glycine gels running buffer (192 mM Glycine, 25 mM Tris, 0.1% (w/v) SDS) until pre-stained protein markers were separated properly. SDS-PAGE gels were then stained using Coomassie staining buffer [0.25% (w/v) Coomassie brilliant blue G-250, 45% (v/v) methanol, 10% (v/v) acetic acid] for 2 h and distained with distaining buffer [40 % (v/v) methanol and 10% (v/v) acetic acid]. Concentrations of these proteins were determined using the Bradford protein assay (Bio-rad). BoNT/DΔH_C-IL-1β, BoNT/DΔH_C-IL-1RA and BoNT/DΔH_C–Atsttrin, BoNT/DΔH_C-CS, Trx-His_6-Gly5-IL-1β were abbreviated /DIL-1β, /DRA, /D-Atsttrin, respectively.

Table 2 Tris-Glycine gel recipes for making 4 gels

Resolving gel		
	10% [ml]	12% [ml]
H_2O	12.3	10.2
1.5M Tris-HCl pH 8.8	7.5	7.5
10 % (w/v) SDS	0.3	0.3
30% (w/v) Acrylamide	9.9	12
20% (w/v) ammonium persulfate(APS)	0.15	0.15
Tetramethylethylenediamine (TEMED)	0.04	0.04
Stacking gel		
H_2O	3.075	
0.5M Tris-HCl pH 6.8	1.25	
10 % (w/v) SDS	0.05	
30% (w/v) Acrylamide	0.67	
20% (w/v) APS	0.025	
TEMED	0.01	

2.2.2.1 Bradford assay

Concentrations of purified recombinant proteins were quantified by Bio-Rad Bradford assay. Briefly, 1 mg/ml BSA (bovine serum albumin) was prepared and standards were set up in 1.5 ml eppendorf tubes, following the table showed below (Table 3). They were then mixed and incubated for 5 min at room temperature, followed by transferring into plastic cuvettes and reading by spectrophotometer at 595 nm. A standard curve of Bradford assay was graphed and is displayed in Figure 2.1. The concentrations of the measured protein were extrapolated from the standard curve. A new standard curve was generated for every assay.

Table 3. Details of setting up Bradford assay standard curve of using 1mg/ml BSA

Standard	Amount of Bradford assay reagent [µl]	Amount of 1mg/ml BSA[µl]	Amount of Distilled Water[µl]	Final concentration in tube[mg/ml]
Blank	200	0	800	0
Standard 1	200	2	798	2
Standard 2	200	4	796	4
Standard 3	200	6	794	6
Standard 4	200	8	792	8
Standard 5	200	10	790	10

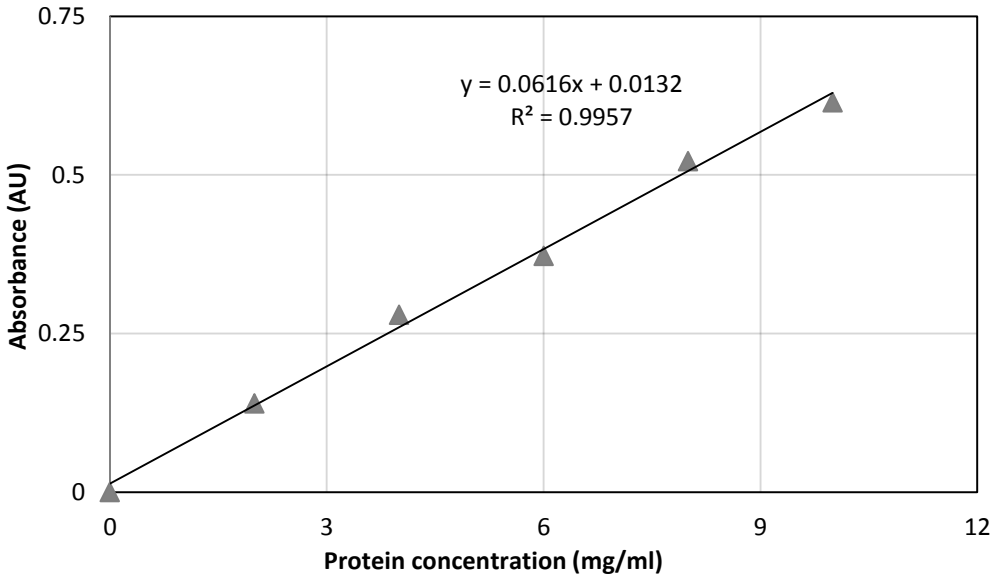

Figure 2.1. Bradford assay standard curve. This figure was graphed in Excel using the linear regression line fit. The value read by spectrophotometer at OD_{595} from the standards was plotted on the y-axis against their known concentrations on the x-axis. The equation of the line generated by excel is shown on the graph.

2.2.3 Nicking of purified /DIL-1β, /DRA, /D-Atsttrin, BoNT/DΔH_C and /DΔH_C –CS with simultaneous His_6 removal and separating Trx-His_6 tag from Gly_5-IL-1β by enterokinase

/DIL-1β, /DRA, /D-Atsttrin, and BoNT/DΔHc and /DΔH_C-CS contain two thrombin sites to allow simultaneous his tag removal and protein activation (nicking of SC to active DC form). Purified recombinant proteins and BoNT/DΔH_C were incubated with thrombin enzyme (1U of thrombin /mg of toxin) for 1.5-2 h at 22 °C. Nicking and His_6 tag removal was confirmed by running on 10% hand-made Tris-glycine SDS-PAGE gels, followed by Coomassie staining and western blotting with antibody against His_6. Upon confirmation of complete nicking to DC, 1mM phenylmethylsulfonyl fluoride (PMSF) (final concentration) was added to inactivate the thrombin. The concentrations of SC or nicked DC were measured by the Bradford protein assay. Only nicked samples were used in function analysis studies or conjugation reaction. IMAC purified fusion protein Trx-H_6-IL-1β were incubated with enterokinase in ratio 1 to 6.25x 10^5 for 3 h at 22°C to separate the Trx-His_6 tag from Gly_5-IL-1β.

2.2.4 Conjugation of /DΔH_C-CS with IL-1β or $CGRP_{8-37}$

/DΔH_C-CS (10 μM final concentration) and sortase A (25 μM, final concentration) were mixed with enterokinase cleaved Trx-His_6 and Gly_5-IL-1β mixture (0.3 M, final concentration) in reaction buffer (50 mM Tris, 150 mM NaCl, 10 mM $CaCl_2$, pH7.4) at 37°C for indicated time. To purify the /DΔH_C-IL-1β conjugated protein (abbreviated as /DIL-1β (conjugate)), the reaction samples were buffer-exchanged into 50 mM Tris buffer (pH 8.0) and loaded onto a Resource Q column following a previously published protocol (Wang et al., 2008). Briefly, after wash with Tris buffer with 30 mM NaCl, a stepwise gradient up to 1M NaCl was used to elute the conjugated protein and other contaminants.

To conjugate /DΔH_C-CS to Gly_3-$CGRP_{8-37}$ or Gly_3-substance P, /DΔH_C-CS (10 μM, final

concentration) and sortase A (25 μM, final concentration) were mixed with peptides (0.3 M, final concentration) at 37°C for 30 min. The reaction mixture was buffer-exchanged into the sample storage buffer using Zeba Spin Desalting Columns to stop the reaction and remove the excess Gly_3-$CGRP_{8-37}$. Final product BoNT /$D\Delta H_C$-$CGRP_{8-37}$ was abbreviated as /D-$CGRP_{8-37}$.

2.2.5 Toxin proteolytic activity assay

The protease activities of /DIL-1β, /DRA, /$D\Delta H_C$-CS, /DIL-1β (conjugate), and /D-$CGRP_{8-37}$, BoNT/$D\Delta H_C$ were measured *in vitro* using a recombinant GFP-$VAMP2_{(2-94)}$-His_6 substrate. Briefly, the proteins were diluted to 100 nM in protease assay buffer HBS-20 (20 mM HEPES, 100 mM NaCl (pH 7.4), 10 μg/ml bovine serum albumin (BSA), 5 mM DTT, and 10 μM $ZnCl_2$) and incubated at 37°C for 30 min to activate proteases. The proteins (100 nM) were serially diluted (2 fold) to a final concentration of 1.56 nM in HBS-20 buffer then mixed with equal volume of 1 mg/ml of GFP-$VAMP2_{(2-94)}$-His_6 substrates. Following additional 30 min incubation at 37°C, the reactions were stopped by adding equal reaction volume of ice-cold 2xLDS (lithium dodecyl sulfate) sample buffer. The samples were analyzed by running on 12% Tris-glycine SDS-PAGE gels and stained by Coomassie solution.

2.2.6 Cell Culture

The murine macrophage cell line (RAW 264.7) is an adherent cell line originally established from the ascites of a tumor induced in a male mouse by intraperitoneal injection of Abselon Leukemia Virus (A-MuLV). The cells were cultured in complete culture medium [DMEM medium containing 10% (v/v) heat-inactivated fetal bovine serum, 1% (v/v) penicillin/ streptomycin], at 37°C, 5% CO_2. A human synovial sarcoma cell line (SW982) is isolated from human synovial sarcoma tissues. The cells were cultured in complete medium [RPMI1640 medium containing 10% (v/v) heat-inactivated fetal bovine serum, 1% (v/v) penicillin/ streptomycin], at 37°C, 5% CO_2.The HFLS, isolated from

normal healthy human synovial tissue, were cultured in commercial human synoviocyte completed growth medium in the same culture condition.

Cells were subcultured every 2-3 days; the cells were harvested by scraping (RAW 264.7 cells) or treating with 0.25% trypsin EDTA for 5 mins (SW982 and HFLS cells) and centrifugation at 120 g for 5 min. Then the supernatant was discarded and the cells were resuspended in fresh medium and re-seeded (1 in 3 dilution).

2.2.7 Isolation and culturing primary mouse peritoneal macrophages

The primary mouse peritoneal macrophages were isolated from peritoneal of around 8 weeks' CD-1 mice and cultured *in vitro*, according to protocol published by Zhang et. al (Zhang et al., 2008). Briefly, the skin at the front of peritoneum were separated and removed from peritoneum. 5 ml of chilled DPBS (no Mg^{2+} and Ca^{2+}) were injected into inter-peritoneal and then collected the fluid from peritoneal cavity. The collected fluid was centrifuged at 120 g for 8 min. The cell pellet was resuspended in culture medium (DMEM/Nutrient F12 ham, 10% (v/v) FBS, 1% penicillin streptomycin and seeded ~4 × 10^5 cells per well into a 24 well plate. After 1 h incubation at 37ºC, 5% CO_2, cells were washed with warmed DPBS (no Mg^{2+} and Ca^{2+}) three times, added fresh culture medium and incubated for further 24 h. More than 90% of cells should be macrophages (Zhang et al., 2008).

2.2.8 Cell proliferation assay

The Cell proliferation assay was used to measure the bio-activity of IL-1β (recombinant or conjugate) and IL-1RA ligands which were fused to BoNT/DΔH_C or ligated to /DΔH_C-CS. The assay measures the incorporation of the nucleoside analog EdU (5-ethynyl-2'-deoxyuridine) into newly synthesized DNA during cell division, by reading the fluorescence emitted from the green-fluorescent Oregon 488 dye. There is a copper-

catalyzed covalent reaction between an azide in the Oregon Green 488 dye and alkyne in EdU to link EdU and the green-fluorescent Oregon 488 dye together. Therefore the fluorescence reading correlates directly with newly synthesized DNA and allows quantification of cell proliferation.

RAW 264.7 cells were plated in a 96 well plate with ~ 0.4 $x10^4$ cells / well, and cultured for 24 h at 37°C, 5% CO_2. After 24 h incubation, a range of two-fold serial dilutions of commercial human IL-1β (from 500 pg/ml to 0.98 pg/ml), serial diluted /DIL-1β, /DRA or BoNT/DΔH_C were added and the plate incubated for a further 48 h at 37°C, 5%CO_2. Treated cells were labelled with 10 μM of EdU for 16 h before fixation. Medium was removed, 50 μl of EdU fixative was added into each well and incubated for 5 min at room temperature, followed by addition 50 μl of 2x Click-iT® reaction cocktail, to label EdU labeled cells, and incubated for an additional 25 min in the dark. The wells were washed twice with blocking buffer to remove any unlinked substrate and then incubated with 50 μl of anti-Oregon Green HRP conjugate for 30 min at room temperature, again avoiding light. After washing twice with 200 μl per well of Amplex® Ultra Red buffer, 100μl of Amplex® Ultra Red reaction mixture [6ml of Amplex® Ultra Red buffer, 6 μl of Amplex® Ultra Red reagent, 6 μl of hydrogen peroxide] was added into each well and incubated for 30 min at room temperature, protecting from light. The reaction was then stopped by adding 10 μl of Amplex® Ultra Red stop reagent. Finally, the fluorescence, excitation/emission maxima 490/525 or 530/590 nm, was read using a plate reader. The brief workflow diagram for this assay was shown in Figure 2.2. A standard curve of commercial human IL-1β was generated. Using the standard curve the readings for /DIL-1β, /DRA, /DIL-1β conjugate, BoNT/DΔH_C or /DΔH_C-CS treated cells were converted to the commercial IL-1β concentration. Finally, the percentage of bio-activity of the test proteins was calculated relative to the original concentration used.

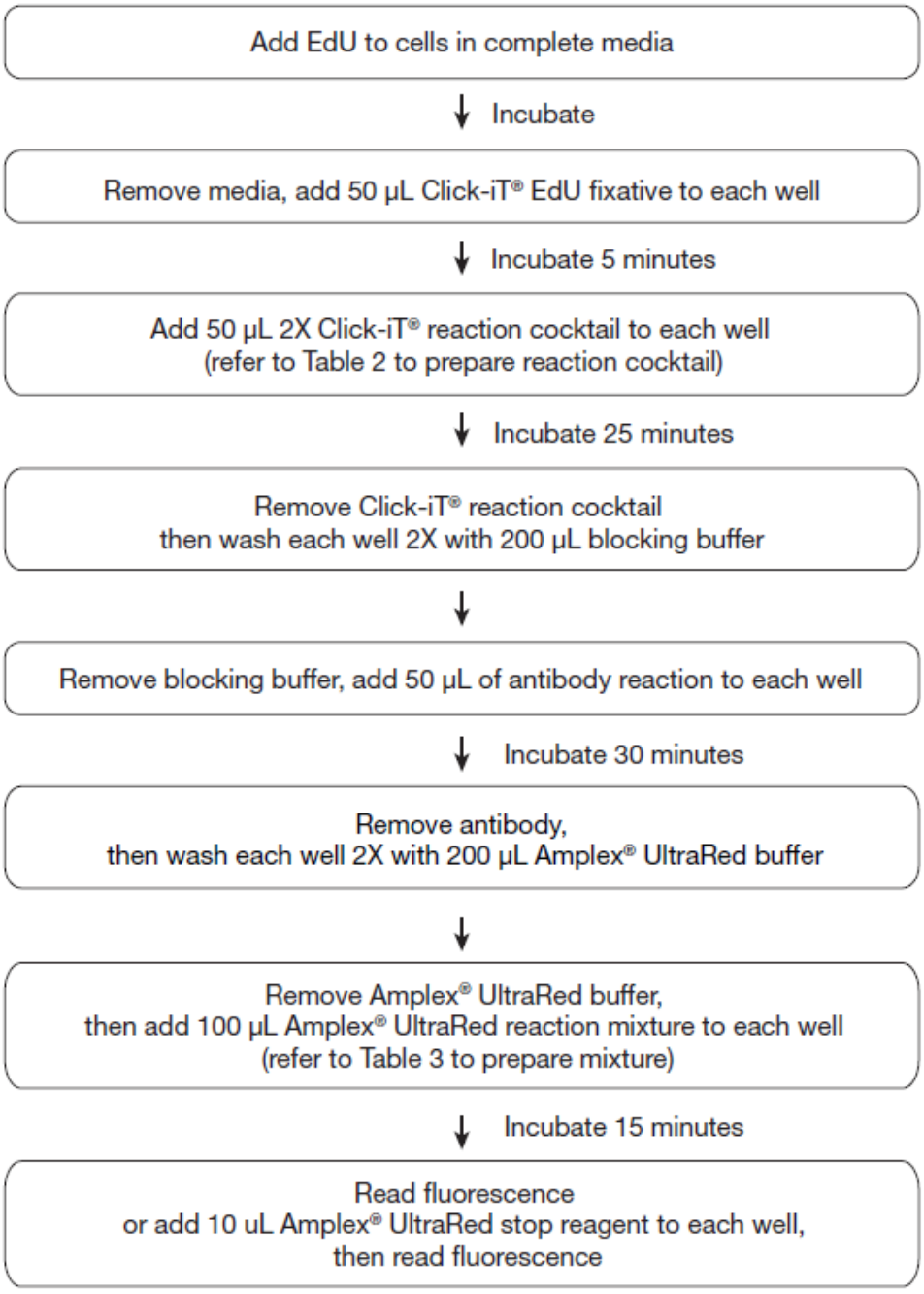

Figure 2.2. Workflow chart for the Click-iT® EdU Microplate Assay (Invitrogen™, 2008).

2.2.9 Murine macrophage cell line or primary macrophages treatment with recombinant or conjugated proteins

The RAW cells or primary mouse macrophages were plated at ~1x10^5 cells per well in a 24 well plate and incubated for 24 h at 37°C, 5% CO_2. On the following day, the cells were treated with a range of two-fold serial dilutions of novel biotherapeutics or control protein and incubated for 6 h at 37°C, 5% CO_2. Treated macrophages were incubated with 200 µl stimulation solution [DMEM medium, containing 100 ng/ml LPS, 1% penicillin/ streptomycin and 500 pg/ml IFNγ] for 42 h at 37°C, 5% CO_2. Then the supernatants were collected and stored at -80°C until ELISA analysis. Treated macrophages were lysed in 70 µl of 2xLDS sample buffer and frozen at -80°C, waiting for western blotting analysis.

2.2.10 Treatment of SW982 cells with /DRA and HFLS cells with/D-Atsttrin

After seeding the SW982 cells or HFLS cells (~5x10^4 cells per well) in a 24 well plate for 24 h at 37°C, 5% CO_2, the cultured cells were incubated with a range of two-fold serial dilutions of /DRA, /D-Atsttrin or control protein (as indicated in the Figure legends) for 44 h at 37°C, 5% CO_2. After removal of the medium, pre-treated SW982 or HFLS cells were incubated with 0.2 ml stimulation solution [RPMI1640 medium, containing 25 ng/ml IL-1β and 1 % penicillin/ streptomycin] for 4 h at 37°C, 5% CO_2. Then the supernatants were collected and stored at -80°C for ELISA analysis. Treated macrophages were lysed in 70 µl of 2xLDS sample buffer and frozen at -80°C for subsequent Western blotting analysis.

2.2.11 Cell viability assay

The mouse macrophages were plated into a 96 well plate with ~ 0.4x10^5 cells / well and cultured for 24 h at 37°C, 5% CO_2. On the following day, the cells were incubated with various concentrations of proteins by two-fold serial dilution for 44 h at 37°C, 5% CO_2. Then each well was replaced with 110 µl culture medium, containing 10 µl alamar blue reagents and further incubated for 4 h, before reading absorbance at 570 nM by plate reader.

2.2.12 Rat dorsal root ganglia (rDRG) isolation, culture and treatment with recombinant proteins

rDRGs were dissected from Sprague Dawley post-natal (P) 0-3 rats (Sacha A Malin, 2007). Firstly, the spine was dissociated from rat pups and the spine was opened to expose spinal cord. The exposed spinal cord was then pushed back to bare the DRG which were cut from their connections and stored in ice-cold DMEM before centrifugation for 1 min at 120 g) (Figure 2.3). The isolated DRGs were then incubated at 37°C for 30 min with DMEM medium, containing 2.4 U/ml dispase II and 5 mg/ml collagenase I. Following centrifugation for 5 min at 120 g, pellets were resuspended in DMEM medium with gentle trituration until cloudy. After centrifugation for 5 min at 120 g, pellets were resuspended in culture medium [DMEM medium containing 5% (v/v) heat-inactivated fetal bovine serum, 1% (v/v) penicillin / streptomycin, 50 ng/ml 2.5S NGF and 1xB-27 supplement] and then ~ $2x10^5$ cells/well were seeded in 48 well plates which were pre-coated with poly-L-lysine (0.1 mg/ml) and laminin (20 μg/ml). From day 1 onwards, cytosine-β-D-arabinofuranoside (Ara-C) (10 μM), an anti-mitotic agent, was added into the culture medium, which was replaced every other day.

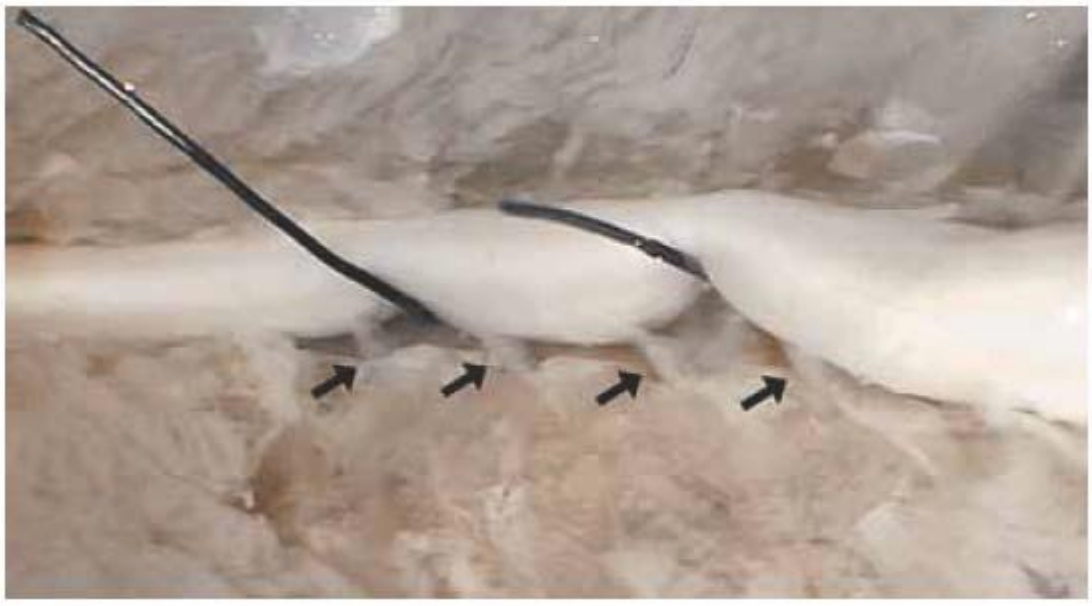

Figure 2.3. DRGs dissection. DRGs were labeled with black arrows (Sacha A Malin, 2007).

After 6-7 days *in vitro*, the rDRGs were incubated with various doses of toxin for 24 h at 37°C, 5% CO_2. Before harvesting, treated rDRGs were incubated with 200 µl of K^+ evoked release stimulation buffer (HBS mM; 22.5 HEPES, 75 NaCl, 63.5 KCl, 1 $MgCl_2$, 2.5 $CaCl_2$, 3.3 glucose, and 0.1% (w/v) BSA, pH 7.4) for 30 min at 37°C, 5% CO_2. Toxin free wells were incubated with basal release buffer (BR-HBS, mM; 22.5 HEPES, 135 NaCl, 3.5 KCl, 1 $MgCl_2$, 2.5 $CaCl_2$, 3.3 glucose and 0.1% (v/v) BSA, pH 7.4) as a control. The supernatants were then collected and stored at -80°C until EIA analysis. Treated rat DRGs were lysed in 60 µl 2xLDS sample buffer and frozen at -80°C.

2.2.13 IL-1, TNF receptor and transmitter staining and imaging

Primary murine peritoneal macrophages, HFLS cells or rat DRGs cultured on coverslips (pre-coated with poly-L-lysine and laminin) were washed with DPBS (no Mg^{2+} and Ca^{2+}) three times and fixed for 20 min at room temperature with DPBS containing 3.7% paraformaldehyde. After additional three times washing with DPBS, the fixed cells were then incubated with 0.2% Triton X-100 in DPBS for 5 min to shift to permeabilized cells, followed by blocking for 1 h with 1% bovine serum albumin (BSA) in DPBS. Primary antibodies diluted in blocking buffer were then added and incubated overnight at 4ºC. On the following day, after the same washing as above, macrophages, HFLS cells or DRGs were incubated with fluorescently-conjugated secondary antibodies for 1 h at room temperature. After the final wash of the secondary antibody, specimens were mounted onto slides using prolong antifade reagents contain (4',6-diamidino-2-phenylindole) DAPI as counter-staining. Specimens were imaged by a Zeiss LSM710 confocal microscope (Carl Zeiss Micro Imaging) with argon and helium/neon lasers, using a 20x0.8 dry Plan-Apochromat objective with the pinhole diameter set for 1 airy unit. Images acquired by Zen software (Universal Imaging, Göttingen).

2.2.14 Western blotting of SNARE proteins

RAW cells, primary mouse macrophages, SW982 cells, HFLS and rat DRGs lysates were heated for 2 min at 100°C and then vortexed three times, to break down the cell's DNA. Samples were then separated by running on 12% pre-cast Bis-Tris gel at 130 volts using MOPs running buffer (250 mM MOPS, 250 mM Tris, 5 mM EDTA, 0.1% (v/v) SDS), once separated, the proteins were then transferred onto PVDF membrane (0.2 µm) using wet transfer for 4 h at 45 volts [transfer buffer: 25 mM Tris base, 38 mM Glycine, 10% (v/v) Methanol], and then blocked in Tris buffered saline with 0.1% (v/v) Tween 20(TBST) (pH 7.4) containing 5% (w/v) milk (TBSM) for 1h at room temperature. The blocked membrane was incubated with different specific primary antibodies overnight at 4°C. Specifically, mouse macrophage and human synoviocytes samples were incubated with Anti-alpha Tubulin, Anti-SNAP-23 and Anti-VAMP-I/II/III antibodies whereas rDRGs samples were probed with Anti-Syntaxin-1(HPC-1) and Anti-VAMP-1 antibodies. Following overnight incubation the membranes were washed 3x 10 min and incubated with the corresponding secondary antibody Horseradish Peroxidase (HRP) donkey anti-rabbit IgG and/or donkey anti-mouse IgG for 1 h at room temperature, followed by washing 3x 10 min in TBST to remove unbound secondary antibody. The membrane was developed using chemiluminescent substrate reagent and images were taken using G BOX CHEMI HR-16 system (Syngene).

Image J software was used to quantify the intensity of each band on the western blot. The intensity of the intact target SNARE protein was divided by the corresponding internal loading control (i.e. a SNARE which is not cleaved by the toxin in use) to normalize any variation in loading/protein concentration between wells.

2.2.15 Enzyme linked immunosorbent assay (ELISA) of inflammatory cytokines and neuropeptides

2.2.15.1 IL-6 and TNF-α ELISA

Duo set ELISA kits from R&D systems was used to measure the content of mouse or human IL-6 or TNF-α release from the RAW cells and primary mouse peritoneal macrophages (mouse IL-6 and TNF-α) or SW982 and HFLS cells (human IL-6 only). The assay utilizes double-antibody sandwich technology to quantify mouse IL-6 between 15.6 pg/ml and 1000 pg/ml and TNF-α between 31.3 pg/ml and 2000 pg/ml or human IL-6 between 9.38 pg/ml and 600 pg/ml. A 96 well MaxiSorp™ plate was coated with 50 µl of 2.0 µg/ml rat anti-mouse IL-6 capture antibody which was diluted 120 fold from original stock in phosphate-buffered saline (PBS) [137 mM NaCl, 2.5 mM KCl, 8.1 mM Na_2HPO_4, 1.5 mM KH_2PO_4, pH 7.2-7.4] solution or 0.8 µg/ml rat anti-mouse TNF-α capture antibody which was diluted 125 fold from original stock or 2.0 µg/ml mouse anti-human IL-6 capture antibody which was diluted 120 fold from original stock in PBS and incubated at 4°C overnight. The following day, the plate was washed with washing buffer (0.1% (v/v) Tween 20 in PBS, pH 7.2-7.4) 3 times and then incubated with 150 µl of blocking buffer 1% (w/v) BSA in PBS, pH 7.2-7.4) for 2 h at room temperature, followed again by 3 washes. 50 µl of either samples or standards were added and incubated for another 2 h at room temperature. After washing, 50 µl of 50 ng/ml biotinylated goat anti-mouse IL-6, TNF-α or anti-human IL-6 detection antibody which was diluted 60 fold from original stock in blocking buffer and incubated for 2 h at room temperature. The plate was washed as before and incubated with 50 µl of streptavidin conjugated to horseradish-peroxidase for 20 min at room temperature, avoiding light. After washing, 50 µl of substrate solution TMB was added into each well and read absorbance at 650 nm, using a plate reader (BioTek). A standard curve was generated by plotting the reading against know standard concentrations (Figure 2.4-2.6). Then, using the value read by plate reader at OD_{650} the concentrations of the treated samples were extrapolated from the standard curve. A new standard curve was generated for every assay.

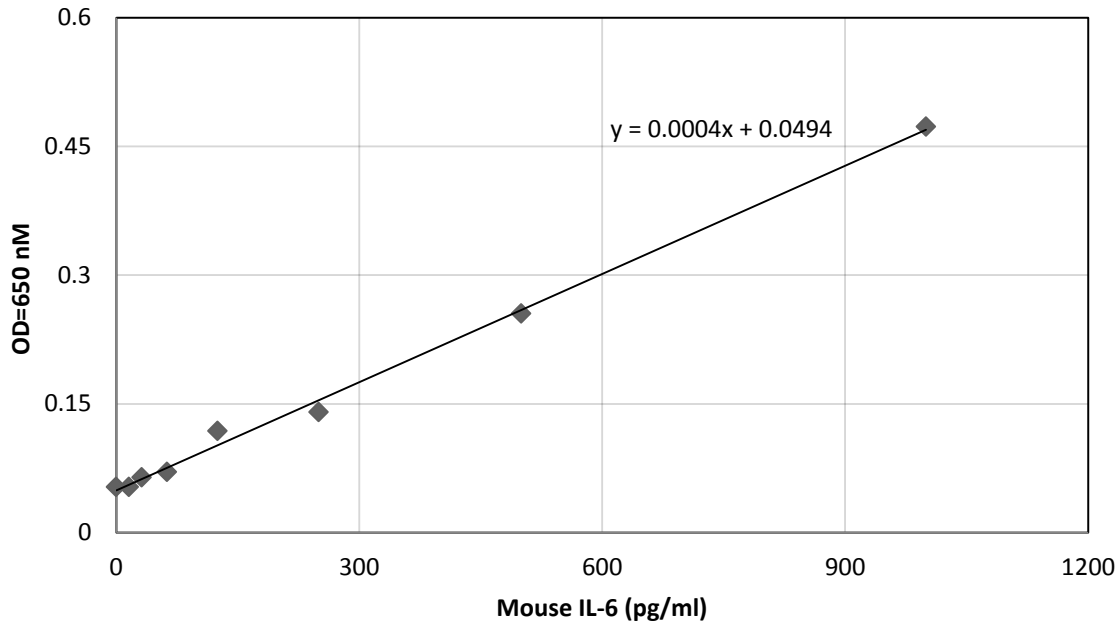

Figure 2.4. Mouse IL-6 standard curve. This figure was graphed in Excel using the linear regression line fit. The OD_{650} from the standards was plotted on the y-axis against their known concentrations on the x-axis. The equation of the line generated by excel is shown on the graph.

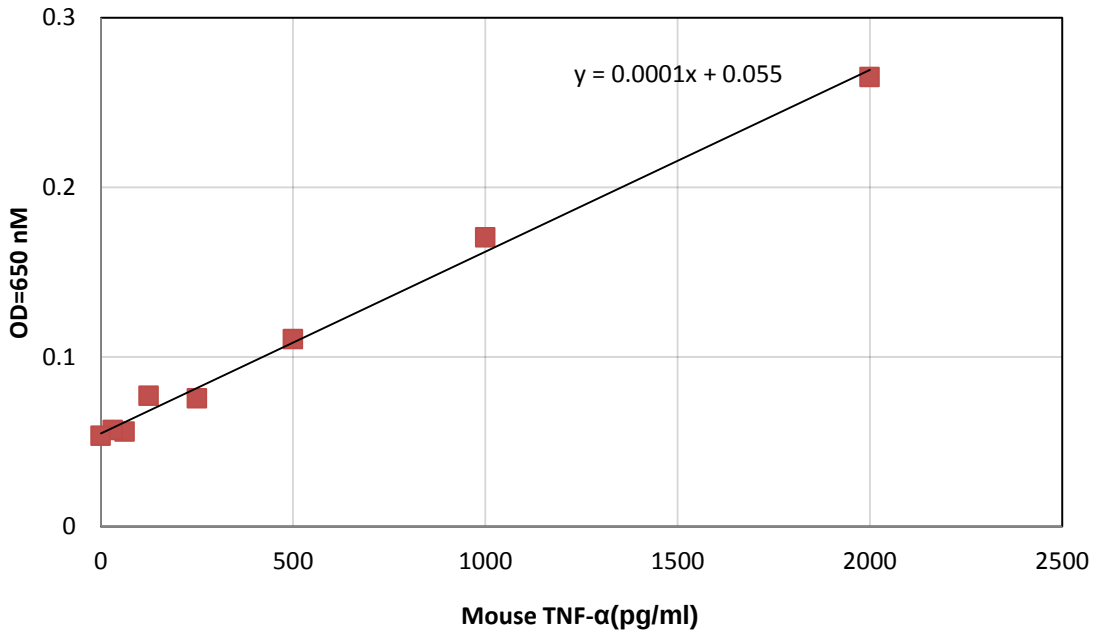

Figure 2.5. Mouse TNF-α standard curve. This figure was graphed in Excel using the linear regression line fit. The OD_{650} from the standards was plotted on the y-axis against their known concentrations on the x-axis. The equation of the line generated by excel is shown on the graph.

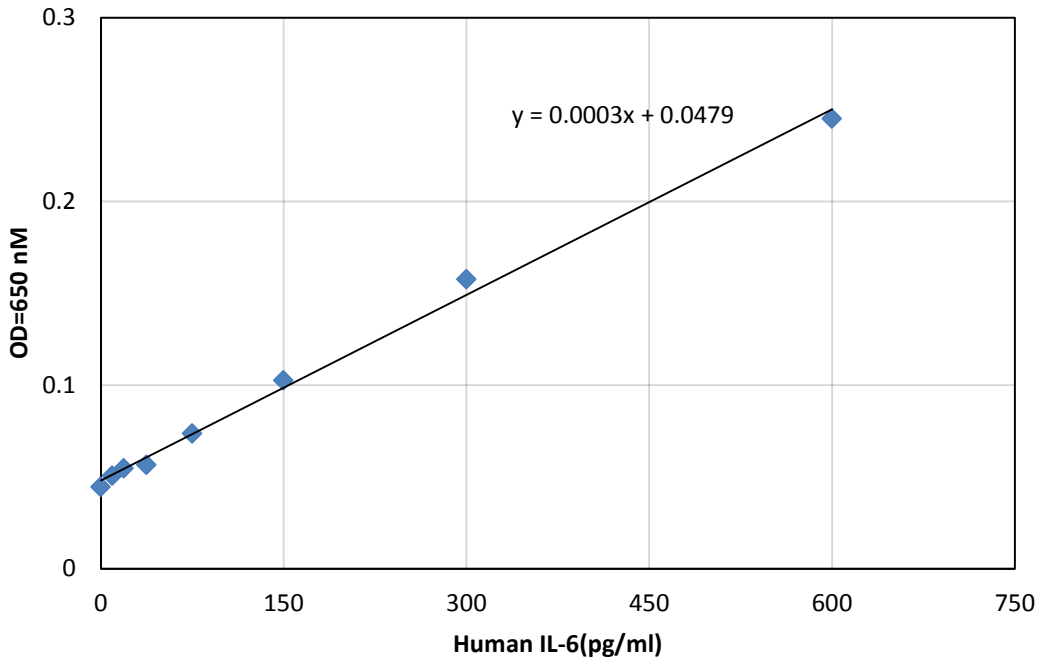

Figure 2.6. Human IL-6 standard curve. This figure was graphed in Excel using the linear regression line fit. The OD_{650} from the standards was plotted on the y-axis against their know concentrations on the x-axis. The equation of the line generated by Excel is shown on the graph.

2.2.15.2 Quantification of substance P

Substance P (SP) EIA kit was used to quantify the amount of SP in treated rDRGs samples. This EIA kit from Cayman chemical is a competition based assay where the plate is coated with a fixed amount of rabbit anti-serum SP binding sites. Treated samples or standards are incubated with a known amount of a SP-conjugate referred to as SP AChE tracer. The absorbance values read directly measure the amount of tracer binding and therefore by keeping the levels of tracer constant the readings are inversely related to the amount of non-conjugated SP binding (Figure 2.7). By generating a standard curve using the assay the concentration of SP in the treated samples can then be quantified.

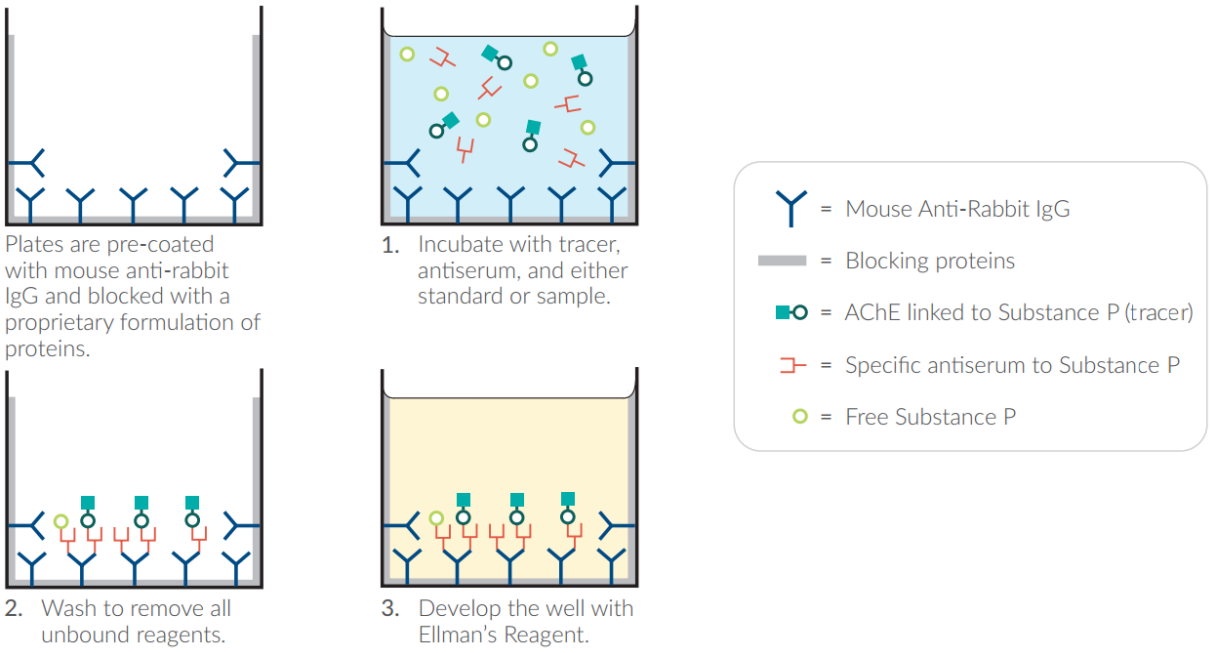

Figure 2.7. Schematic diagram of SP EIA assay (Cayman, 2013).

50 µl of collected samples or prepared SP standards were added into each well, containing pre-coated mouse monoclonal anti-rabbit IgG, followed by 50 µl of SP-tracer and 50µl of the rabbit antiserum-SP and incubated at 4°C overnight. On the following day, the plates were washed with washing buffer 5 times before 200 µl of Ellman's reagent was added into each well and incubated for 90-120 min at room temperature. Finally, the plate's absorbance at 405 nm was read using a plate reader (BioTek). A standard curve of SP was graphed and is displayed in Figure 2.8. The unknown amount of SP in the samples was calculated from the standard curve where % (B/B_0) is the ratio of the OD_{405} of the sample or standards minus non-specific binding (NSB) to the maximum binding minus non-specific binding (NSB). NSB is the absorbance value for the well without any sample or standard and anti-serum. Maximum binding is the absorbance value for the well containing the tracer and anti-serum without any sample or standard. The concentrations of unknown samples were extrapolated from the graphed standard curve using the OD_{405} (y-axis value). A new standard curve was generated for each assay.

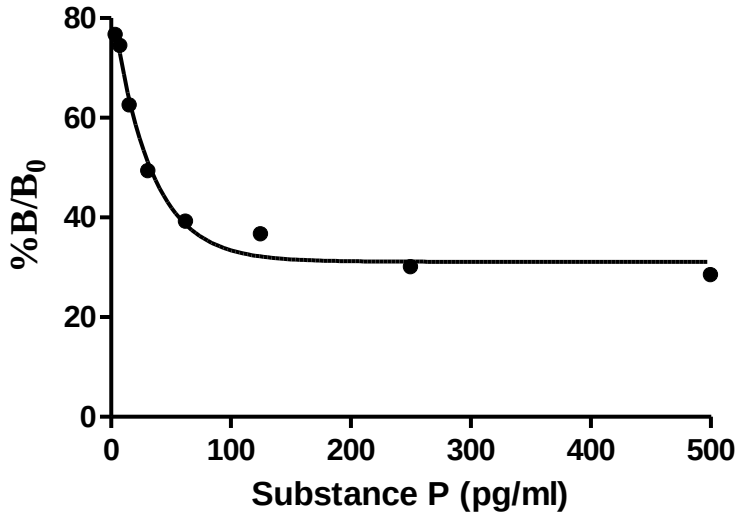

Figure 2.8. SP standard curve. This standard curve was graphed using Prism software 4.0 using nonlinear regression curve fit - two site binding (hyperbola) equation**.** The amount of SP in the unknown samples was calculated from the curve which plots $\%B/B_0$ ($\%OD_{405}$ of standard- non-specific binding (NSB)/ maximum binding - non-specific binding (NSB)) on the y-axis against the known concentrations of SP standards on the x-axis.

2.2.16 Statistical analysis

All raw data were analyzed using Microsoft Excel 2010. Graph Pad Prism 4.0 was used to plot the calculated data points and statistical analysis. The number of independent experiments (n value) represented in a graph is highlighted in the corresponding figure legends. The significance between treatments was evaluated using the student's unpaired t-test.

Chapter 3: Engineering novel SNARE-inactivating therapeutics targeting to IL-1 receptors on the inflammatory cells and sensory neurons for inhibiting the release of cytokines/pain-mediators

3.1 Overview

Cytokines and pain peptides are known to be important mediators in both inflammatory and neuropathic pain, they are both involved in a signaling feed forward loop which leads to persistent activation of both immune cells and sensory neurons. Specifically, inflammatory cells (macrophages) secrete pro-inflammatory cytokines, such as TNF-α and IL-6 while sensory neurons (DRGs) secrete pain peptides such as SP or CGRP, which contribute to chronic pain. Macrophages are also critically involved in the pathogenesis of RA. SW982 cells are introduced as a good model to measure the efficacy of therapeutics on the inhibition of cytokine release (Chang et al., 2014, Boddul et al., 2014). VAMP-3 is necessary for the release of pro-inflammatory cytokines from macrophages whereas VAMP-1 is involved in pain peptide release from sensory neurons. The IL-1 receptor is known to be expressed on macrophages, SW982 cells and DRGs (Li et al., 2005, Wijelath et al., 1997)

3.1.1 Aim and objectives

In this chapter, our aim was to produce a novel therapeutic, which retargeted the SNARE cleaving BoNT/D protease into inflammatory cells and sensory neurons via binding IL-1 receptor. Therefore, we designed a therapeutic by replacing the binding domain of BoNT/D with IL-1β or IL-1RA, using recombinant technology. These constructs, encoding novel BoNT/D based therapeutics were then expressed in *E.coli* and purified by IMAC. The resultant products were investigated for their ability to cleave their target SNARE proteins and attenuate either cytokine or pain peptide release in immune cells or sensory neurons respectively.

3.2 Results

3.2.1 Primary mouse macrophages and rat DRGs express IL-1 receptors

As we expect, after staining with a specific antibody against IL-1 receptor or IL-6, images demonstrated that IL-1 receptors (green) were presented in nearly all cultured primary mouse macrophages (Figure 3.1A) which also expressed pro-inflammatory cytokine IL-6 (red) (Figure 3.1 B). Confocal images showed IL-1 receptor was expressed in the majority of SP positive neurons (Figure 3.1C, D). Thus, we confirmed cultured primary mouse macrophages and rat DRGs express IL-1R.

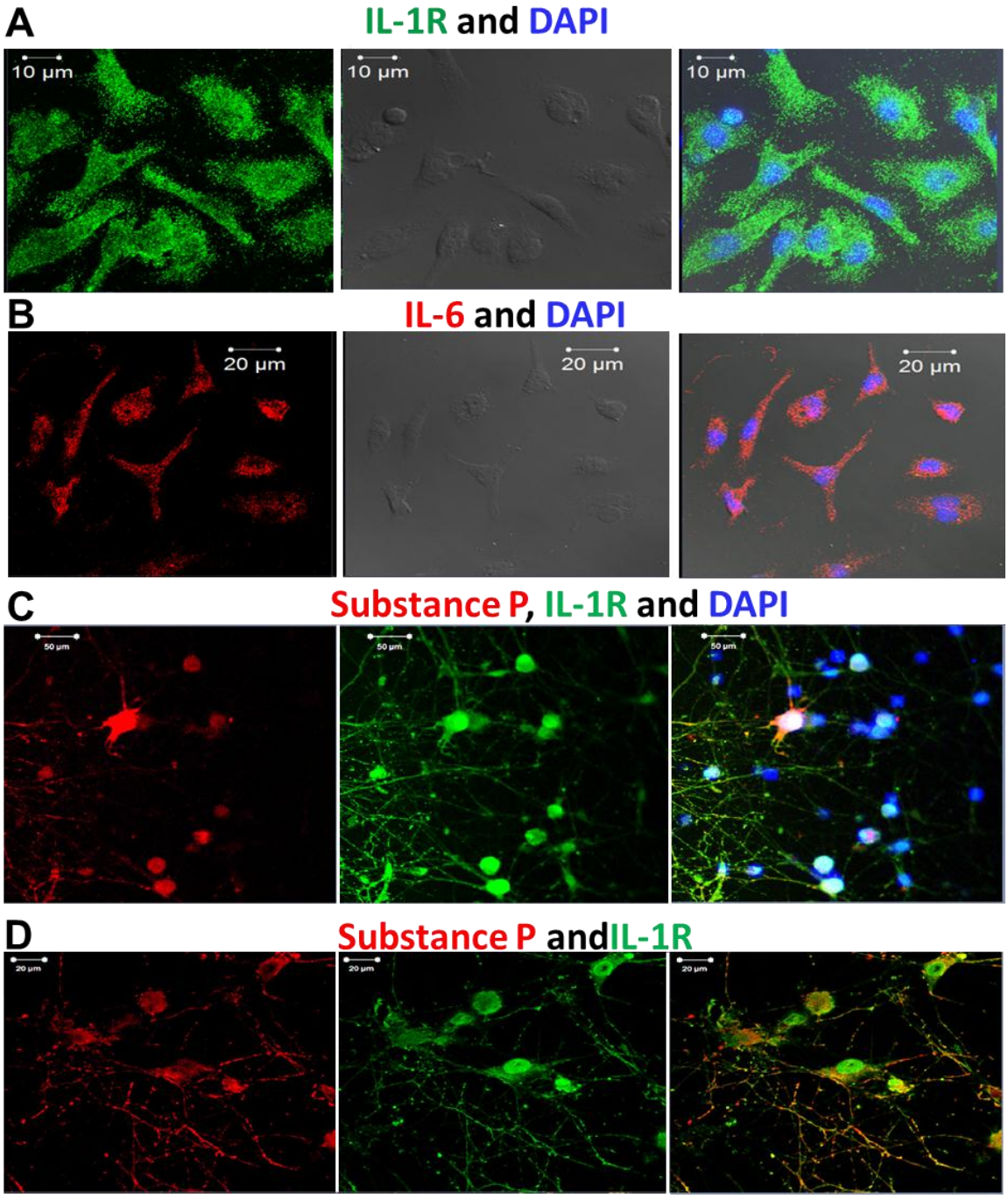

Figure 3.1. Primary mouse macrophages express IL-1R and IL-6, whereas IL-1R was expressed on the majority of SP-positive neurons.

Primary macrophages grown on coverslips for 2 DIV (A, B) and rat DRGs 7 DIV (C) were fixed, permeabilised and then incubated with (A) rabbit anti-IL-1 receptor (1:200), (B) rabbit anti-IL-6 (1:400), or (C, D) rabbit anti-IL-1 receptor (1:500) and mouse anti-SP (1:500) overnight at 4 ºC followed by goat anti-rabbit Alexa Fluor-488 (1:1000) (A), goat

anti-rabbit Alexa Fluor-555 (1:1000) (B), goat anti-mouse Alexa Fluor-555 (1:1000) and anti-rabbit Alexa Fluor-488 (1:1000) (C, D) for 1 h at room temperature. After three washes, samples were mounted in ProLong Gold antifade reagent containing DAPI. Images were captured using a confocal microscope under fluorescent and phase contrast mode. Scale bar as indicated.

3.2.2 Recombinant fusion proteins (/DIL-1β and /DRA) were expressed, purified and nicked to tag less DC forms

Dr. Jiafu Wang has previously engineered a construct encoding recombinant BoNT/D which contains a catalytic domain (LC), a translocation domain (H_N), and a binding domain (H_C), followed by a His_6 tag for purification. Two thrombin sites were also included for simultaneous protein nicking and tag removal (Figure 3.2A). To engineer targeted therapeutics, Dr. Jiafu Wang further designed constructs, encoding /DIL-1β and /DRA, by replacing the Hc gene in BoNT/D with that for IL-1β or IL-1RA targeting ligand (Figure 3.2B and C). Deletion of Hc gene from BoNT/D yielded the construct, encoding the non-targeted control protein BoNT/DΔHc (Figure 3.2D). The positive clones of /DIL-1β, /DRA and BoNT/DΔH_C were identified using the restriction enzyme digestion. As illustrated in Figure 3.2E, restriction digestion with indicated combinations of enzymes confirmed the presence of respective inserts (Figure 3.2F).

Once the construct was further confirmed by DNA sequencing, /DIL-1β, /DRA, and control protein were then expressed in *E. coli* BL21. DE3 strain and purified by IMAC with high purity and reasonable yields (~ 6, 5 and 6 mg/L, respectively). /DIL-1β and /DRA have similar sizes and can be visualised as a band at ~117k (Figure 3.3 A and B). The purified control protein migrated as predicated molecular size (~ 100k) (Figure 3.3C). As purified /DIL-1β, /DRA and /DΔH_C are SC forms, they were then nicked into DCs, by thrombin. The resultant products were confirmed by SDS-PAGE in the presence or absence of DTT. Their LCs were only separated from the H_N or H_N-TL(H_N-targeting ligands) constituents in the presence of DTT confirming that inter-chain di-sulphide bond had been formed (Figure 3.4 A and B). Only the unnicked SCs of /DIL-1β, /DRA and

control protein were recognized by a mouse anti-His_6 antibody, confirming the removal of His_6 by thrombin while nicking (Figure 3.4C-E).

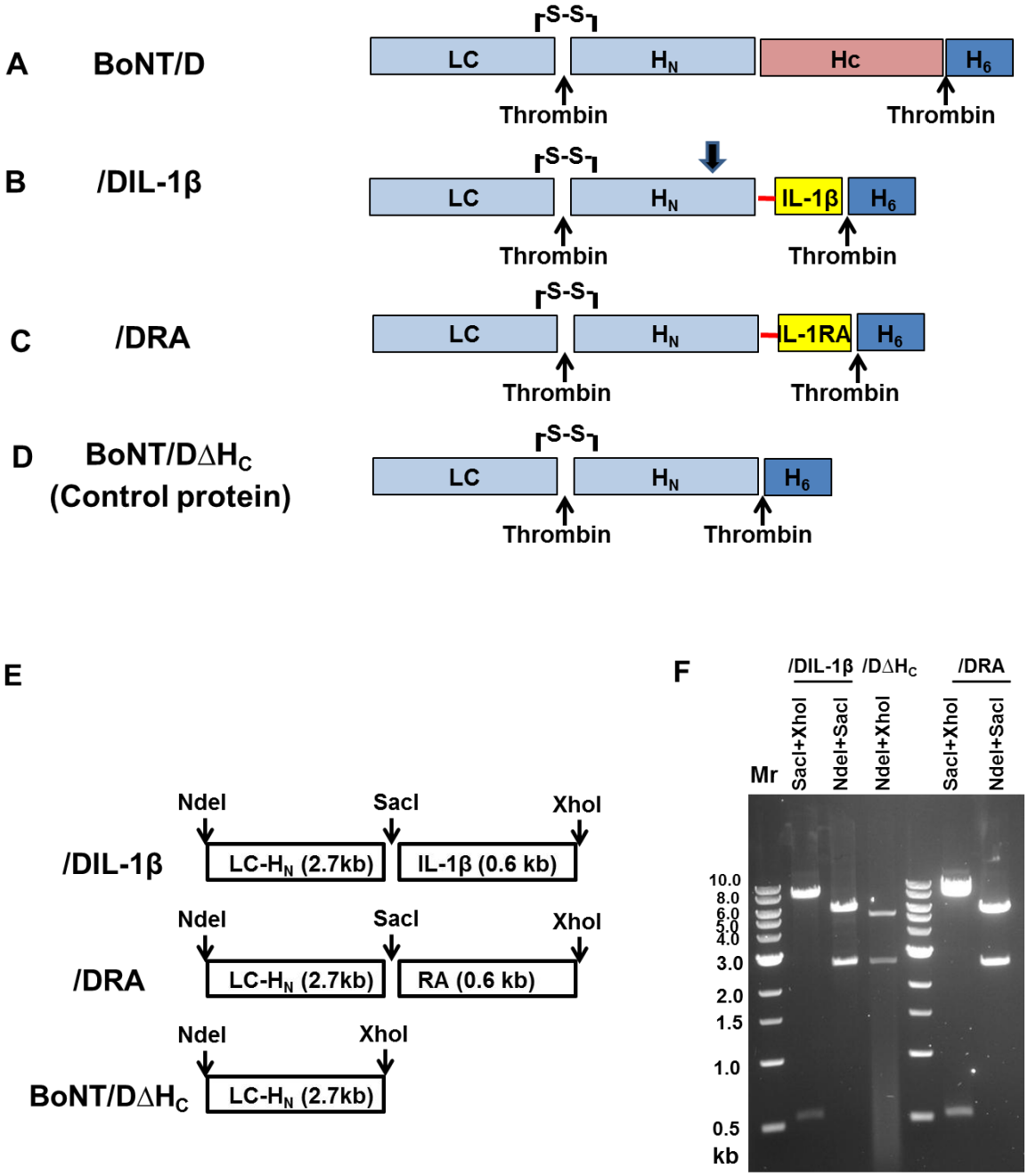

Figure 3.2. Protein engineering BoNT/D based therapeutics.

Substituting the H_C gene in BoNT/D construct **(A)** with either IL-1β or IL-1RA gene

yielded the constructs encoding **(B)** /DIL-1β and **(C)** /DRA. Removing H_C gene in BoNT/D created the construct encoding **(D)** a non-targeted control protein BoNT/DΔH_C. Note that, all these proteins have a His_6 tag and two thrombin sites as indicated. (**E**) Schematic of cloning sites for /DIL-1β, /DRA and /DΔH_C. (**F**) Restriction digestion with indicated enzymes confirmed the presence of inserts with predicated size.

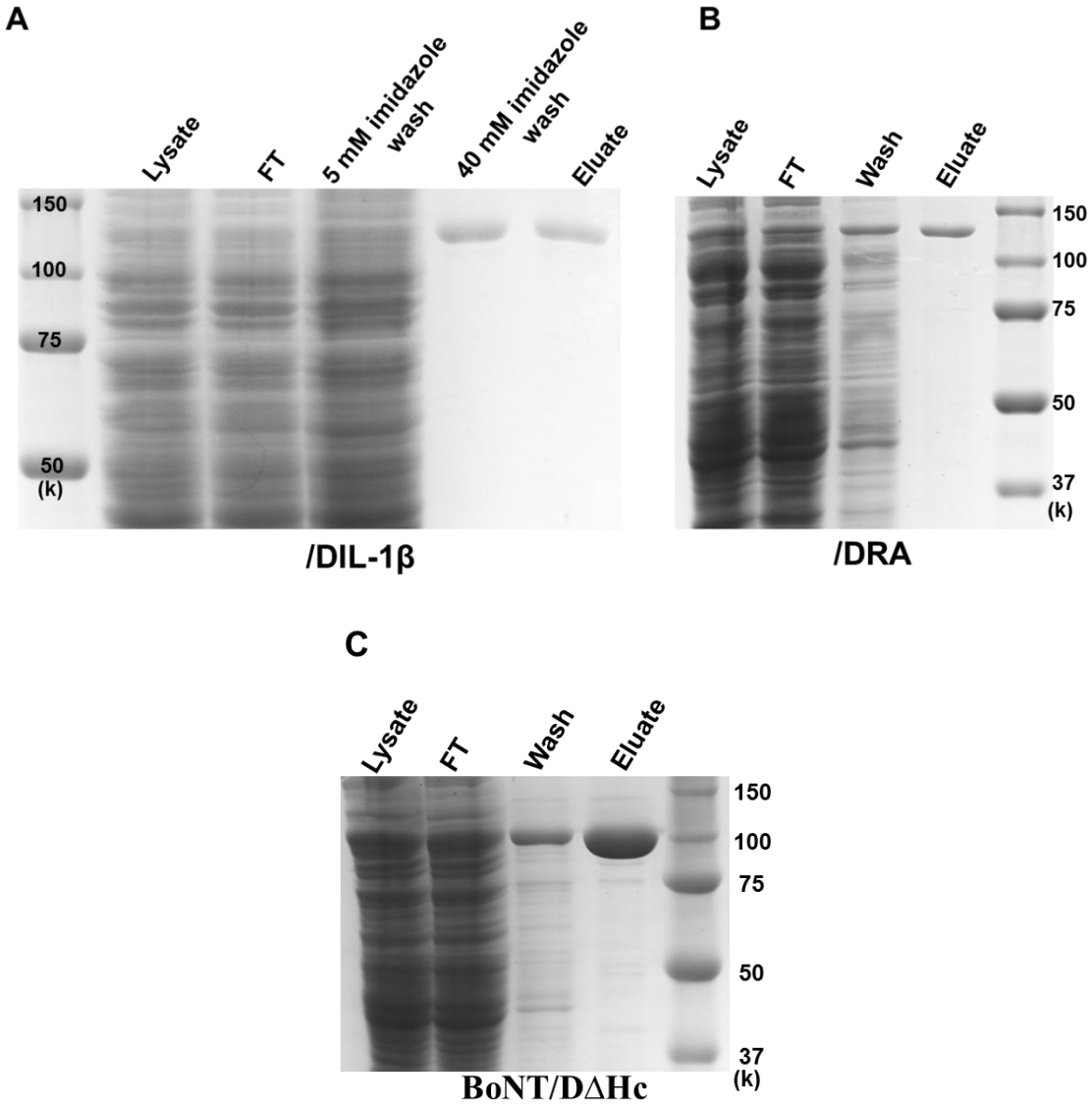

Figure 3.3. IMAC purification of /DIL-1β, /DRA and control BoNT/DΔHc proteins. /DIL-1β (A), /DRA (B) and BoNT/DΔH_C (C) were expressed in *E.coli* and purified by IMAC. Samples were taken at various stages of the process and analyzed by running a 10% hand-made Tris-glycine SDS-PAGE gel, followed by Coomassie staining, FT: flow through.

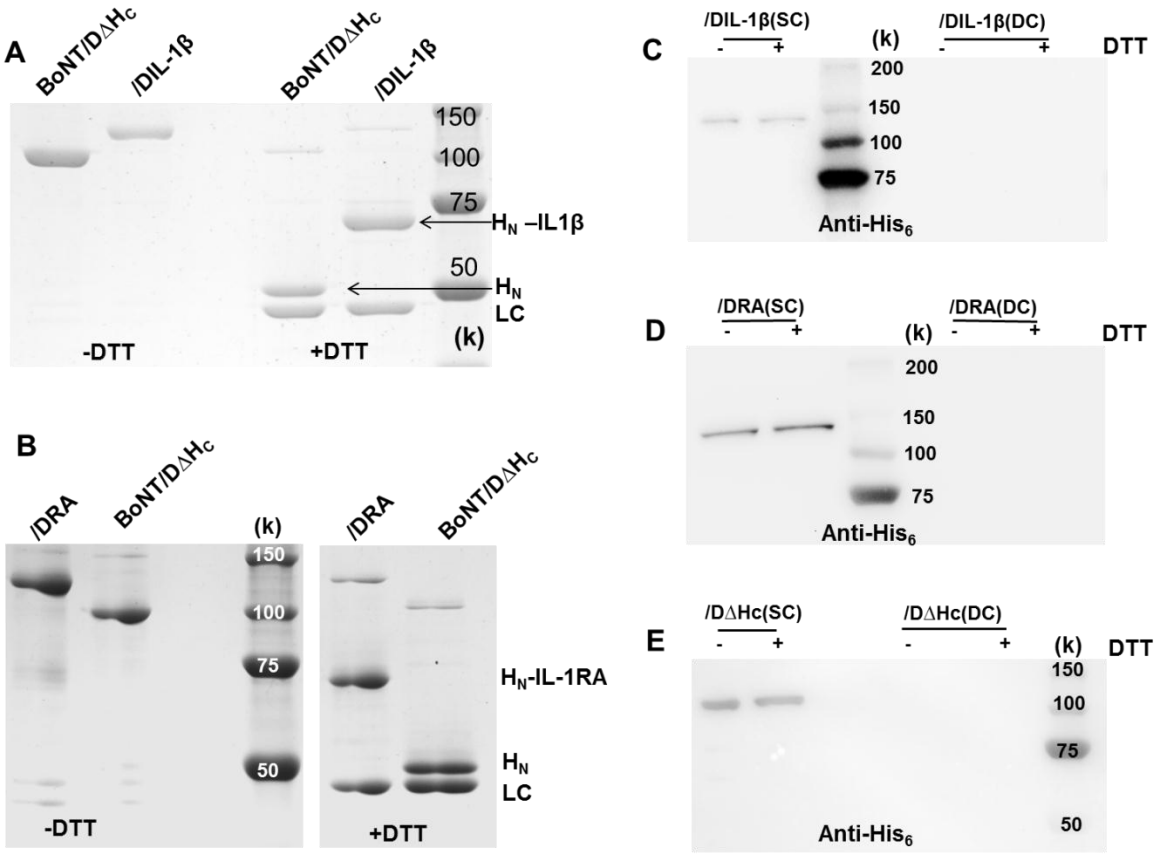

Figure 3.4. Thrombin nicked /DIL-1β, /DRA and control protein to DC forms with simultaneous removal of His_6 tag.

A-B. Thrombin nicked /DIL-1β, /DRA and control protein were analyzed, with and without dithiothreitol (DTT) (50 mM), using 10% SDS-PAGE followed by Coomassie staining. Nicked and non-nicked /DIL-1β (C), /DRA (D) and control protein BoNT/DΔH_C (E) were subjected to SDS-PAGE followed by Western blotting with a mouse anti-His_6 antibody.

3.2.3 Recombinant /DIL-1β, /DRA and BoNT/DΔH_C retained the proteolytic activity of BoNT/D and /DIL-1β showed comparable proliferation activity as commercial IL-1β

The protease activities of /DIL-1β, /DRA and BoNT/DΔH_C were measured in *vitro* using a

recombinant substrate, GFP-VAMP$_{(2-94)}$-His$_6$. /DIL-1β, /DRA and BoNT/DΔH$_C$ exhibited similar levels of GFP-VAMP$_{(2-94)}$-His$_6$ substrate cleavage (Figure 3.5). Thus, inserting the desired targeting ligands into BoNT/DΔH$_C$ construct did not affect the proteolytic activity of its LC in *vitro*.

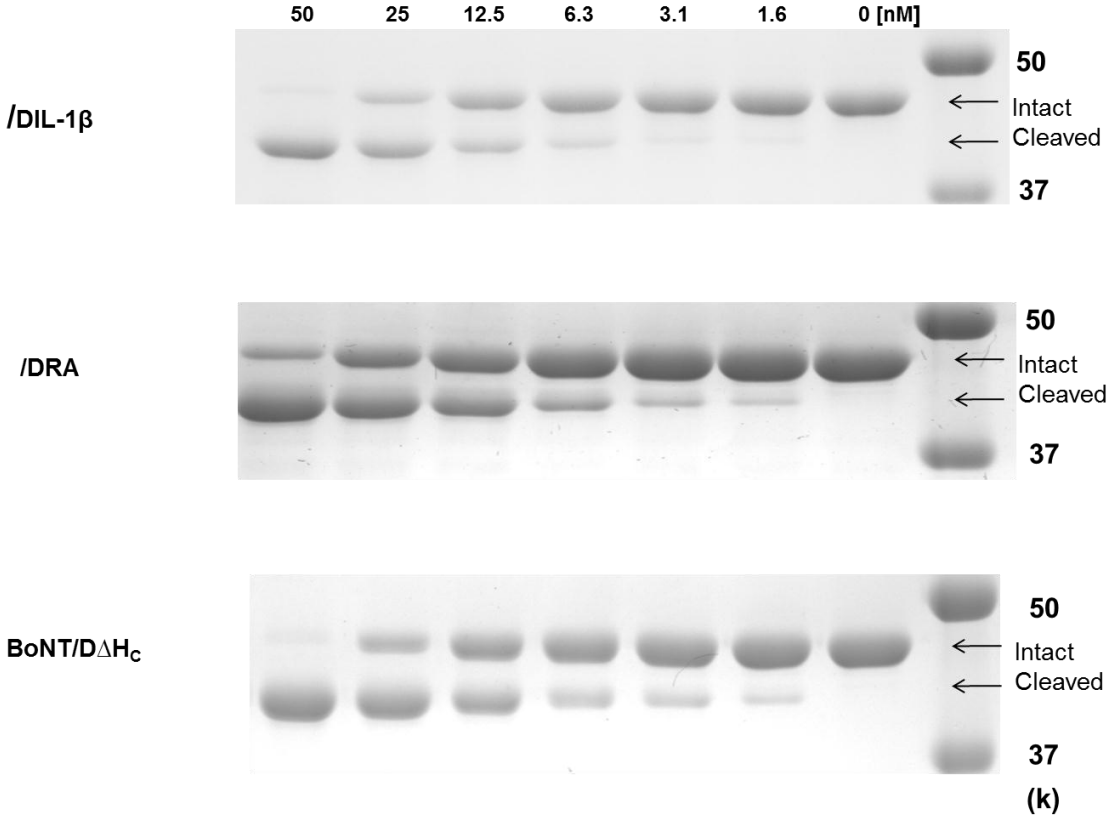

Figure 3.5. *In vitro* protease activity assay for /DIL-1β, /DRA and /DΔH$_C$.
/DIL-1β, /DRA and BoNT/DΔH$_C$ were diluted to 50 nM in protease assay buffer containing 5 mM DTT and incubated at 37ºC for 30 min to activate the protease domain. They were then serially diluted to 1.6 nM in assay buffer and mixed with equal volume of 1 mg/ml of GFP-VAMP$_{(2-94)}$-His$_6$ substrate for additional 30 min at 37ºC. Samples were resolved on 12% hand-made Tris-glycine SDS-PAGE gels and stained by Coomassie blue.

It was also important to confirm that recombinantly expressed /DIL-1β retains the desired bio-activity of its ligand. Therefore, to assess this bioactivity we compared its effects on cell proliferation with commercial human IL-1β in macrophage cells. The results confirmed that the recombinant IL-1β was active and only displayed a decrease of ~40%

compared to the commercial human IL-1β (Figure 3.6A and B). /DRA and the control protein did not show any effect on cell proliferation, as expected (Figure 3.6B). In conclusion, IL-1β targeting ligand in /DIL-1β retained its anticipated bio-activity after being recombinantly fused to BoNT/DΔH_C protein.

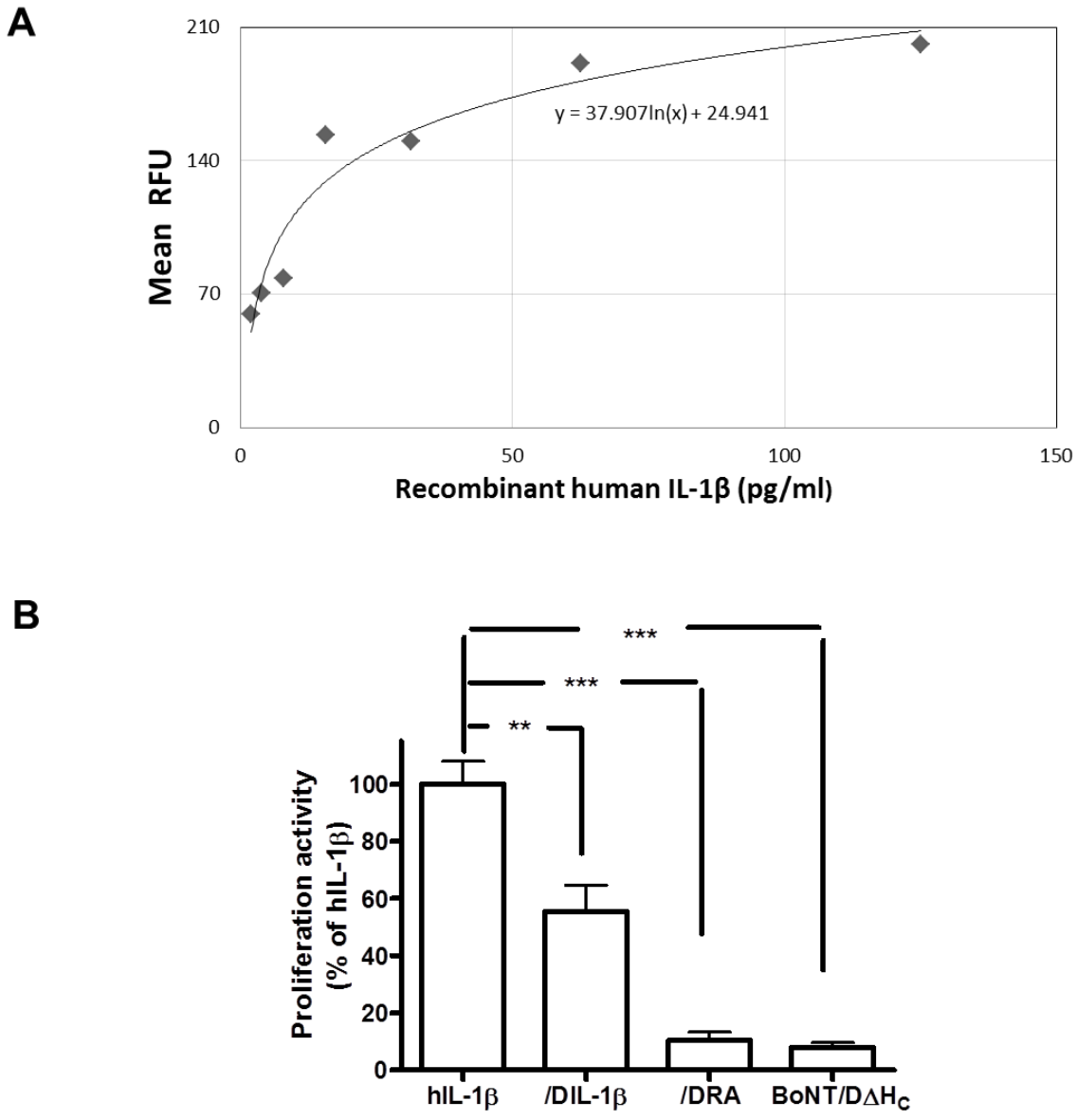

Figure 3.6. Effects of recombinant proteins on cell proliferation.

A. Standard curve showing dose dependent effects of commercial human IL-1β (R&D) on

cell proliferation. RAW 264.7 cells were treated with IL-1β for 48 h and the % of cell proliferation quantified by measuring newly synthesized DNA during cell division using Click-iT® EdU microplate assay kit (Invitrogen). This standard curve was generated in Excel using nonlinear regression curve fit. The generated line equation used for calculating the test sample activity is shown on the graph.

B. RAW cells were treated with serial dilutions of /DIL-1β, /DRA or /DΔH_C and cell proliferation quantified using kit as above. Using the equation from the standard curve **(A)** the values obtained for /DIL-1β, /DRA or /DΔH_C treated cells were converted to the corresponding commercial IL-1β concentration. Finally, the percentage of bio-activity of the test proteins was calculated using the formula: concentration calculated from commercial IL-1β standards/original treated concentration. Data plotted are mean ±S.E.M. (n=3). Students unpaired T-test was chosen for statistical analysis **: $P<0.01$ and ***: $P<0.001$.

3.2.4 Murine RAW 264.7 cells contain SNARE proteins VAMP-3 and SNAP-23 and secrete pro-inflammatory cytokines upon stimulation

To confirm the murine RAW 264.7 cell line was a suitable model for our study we firstly investigated whether the cells expressed BoNT/D protease substrates, SNARE proteins. We also investigated the release of pro-inflammatory cytokines upon stimulation. Raw cells were incubated with serum free DMEM medium for 6 h before stimulation with IFNγ (500 pg/ml) and LPS (100 ng/ml) in DMEM medium for 42 h. Western blotting confirmed that the RAW cells did in fact express SNARE proteins, specifically SNAP-23 and VAMP-3 (Figure 3.7A). VAMP-3 has been reported to play a key role in the release of pro-inflammatory cytokines from immune cells. After 42 h stimulation, the secretion of TNF-α and IL-6 were significantly increased compared to non-stimulated controls (Figure 3.7 B-C).

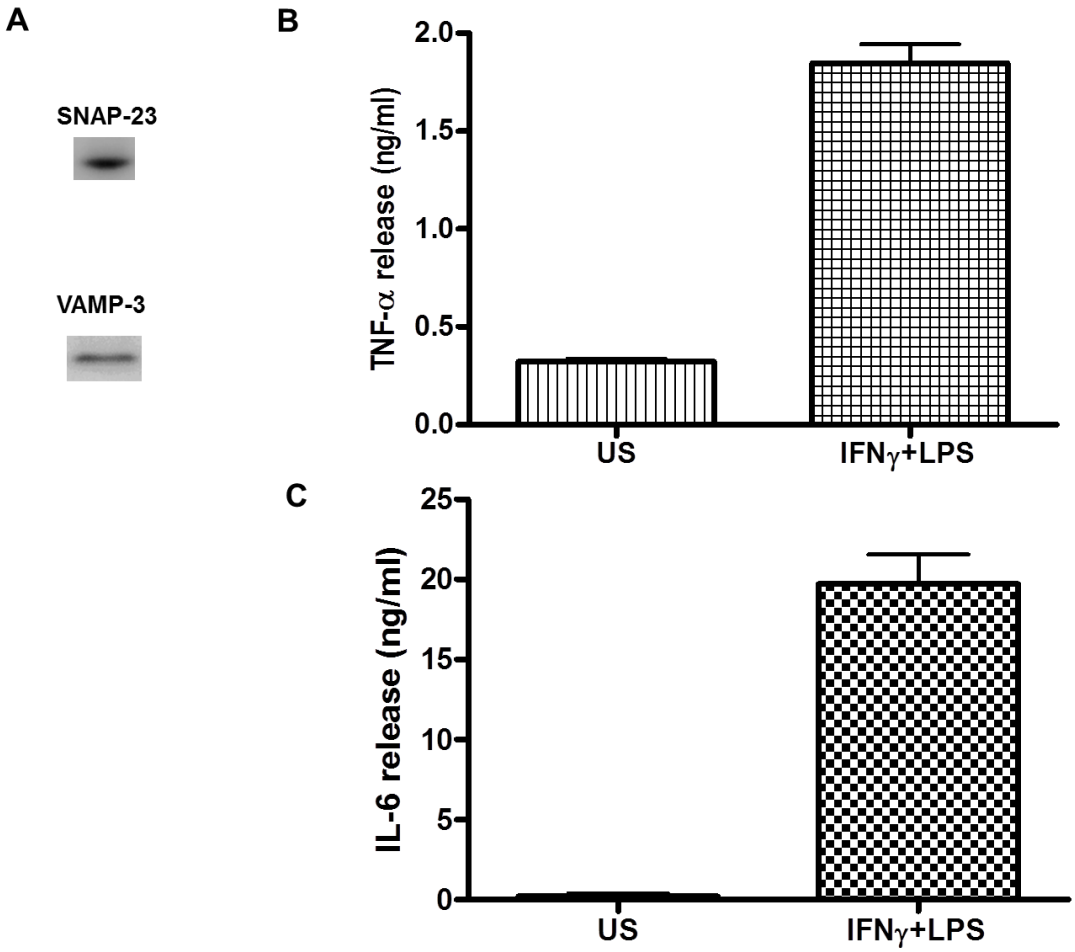

Figure 3.7. Evaluation of SNARE protein expression and stimulated cytokine release in RAW 264.7 cells.

A. Cultured raw cells were lysed in 70 µl of 2×LDS sample buffer and analysed by Western blotting with anti-SNAP-23 and anti-VAMP-3 antibodies. **(B, C) M**acrophages were cultured in DMEM for 6 h before stimulation with or without IFNγ (500 pg/ml) and LPS (100 ng/ml) for 42 h. TNF-α (B) and IL-6 (C) content in stimulated or unstimulated (US) cells were quantified by ELISA. Data plotted in panel B and C are mean ± S.E.M. (n=3).

3.2.5 /DIL-1β and /DRA entered into cultured mouse macrophage cells, cleaved VAMP-3 and attenuated evoked TNF-α and IL-6 release

To investigate the ability of the targeted therapeutic to be taken up by RAW cells and cleave its target substrate VAMP-3 the cells were treated with varying concentrations of /DIL-1β or /DRA for 6 h and stimulated with IFNγ (500 pg/ml) and LPS (100 ng/ml) for 42 h before harvesting. Analysis by Western blotting displayed dose dependent cleavage of VAMP-3 from 6.3 nM to 50 nM of both therapeutics (Figure 3.8A), with approximately 70% of VAMP-3 cleaved by the highest concentration (Figure 3.8B). In contrast, the control protein treated samples only showed ~20% cleavage at 50 nM (Figure 3.8B).There was no significant difference between either /DIL-1β or /DRA confirming both targeting ligands bind to the IL-1 receptor and become internalised with similar capabilities.

After ELISA analysis, IFNγ and LPS-evoked TNF-α and IL-6 release was attenuated dose dependently and especially in high concentration, approximate 80% of IL-6 and 65% of TNF-α release were inhibited (Figure 3.9 B and C). There is only ~25% inhibition of IL-6 release and no inhibition of TNF-α release after treatment with 50 nM of the control protein (Figure 3.9 B and C), thus, confirming the targeted uptake of /DIL-1β and /DRA by RAW cells.

Results from the cell viability assay on macrophages also showed /DIL-1β and /DRA did not affect RAW cells viability. It was demonstrated the inhibition of TNF-α and IL-6 release were not caused by cell death (Figure 3.10).

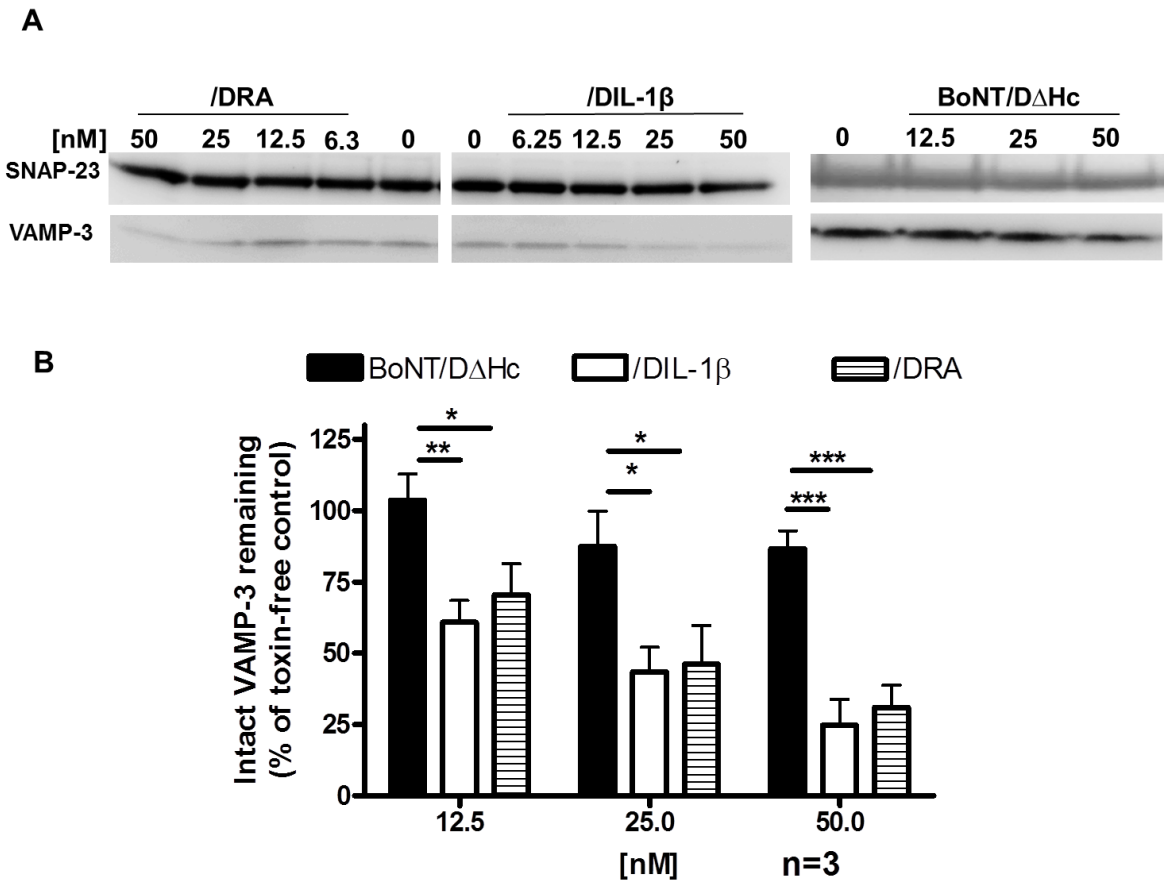

Figure 3.8. The differential effects of /DIL-1β, /DRA or control protein on the cleavage of VAMP-3.

A. RAW 264.7 cells were incubated with various doses of /DIL-1β, /DRA or BoNT/DΔH_C for 6 h. Toxins were then removed and cells were cultured in medium with LPS (100 ng/ml) and IFNγ (500 pg/ml) for 42 h. The cells were then harvested and probed for VAMP-3 cleavage via Western blotting. SNAP-23 was blotted as an internal loading control. **B.** The intensity of VAMP-3 was divided by the corresponding internal loading control (SNAP-23) to normalize any variation in loading/protein concentration between wells. VAMP-3 remaining after treatment with toxin was calculated by expressing the above ratio as a % of the toxin free control sample. Data plotted in panel B is mean ± S.E.M. (n=3). Statistical analysis was carried out using the Students unpaired T-test *: $P<0.05$, **: $P<0.01$ and ***: $P<0.001$.

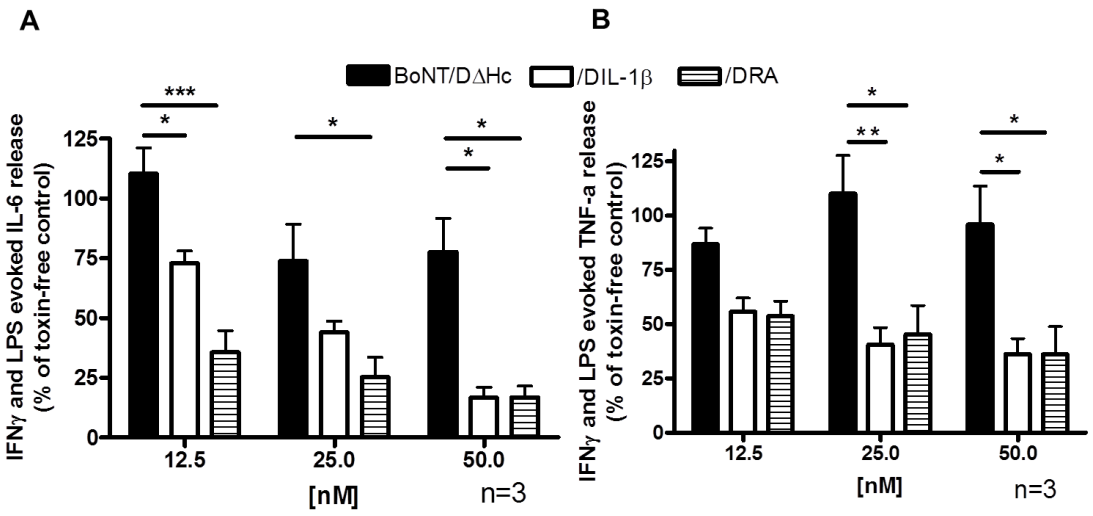

Figure 3.9. Effects of therapeutics on inhibition of IL-6 and TNF-α release from mouse macrophages.

A-B. Murine macrophages were incubated with various dose of /DIL-1β, /DRA or BoNT/DΔH_C for 6 h. After removal of toxin, cells were further cultured in DMEM with IFNγ (500 pg/ml) and LPS (100 ng/ml) for 42 h. IL-6 (A) and TNF-α (B) release in the supernatant were measured using the relevant ELISA kits. Data plotted in panel **A-B** are mean ±S.E.M. (n=3). Statistical analysis was carried out using the Students unpaired T-test *: $P<0.05$, **: $P<0.01$ and ***: $P<0.001$.

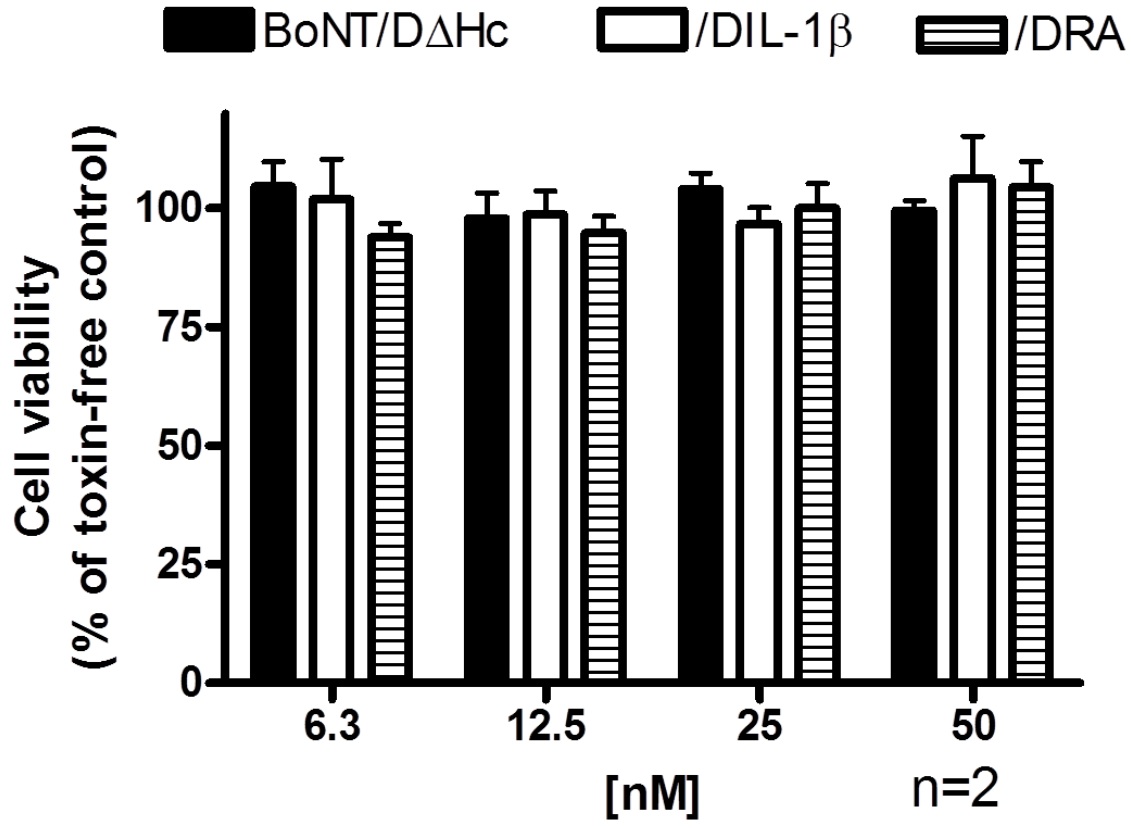

Figure 3.10. Effect of therapeutics (/DIL-1β and /DRA) on RAW cells viability.
RAW cells were incubated with a various doses of /DIL-1β, /DRA and control protein BoNT/DΔ$H_C$for 44 h, followed by 4 h incubation with alamar blue contained culture medium, avoiding light, before reading at absorbance 570 nm by plate reader. Cell viability was quantified by expressing the above ratio as a % of the toxin free control samples. Data graphed is mean ± S.E.M. (n=2).

3.2.6 Cultured primary mouse peritoneal macrophages contain SNARE proteins VAMP-3 and SNAP-23 and release TNF-α and IL-6 after stimulation

Similarly, cultured primary mouse peritoneal macrophages have been confirmed that they did in fact express SNARE proteins, specifically SNAP-23 and VAMP-3 (Figure 3.11A). After 42 h stimulation, TNF-α and IL-6 were increased significantly, compared to non-

stimulated control cells (Figure 3.11B and C).

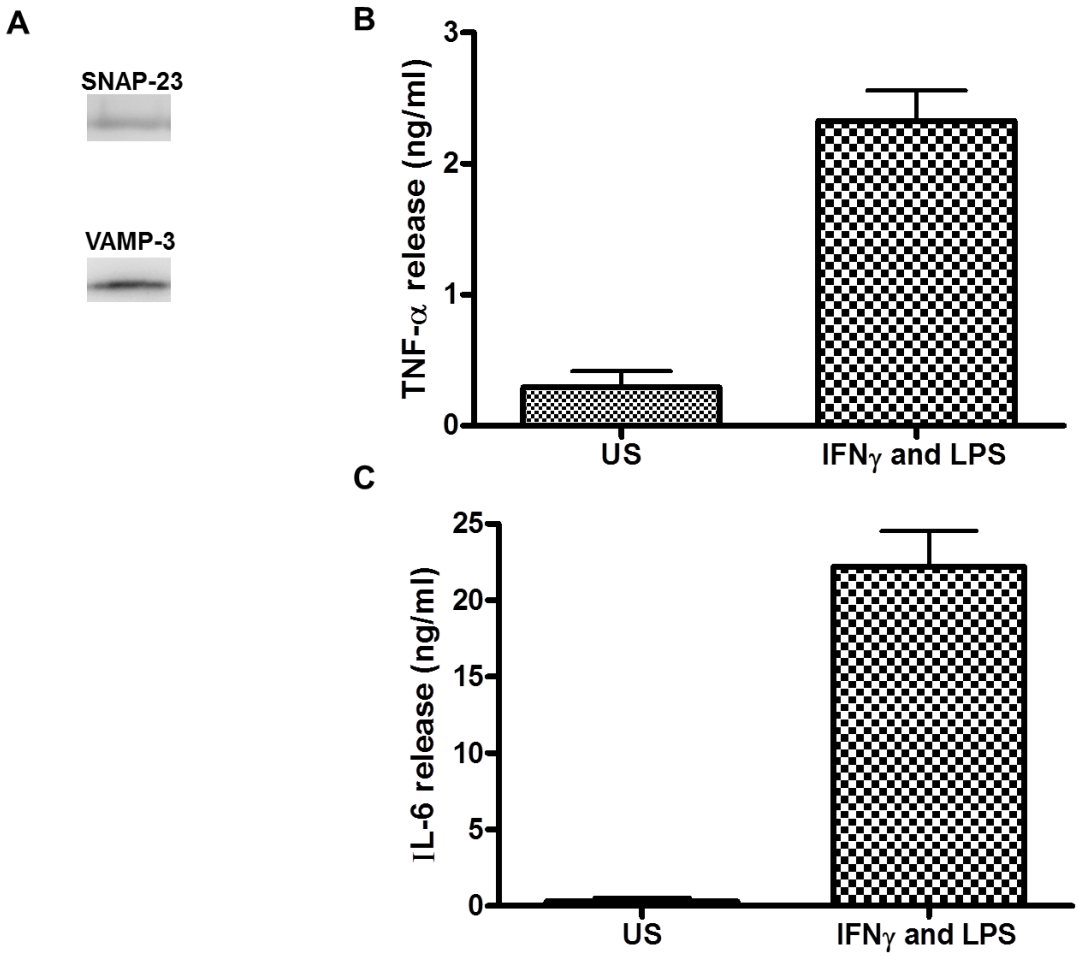

Figure 3.11. Investigation of SNARE protein expression and stimulated cytokine release in primary macrophages.

A. Cultured primary macrophages were lysed in LDS sample buffer and analysed by Western blotting with anti-SNAP-23 and VAMP-3 antibodies. TNF-α (**B)** and IL-6 (**C**) content in IFNγ (500 pg/ml) & LPS (100 ng/ml) stimulated or unstimulated (US) cells for 42 h were quantified by ELISA. Data plotted in panel **B -C** are mean ±S.E.M. (n=3).

3.2.7 Targeted delivery of BoNT/D protease into cultured primary mouse macrophages via binding to IL-1 receptor, cleaved VAMP-3 and inhibited evoked TNF-α and IL-6 release

RAW264.7 is an altered mouse macrophage cell line. As a cell line, it may display the characteristics of heterogeneity. Therefore, the results obtained from RAW cells may not represent the function of macrophages *in vivo*. Herein, we cultured primary mouse peritoneal macrophages and then exactly the same experiment carried on RAW cells was done on these primary mouse macrophages, followed by western blotting and mouse TNF-α and IL-6 ELISA analysis. After western blotting analysis, blots exhibited VAMP-3 was cleaved at ≥ 12.5 nM of both therapeutics (Figure 3.12A and B). Similarly, results from ELISA analysis also displayed reduction of IFNγ and LPS-evoked IL-6 and TNF-α release. Approximate 50% of IL-6 and TNF-α release were attenuated by treatment with 25 nM of /DIL-1β and /DRA (Figure 3.13 A and B). BoNT/DΔH_C was significantly less effective in inhibiting these two cytokine release than targeted therapeutics. Therefore, double confirming the targeted delivery of /DIL-1β and /DRA into mouse macrophages.

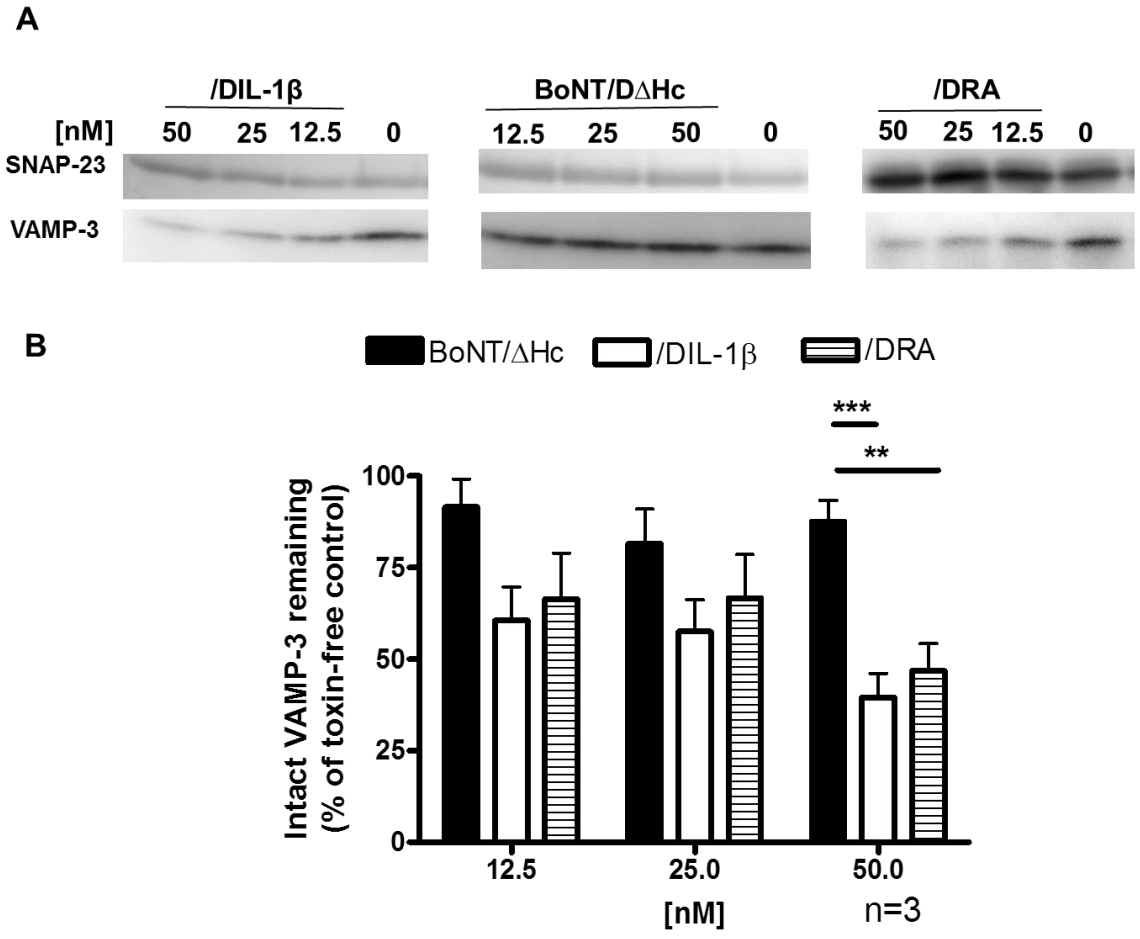

Figure 3.12. /DIL-1β, /DRA or control protein on the cleaving ability of VAMP-3.

A. Various doses of /DIL-1β, /DRA or BoNT/DΔH_C were treated into primary mouse peritoneal macrophages for 6 h, followed by stimulation with IFNγ (500 pg/ml) and LPS (100 ng/ml) for 42 h. The cells were then lysed in 70 µl LDS buffer and analysed by Western blotting to probe VAMP-3 cleavage. SNAP-23 was detected as an internal loading control. **B**. The amount of VAMP-3 remaining relative to the SNAP-23 internal loading control was calculated by expressing the above ratio as a % of the toxin free control cells. Data plotted in panel B is mean ± S.E.M. (n=3). Statistical analysis was carried out using the Students unpaired T-test **: P<0.01 and ***: P<0.001.

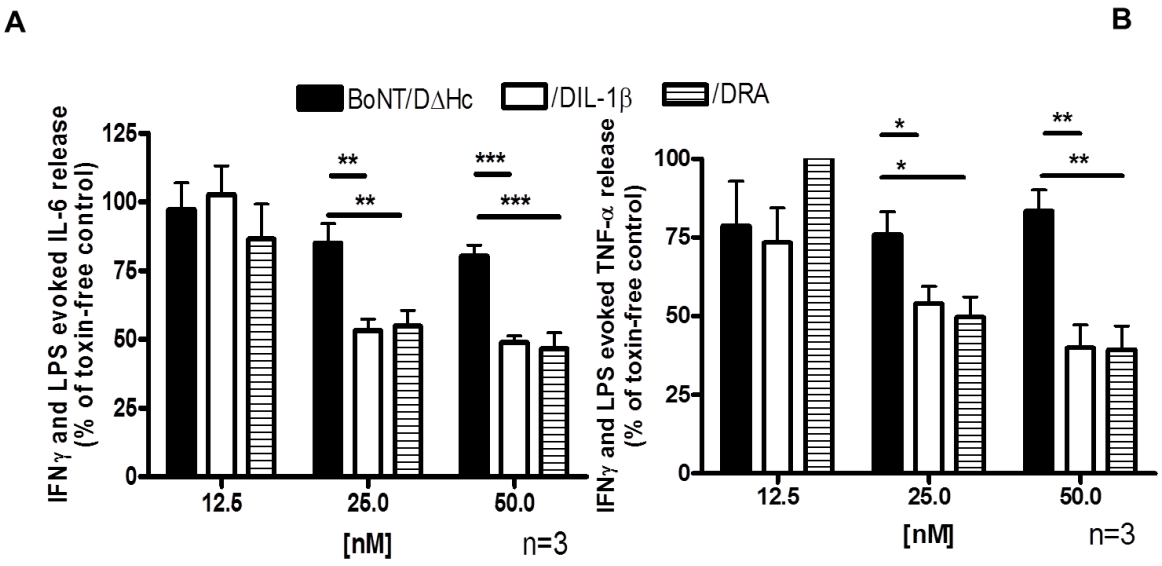

Figure 3.13. The ability of therapeutics on attenuating IL-6 and TNF-α release from mouse primary macrophages.

After 6 h treatment with recombinant protein, cells were stimulated with IFNγ (500 pg/ml) and LPS (100 ng/ml) in medium for another 42 h. Then collected supernatants were used to measure evoked IL-6 (**A)** and TNF-α **(B**) release using the relevant ELISA kits. Data plotted are mean ±S.E.M. (n=3). Students unpaired T-test was chosen for statistical analysis *: P<0.05, **: P<0.01 and ***: P<0.001.

3.2.8 SNARE proteins, VAMP-3 and SNAP-23 were expressed in SW982 cells which secrete IL-6 in response to IL-1β

Similarly, we also investigated SNARE protein expression in SW982 cells and the secretion of IL-6 from them upon stimulation. SW982 cells were cultured with serum free completed RPMI 1640 medium for 44 h and stimulated with IL-1β (25 ng/ml) for 4 h. Western blotting confirms that they did in fact express SNARE proteins, SNAP-23 and VAMP-3 (Figure 3.14A). After 4 h stimulation, IL-6 level in the supernatant was raised up significantly, compared to non-stimulated control cells (Figure 3.14 B). The secretion of TNF-α was analyzed by ELISA as well. However, upon stimulation with IL-1β (25 ng/ml), only a tiny amount of TNF-α release can be detected from SW982 cells.

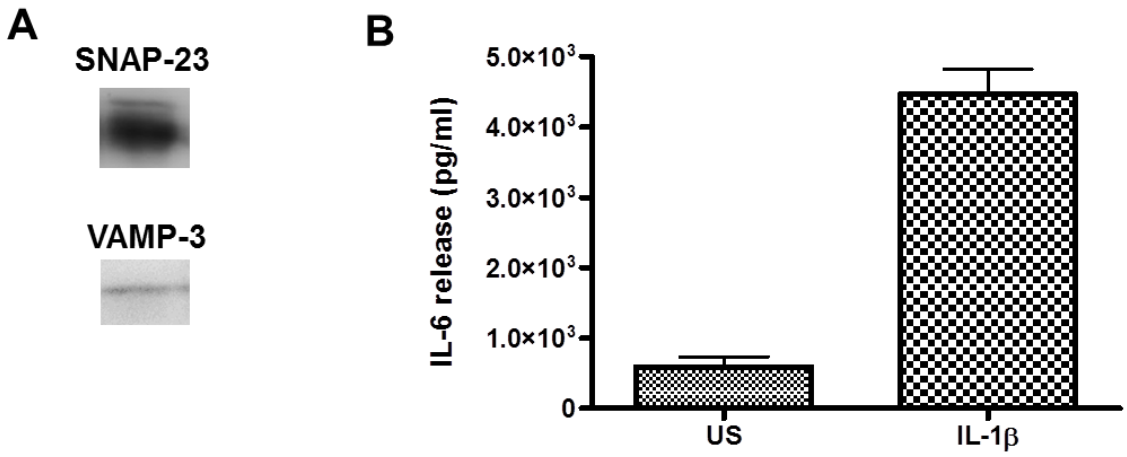

Figure 3.14. Confirmation of SNARE protein expression and IL-6 release from SW982.

A. Cultured SW982 were lysed in 70 ul 2×LDS sample buffer and analysed by Western blotting with anti-SNAP-23 and VAMP-3 antibodies. (B) IL-6 content in IL-1β (25 ng/ml) stimulated or unstimulated (US) cells were quantified by ELISA. Data plotted are mean ±S.E.M. (n=3).

3.2.9 /DRA entered into SW982 cells via binding to IL-1 receptor, cleaved VAMP-3 and inhibited evoked IL-6 release

SW982 cells are a suitable model to study RA (Chang et al., 2014) and express IL-1 receptor. Our colleagues have also confirmed VAMP-3 contributes to IL-6 release (Boddul et al., 2014). Thus, I studied the ability of /DRA to enter into SW982 cells and cleave its target substrate VAMP-3. The cells were incubated with varying concentrations of /DRA for 44 h and then stimulated with IL-1β (25 ng/ml) for 4 h before harvesting. After analyzing by Western blotting, western blots showed significant cleavage of VAMP-3 especially at higher concentration (100 nM of /DRA (Figure 3.14A), with approximately 45% of VAMP-3 cleaved (Figure 3.14B). In contrast, no cleavage was observed in the control protein treated samples (Figure 3.14 A and B).

After ELISA analysis, IL-1β-evoked IL-6 release was inhibited dramatically by /DRA at 50 nM or higher, approximate 70% of IL-6 release was attenuated (Figure 3.14 C). There is only ~25% inhibition of IL-6 release after treatment with the control protein at the highest concentration (Figure 3.14 C), thus, confirming the preferential uptake of /DRA by SW982 cells.

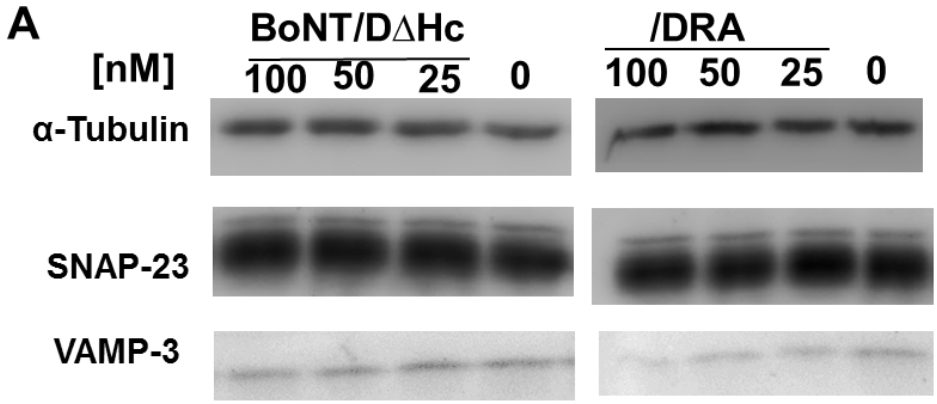
A
BoNT/DΔHc
/DRA
[nM]
100 50 25 0
100 50 25 0
α-Tubulin
SNAP-23
VAMP-3

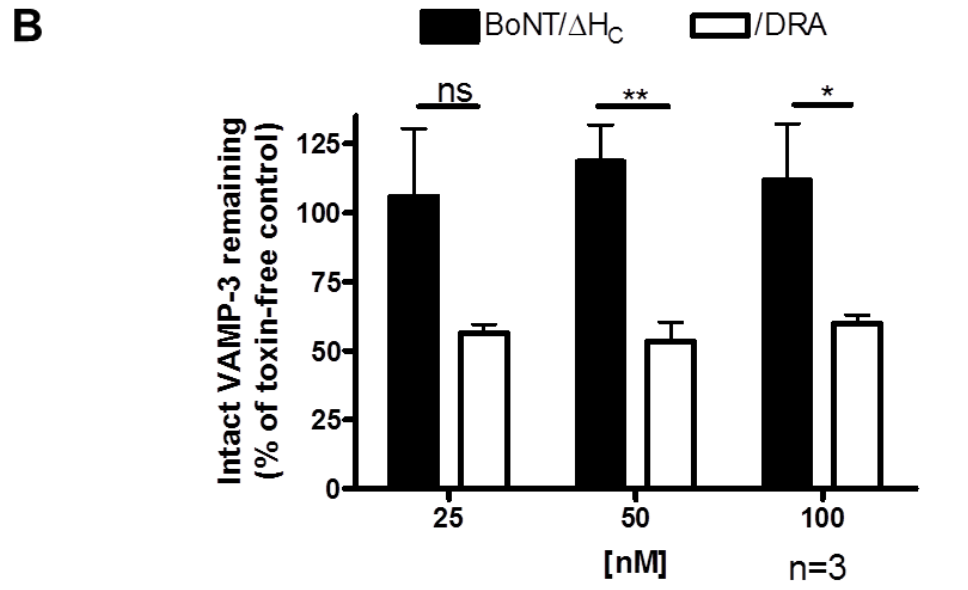
B
BoNT/ΔHC
/DRA
ns
**
*
Intact VAMP-3 remaining
(% of toxin-free control)
125
100
75
50
25
0
25
50
100
[nM]
n=3

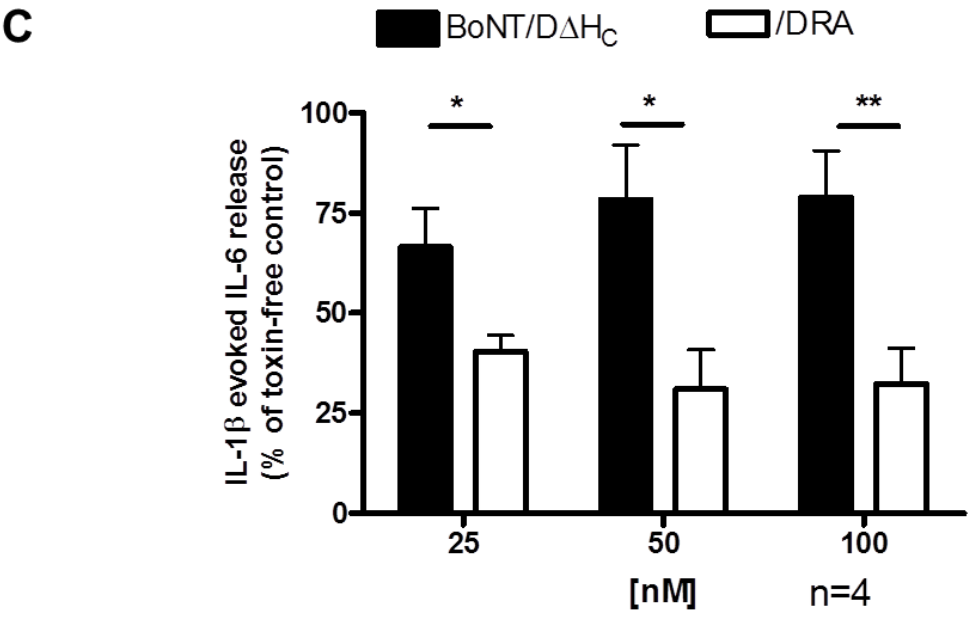
C
BoNT/DΔHC
/DRA
*
*
**
IL-1β evoked IL-6 release
(% of toxin-free control)
100
75
50
25
0
25
50
100
[nM]
n=4

Figure 3.15. /DRA was uptaken by SW982 cells resulting in cleavage of VAMP-3, and inhibition of IL-1β stimulated IL-6 release.

A. SW982 cell were incubated with /DRA for 44 h and stimulated with IL-1β (25 ng/ml) for 4 h. Harvested cells were analyzed by westen blotting to detect VAMP-3. SNAP-23 and α-Tublin were probed as loading controls. **B**. VAMP-3 remaining after treating with /DRA was calculated by expressing the ratio (intensity of VAMP-3 / the corresponding internal loading control (SANP-23)) as a % of the toxin free control sample. **C.** Stimulated IL-6 release was quantified by ELISA and plotted as % of the toxin free stimulated sample. Data plotted in panel (**B-C)** are mean ±S.E.M. (n indicated). Statistical analysis was carried out using the Students unpaired T-test, ns: non-significant, *: $P<0.05$, and **: $P<0.01$.

3.2.10 IL-1β and IL-1RA ligands re-targeted BoNT/D protease into rDRGs to cleave VAMP-1 and inhibit SP release

The IL-1 receptor is known to be expressed by DRGs. Therefore, cultured rDRGs (Figure 3.16) were incubated with 50 or 100 nM of /DIL-1β or /DRA for 24 h (Results from 24 h and 48 h incubation were no difference between each other.) to assess the ability of the therapeutics to enter rDRGs and cleave their target substrate VAMP-1, hopefully resulting in inhibition of SP release. Before harvesting, treated rDRGs were stimulated with 60 mM KCl for 30 min. Western blotting results showed both /DIL-1β and /DRA cleaved VAMP-1especially at 100 nM, however no significant cleavage was observed in control protein treated rDRGs (Figure 3.17A and B). After stimulation with high KCl, the amount of SP release from untreated rDRGs control cells was 4 fold higher than the basal condition (Figure 3.18A). Due to the ability of /DIL-1β and /DRA to cleave VAMP-1, potassium evoked SP release was attenuated, especially by 100 nM; about 40% - 50% of SP was blocked (Figure 3.18B). Non-ligand control protein failed to inhibit the SP release. These results confirmed IL-1β and IL-1RA can direct BoNT/D protease into rDRGs.

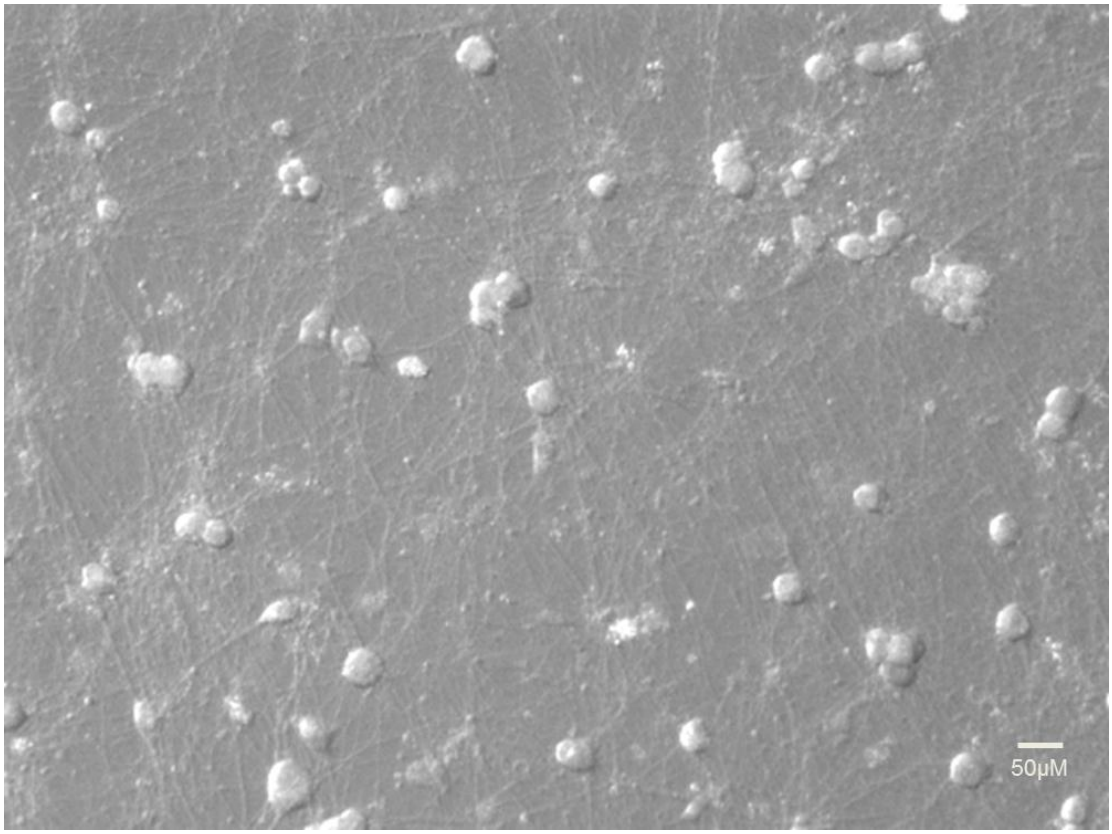

Figure 3.16. The morphology of cultured rat DRGs at day 9 *in vitro*.

The picture was taken by an inverted Olympus IX71 microscope in phase contrast mode Scale bar, 50 μm.

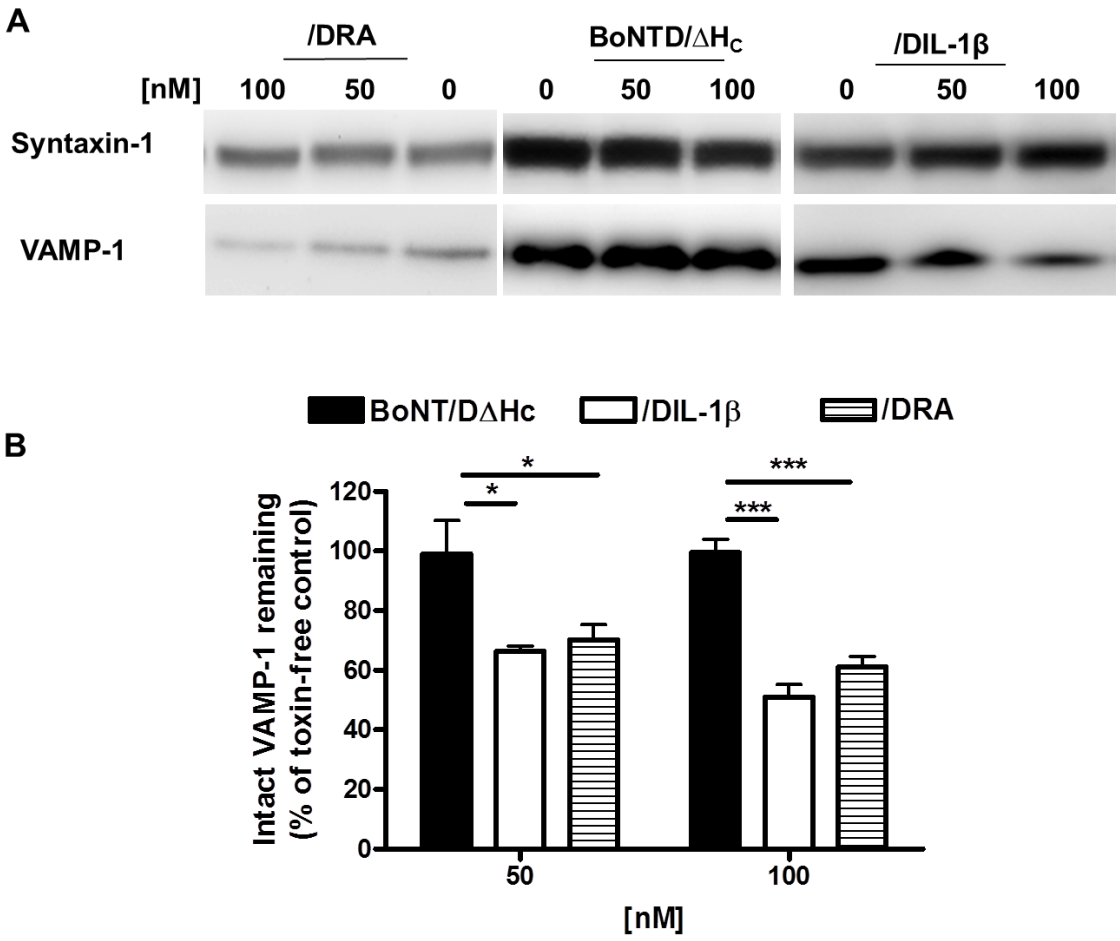

Figure 3.17. /DIL-1β and /DRA entered rDRGs and cleaved VAMP-1, unlike control protein.

A. rDRGs were treated for 24 h, stimulated with either high or low potassium and the cells harvested for Western blotting to detect VAMP-1 and Syntaxin-1, the latter probed as a loading control. **B.** VAMP-1 remaining after incubating with 50 nM or 100 nM of either biotherapeutic was calculated by expressing the ratio (intensity of VAMP-1 / the corresponding internal loading control (Syntaxin-1)) as a % of the toxin free control sample. Data plotted in panel **B.** is mean ±S.E.M. (n=3). Statistical analysis was carried out using the Students unpaired T-test *: $P<0.05$, and ***: $P<0.001$.

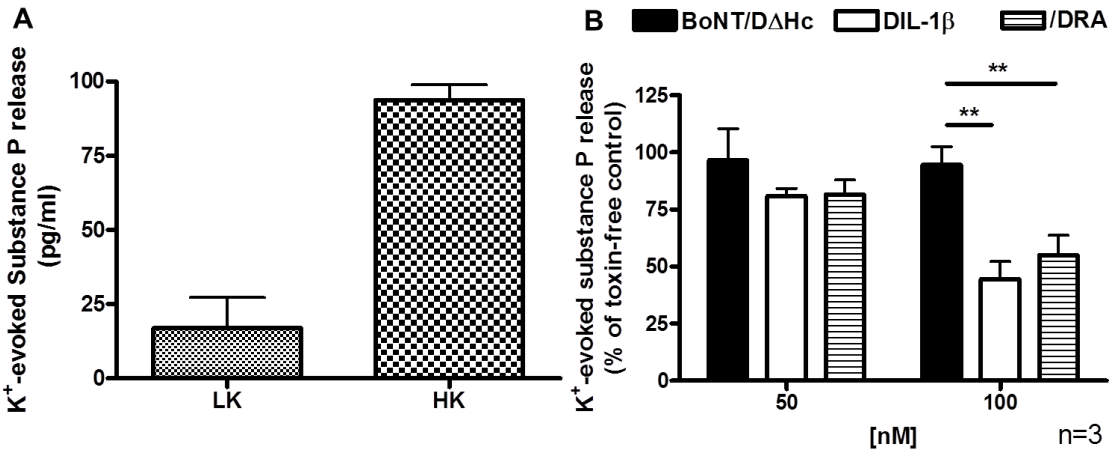

Figure 3.18. The inhibition of SP release by targeted therapeutics in DRGs.

A. Evoked SP release from rDRGs after 30 min of either low k^+ (3.5 mM) (LK) or high k^+ (60 mM) (HK) was quantified using an ELISA kit. **B**. SP release was quantified after 24 h treatment followed by stimulation. % of potassium (K^+) evoked SP release was calculated by setting the toxin free stimulated sample as 100%. Data plotted in panel **A.** and **B.** are mean ±S.E.M. (n=3). Statistical analysis was carried out using the Students unpaired T-test **: $P<0.01$.

3.3 Discussion

Chronic pain is currently a major medical challenge in need of new improved therapeutics. The increased release of pro-inflammatory cytokines and pain peptides contribute to inflammation and pain. Thus, by blocking the release of pro-inflammatory cytokines and/or pain peptides release we may be able to successfully treat chronic pain. During this research project, new dual targeting therapeutics, based on botulinum neurotoxin combined with potential targeting ligands (IL-1β and IL-1RA), with potential as anti-inflammatory and/or anti-nociceptive agents were successfully designed and created. The results presented in this chapter demonstrate that /DIL-1β and /DRA can enter non-neuronal cells (mouse macrophages) and neurons (DRGs) via the targeting ligands IL-1β or IL-1RA and effectively cleave VAMP-3 and VAMP-1, respectively, resulting in attenuation of pro-

inflammatory cytokines (TNF-α and IL-6) and pain peptide (SP) release. This result confirms the potential of these proteins as therapeutics to treat chronic pain.

Native BoNT/D is a potent neurotoxin, which cleaves VAMPs resulting in inhibition of transmitter release from neurons via binding to synaptic vesicle protein 2 (SV2) receptor. However, the SV2 receptor is predominately expressed on neurons and neuronal cells. Researchers have previously tried to use different strategies to replace either the full or minimal binding moiety of BoNTs' binding domain with a potential targeting ligand in the attempt to re-target BoNTs' protease to a variety of receptors on sensory neurons or some secretory cells, hopefully reducing its associated toxicity. For instance, Chaddock *et al* choose NGF as a potential targeting ligand to engineer and produce a novel protein named NGF-LC-H_N/A which can enter PC12 cells by binding to tropomyosin receptor kinase A (TrkA), cleave SNAP-25 and attenuate [^{3}H]-NA release (Chaddock et al., 2000). Duggan *et al* coupled an *Erythrina cristagalli* lectin, which can recognize and bind to carbohydrates, to LC-H_N/A to form LC-H_N/A-ECL conjugates. The latter conjugates bind to carbohydrates involved in galactose to enter into cultured embryonic DRGs to cleave SNAP-25 and attenuate substance P release (Duggan et al., 2002). Ma *et al* reports using the recombinant fusion strategy for the successful production of a therapeutic named LC-H_N-H_{CN}/A-MH7C, by fusing an antibody (MH7C) to BoNT/AΔH_{CC} core-therapeutic domains (Ma et al., 2014). They firstly generated the targeting ligand-MH7C which is a single chain antibody recognizing the $P2X_3$ receptor on the surface of sensory neurons using a phage display strategy. This antibody was then fused to BoNT/AΔH_{CC} by recombinant technology to generate LC-H_N-H_{CN}/A-MH7C. A similar study by Yeh *et al* also reported two new retargeted BoNT/B based therapeutics; BoNT/B or BoNT/BΔHc mixed with an anti-BoNT/B antibody (Yeh et al., 2011). They reported the delivery of these BoNT/B protease containing complexes into primary human blood monocyte-derived macrophages and murine RAW 264.7 cell line and their ability to attenuate TNF-α release, indicating their potential for treatment of chronic inflammation. Their strategy utilizes the interaction between the Fc fragment of antibody and complement receptor-mediated endocytosis pathway in the above-mentioned cells.

As we know, Il-1β and IL-1RA are an IL-1 receptor agonist and antagonist, respectively. The IL-1 receptor is also known to be expressed on both macrophages and DRGs. In this project, we directly use the recombinant strategy to successfully engineer and produce BoNT/DΔ$H_C$protease based therapeutics (/DIL-1β and /DRA) by recombinantly replacing the H_C domain of BoNT/D with IL-1β or IL-1R. Therefore, the resultant therapeutics are dual targeting as they can enter into both immune cells (macrophages) and sensory neurons (DRGs) and therefore present greater potential to control chronic inflammatory pain.

/DIL-1β and /DRA have several advantages over current biotherapeutics due to their recombinant nature, which is much simpler making the production much easier. They can be produced with high yield and purity using this highly reproducible method which is extremely cost effective. We normally can obtain ~ 20 mg therapeutics with ~ 90% purity from 4 L expression. If these proteins were to become potential therapeutics for the treatment of chronic pain in the future, our method/strategy also provides the benefit of large scale production.

TNF-α and IL-6 are two main types of pro-inflammatory cytokines and secreted from immune cells such as macrophages and mast cells. They play an important role in the pathophysiology of chronic inflammatory pain. In contrast to these inflammatory cytokines, their inhibitors (anti-TNF-α and anti-IL-6) block transduction of signalling pathways for inflammatory response, resulting in controlling inflammation and pain. A class of anti-TNF-α (TNF-α inhibitors) drugs such as adalimumab, etanercept, golimumab, and infliximab were studied by Maxwell *et al*. They found clinical symptoms of ankylosing spondylitis are in remission after treating with these anti-TNF agents (Maxwell et al., 2015). Similarly, Kremer *et al* reported an IL-6 inhibitor based therapeutic - tocilizumab improves clinical symptoms in the treatment of rheumatoid arthritis (RA) from Phase III clinical trials (Kremer et al., 2011). Except TNF-α and IL-6, SP is also involved in pain transmission (Besson, 1999). It is secreted from primary sensory neurons located at the peripheral nerves **(**O'Connell et al. 2004). Following peripheral inflammation, the release of SP is increased to induce inflammatory and neuropathic pain. Therefore, blocking the release of SP may contribute to anti-inflammatory and the treatment of chronic pain. For

example, in Li *et al*'s study, their results show Dragon's blood (DB) which is a traditional Chinese medicine can control inflammation and relief pain symptoms by inhibiting the secretion of SP (Li et al., 2012).

Our results show /DIL-1β and /DRA dose dependent inhibition of IL-6 and TNF-α release from macrophage cells which correlated with the cleavage of VAMP-3. The efficacy of /DIL-1β and /DRA may be 1.5-2 folds lower than BoNT/BΔH_C + αB (anti-BoNT/B); however they have the advantage of being able to attenuate not only TNF-α release but also IL-6 release. In addition, they can also enter into DRGs to cleave VAMP-1 and reduce SP neuropeptide release. These further showed promising potential as a treatment for chronic inflammatory pain.

Chapter 4: Targeting TNF-α receptor for delivery of botulinum neurotoxin protease into sensory neurons and inflammatory cells to normalize the exocytosis of pain-transmitters for pain relief

4.1 Overview

To this day, administration of monoclonal antibodies against TNF-α or its receptor has proved beneficial in clinical therapy of patients with chronic pain such as Rheumatoid arthritis (RA) (McInnes and Schett, 2011, Feldmann, 2002). In 2011, Tang, Liu et al. also reported Atsttrin which is a TNF receptor (TNFR) antagonist exhibited selective TNFR binding ability and Atsttrin alone is more efficacious in preclinical models of inflammatory arthritis than currently available clinical therapies (Tang et al., 2011). It is known that TNFR is expressed in immune cells, HFLS cells and neurons (Shao et al., 2005, Idriss and Naismith, 2000, Meng et al., 2016).

4.1.1 Aim and objectives

Herein, we decided to choose TNFR as a specific target and atsttrin as a targeting ligand for selective TNFR binding to achieve targeted delivery of long-lasting BoNT/D protease into inflammatory cells, HFLS cells and peripheral sensory (but not motor) neurons. We ~~then~~ designed a therapeutic by replacing the binding domain of BoNT/DΔH_C with atsttrinusing recombinant technology. We report the successful engineering, expression and characterisation of this novel BoNT/D based therapeutic named BoNT/DΔH_C-atsttrin (abbreviated as /D-Atsttrin). We investigated its ability to cleave SNARE target proteins (VAMP-1 and 3) and inhibit either TNF-α and IL-6 pro-inflammatory cytokines or pain peptide (SP) release in immune cells and sensory neurons, respectively.

4.2 Results

4. 2.1 Cultured primary macrophages, HFLS cells and DRGs express TNF receptor

After staining cultured primary macrophages with anti-TNFR, confocal images show virtually all of macrophages express TNFR (Figure 4.1A). Interestingly, TNFR is

predominantly localized on the surface of cultured rat DRGs. Nearly majority of substance P positive neurons also express TNFR (Fig. 4.1B). As expected, cultured HFLS cells also express TNFR as visualized by anti-TNFR. Confocal pictures demonstrated all of cultured HFLS cells express TNFR (Fig. 4.1C).

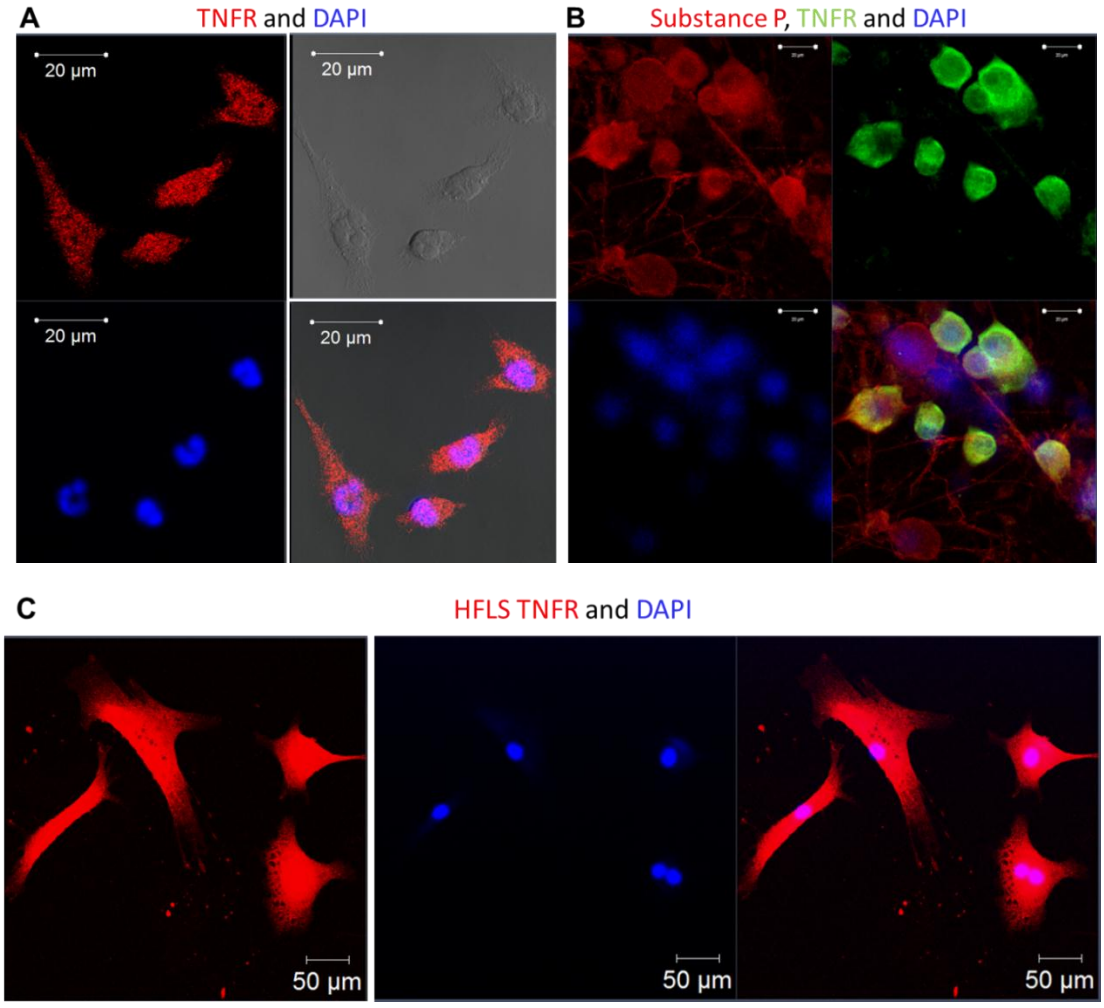

Figure 4.1. Primary macrophages, substance P-positive rat DRGs and HFLS cells express TNFR.

Primary macrophages (A) and HFLS cells (C) were grown on coverslips for 2 DIV and 7 DIV for DRGs (B), fixed, permeabilised and then incubated with rabbit anti-TNF receptor (1:400) alone (A and C), or together with mouse anti-SP (1:500) overnight at 4 ºC followed

by goat anti-rabbit Alexa Fluor-555 (1:1000) (A and C), goat anti-mouse Alexa Fluor-555 (1:1000) together with goat anti-rabbit Alexa Fluor-488 (1:1000) (B) for 1 h at room temperature. Cell nuclei are stained by DAPI. Images were captured by a confocal microscope under fluorescent or phase contrast mode. Scale bar, 20 μm (A and B) and 50 μm (C).

4. 2.2 Targeted biotherapeutic (/D-Atsttrin) was produced recombinantly with high yield and good purity

Dr. Jiafu Wang designed the construct, encoding /D-Atsttrin, by inserting the gene encoding Atsttrin targeting ligand into BoNT/DΔHc (Fig. 4.2A) between H_N and His_6 tag (Fig. 4.2B). As cloning sites illustrated in Figure 4.2C, selected clone gave expected size after double digestion with SacI+XhoI, NdeI+SacI or NdeI+XhoI (Figure 4.2D).

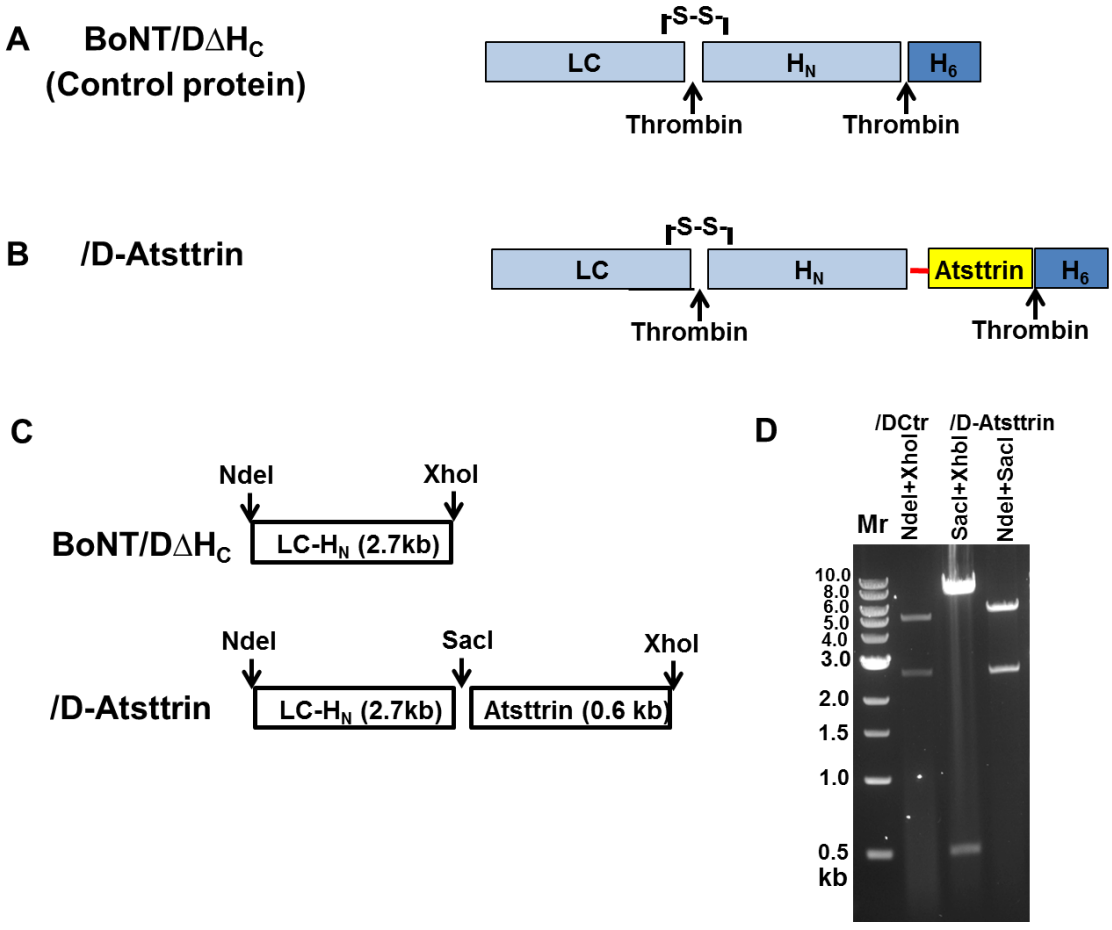

Figure 4.2. Schematics showing the design of /D-Atsttrin and its restriction digestion. A. Removing Hc gene in BoNT/D created the construct encoding a non-targeted control protein BoNT/DΔH_C. **B.** inserting Atsttrin gene yielded the construct encoding /D-Atsttrin. Note that, all these proteins have a His_6 tag and two thrombin sites as indicated. **C**. Schematic of /D-Atsttrin construct with indicated cloning sites D. /D-Atsttrin and BoNT/DΔHc clones were digested by Sacl+Xhol, Ndel+Sacl and Ndel+Xhol restriction enzymes for 2 h at 37℃and then analysed by running a 0.8% agarose gel.

Once the construct was confirmed by MWG-Biotech AG using DNA sequencing, /D-Atsttrin was then successfully purified following the outlined methods with high purity, giving a yield around 3.3 mg/L (Figure 4.3). /D-Atsttrin was expressed in a SC form, as revealed by the single bands of the expected molecular weights (~120k) observed in both the absence and presence of reducing agent (Figure 4.4A). After nicking with thrombin, its LC/D (50k) and H_N/D-Atsttrin (70k) were separated from a gel under reducing conditions (Figure 4.4A). This confirms the successful nicking into the DC form as well as the successful formation of the inter-chain di-sulphide bridge. Western blots displayed His_6 tag contained in SC form was completely removed after successfully nicking into the DC form (Figure 4.4B).

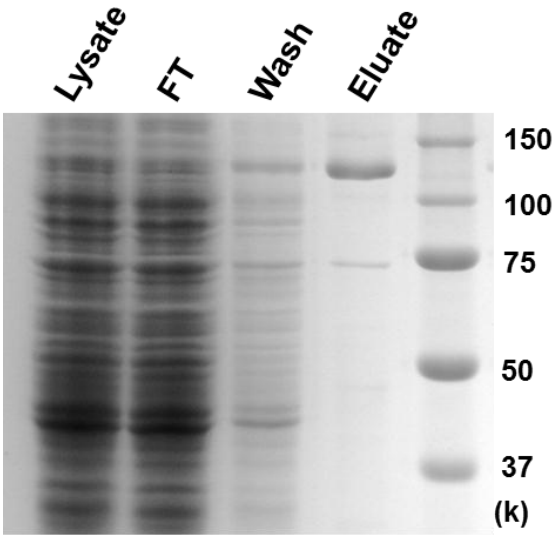

Figure 4.3. IMAC purification of /D-Atsttrin.

A. /D-Atsttrin was expressed in *E.coli* and purified by IMAC. Samples were taken at various stages of the process and analyzed by running a 10% hand-made Tris-glycine SDS-PAGE gel, followed by Coomassie staining, FT: flow through

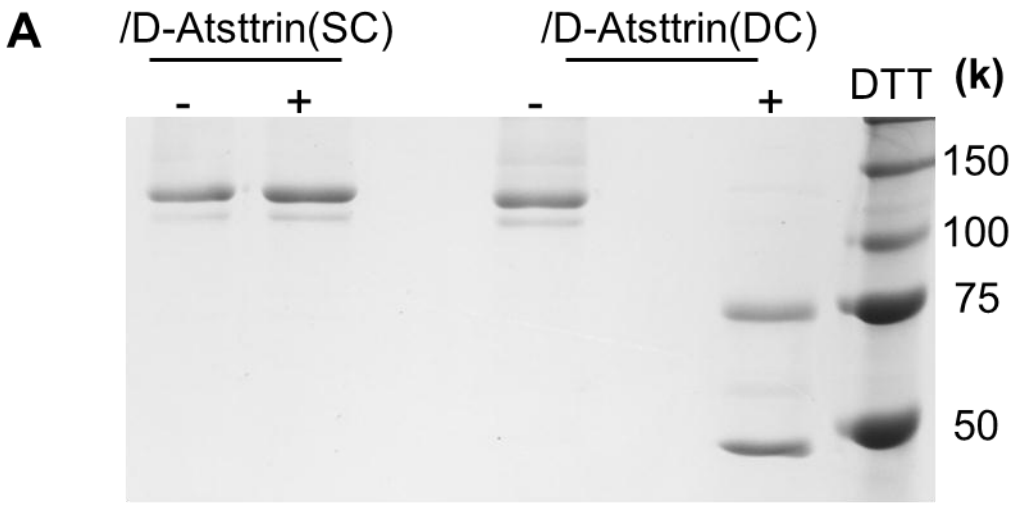

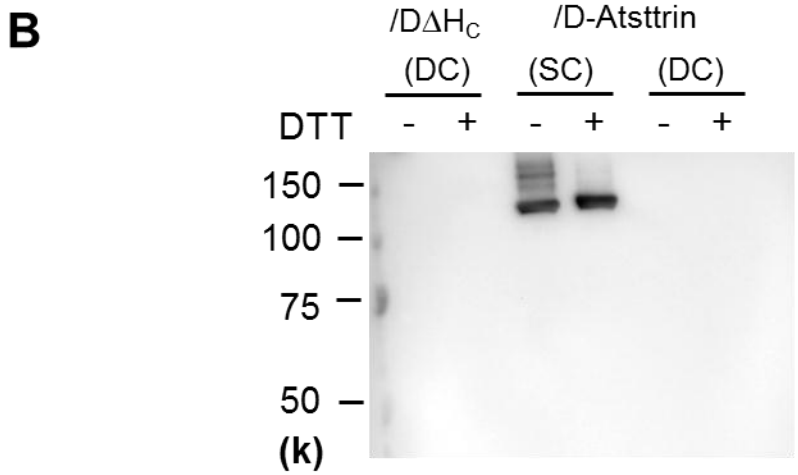

Figure 4.4. Simultaneous nicking and His_6 tag removal from/D-Atsttrin.

A. /D-Atsttrin SC and DC were analyzed, with and without dithiothreitol (DTT) (50 mM), using 10% SDS-PAGE followed by Coomassie staining. **B**. /D-Atsttrin SC and DC were subjected to SDS-PAGE followed by Western blotting with mouse anti- His_6 antibody.

4.2.3 Recombinant /D-Atsttrin and BoNT/DΔHc have the same protease activity

To confirm the protease activities of /D-Atsttrin and BoNT/DΔHc in *vitro*, a recombinant substrate (GFP-VAMP2$_{(2-94)}$-His$_6$) cleavage assay was carried out. After measuring, /D-Atsttrin and BoNT/DΔH$_C$ performed similar ability to cleave GFP-VAMP2$_{(2-94)}$-His$_6$ substrate(Figure 4.5). At 12.5 nM, GFP-VAMP2$_{(2-94)}$-His$_6$substrate was cleaved approximately 50% (Figure 4.5). This confirmed inserting the desired targeting ligand Atsttrin into BoNT/DΔH$_C$ construct did not affect the protease function of the LC of BoNT/D in *vitro*.

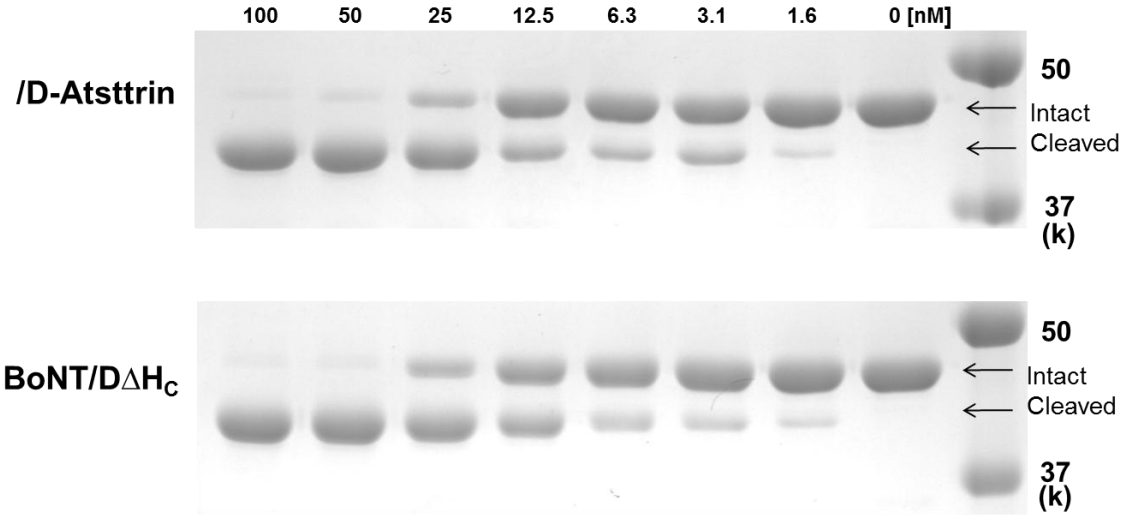

Figure 4.5. *In vitro* protease activity assay for /D-Atsttrin and BoNT/DΔHc.
/D-Atsttrin and BoNT/DΔH$_C$ were diluted to 100 nM in protease assay buffer and incubated at 37ºC for 30 min to activate the protease domain. They were then serially diluted to 1.6 nM in assay buffer and mixed with GFP-VAMP2$_{(2-94)}$-His$_6$substrate for additional 30 min at 37ºC, followed by addition of ice-cold LDS sample buffer. Samples were resolved on 12% hand-made Tris-glycine SDS-PAGE gels which were then Coomassie stained.

4.2.4 /D-Atsttrin entered into RAW 264.7 cell line, cleaved VAMP-3 and attenuated TNF-α and IL-6 release

In Chapter 3, the mouse RAW 264.7 cell line has been confirmed as a suitable model for our study. Herein, in this chapter, RAW cells were also used to investigate the ability of the targeted therapeutic to cleave VAMP-3 and inhibit secretion of IL-6 and TNF-α. The cells were incubated with various doses of /D-Atsttrin for 6 h and stimulated with IFNγ (500 pg/ml) and LPS (100 ng/ml) for 42 h before harvesting. Analysis by Western blotting showed VAMP-3 was cleaved significantly when treatment was ≥ 12.5 nM of /D-Atsttrin (Figure 4.6A and B). In contrast, the control protein treated samples only exhibited 25% cleavage at the highest concentration tested (Figure 4.6B). IFNγ and LPS-evoked IL-6 and TNF-α release were inhibited by the re-targeted therapeutic (Figure 4.7). Treatment with 50 nM of /D-Atsttrin resulted in cleavage of 60% of VAMP-3 which correlated with around 65% reduction in IL-6 release and inhibiting ~45% of TNF-α release (Figure 4.7A and B). In contrast, the control protein treated samples only blocked 20% of IL-6 release and no reduction in TNF-α release at the highest concentration tested (Figure 4.7A and B).

Importantly neither the targeted or non-targeted control toxin had an effect on cell viability (Figure 4.8).

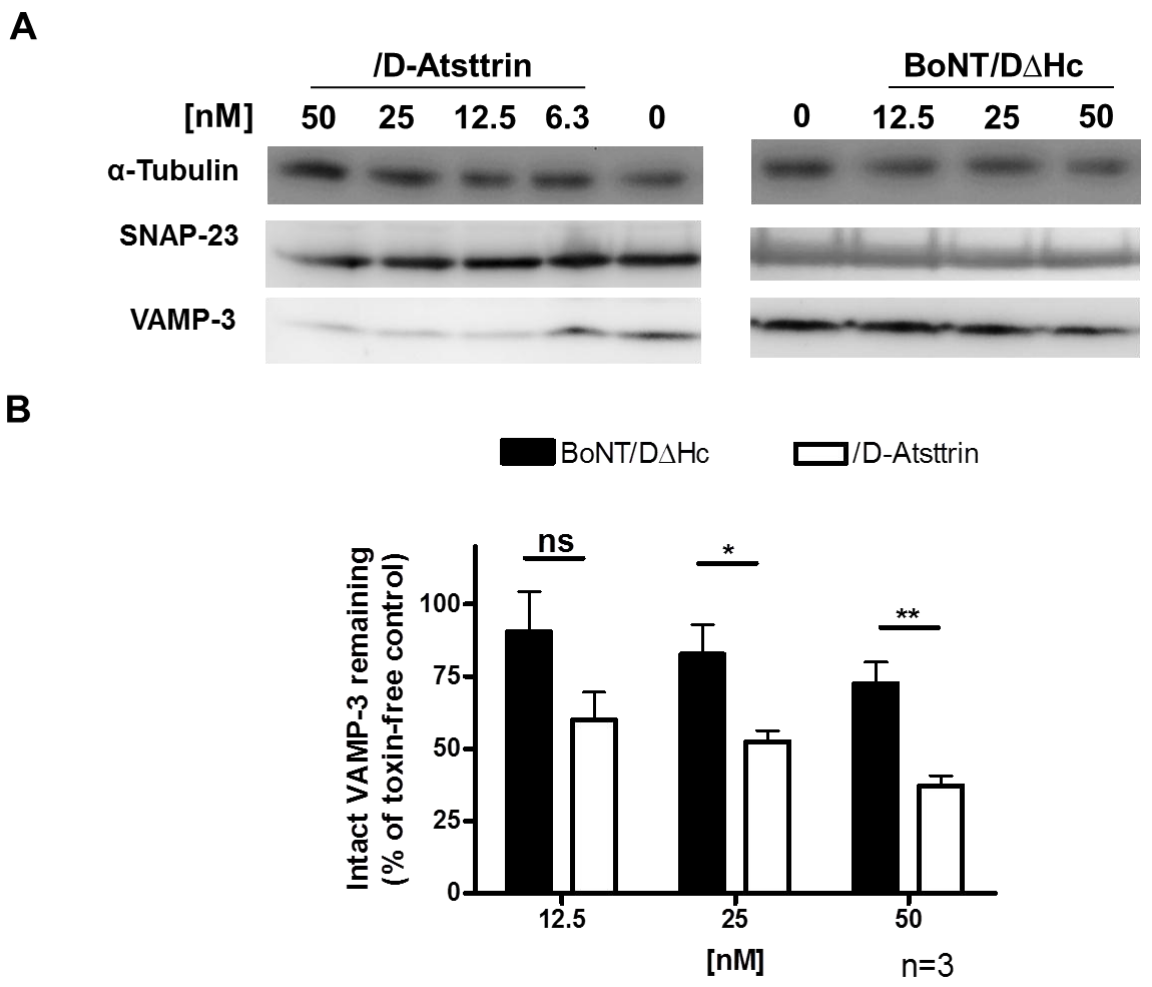

Figure 4.6. The differential effects of /D-Atsttrin and control protein on the cleavage of VAMP-3.

A. RAW cells were incubated with various doses of /D-Atsttrin or BoNT/DΔH_C for 6 h before stimulation with IFNγ and LPS for 42 h. The cells were then harvested and probed for VAMP-3 cleavage. α-Tubulin (an non-SNARE protein) and SNAP-23 were detected as an internal loading controls. **B**. The intensity of VAMP-3 was divided by the corresponding internal loading control (SNAP-23) to normalize any variation in loading/protein concentration between wells. VAMP-3 remaining after treatment with toxin was calculated by expressing the above ratio as a % of the toxin free control sample. Data plotted in panel B is mean ± S.E.M. (n=3). Statistical analysis was carried out using the Students unpaired T-test, *: $P<0.05$ and **: $P<0.01$.

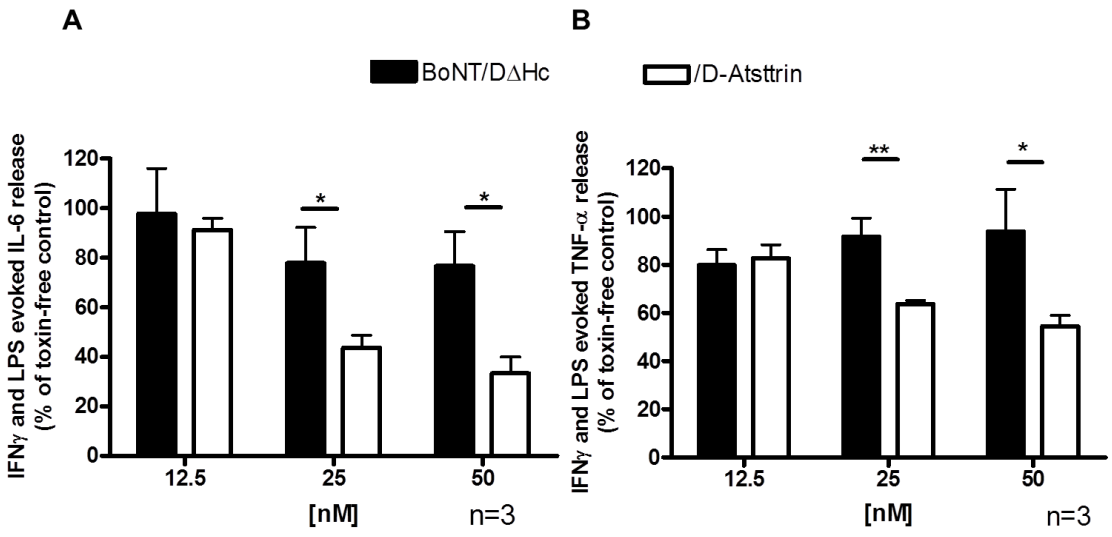

Figure 4.7. Effects of /D-Atsttrin on TNF-α and IL-6 release from mouse macrophages.

Murine RAW cells were incubated with various dose of /D-Atsttrin or BoNT/DΔH_C for 6 h before stimulation with IFNγ and LPS for 42 h. IL-6 and TNF-α content were then measured using the relevant ELISA kits. Data plotted were mean ±S.E.M. (n=3). Statistical analysis was carried out using the Students unpaired T-test *: $P<0.05$, **: $P<0.01$.

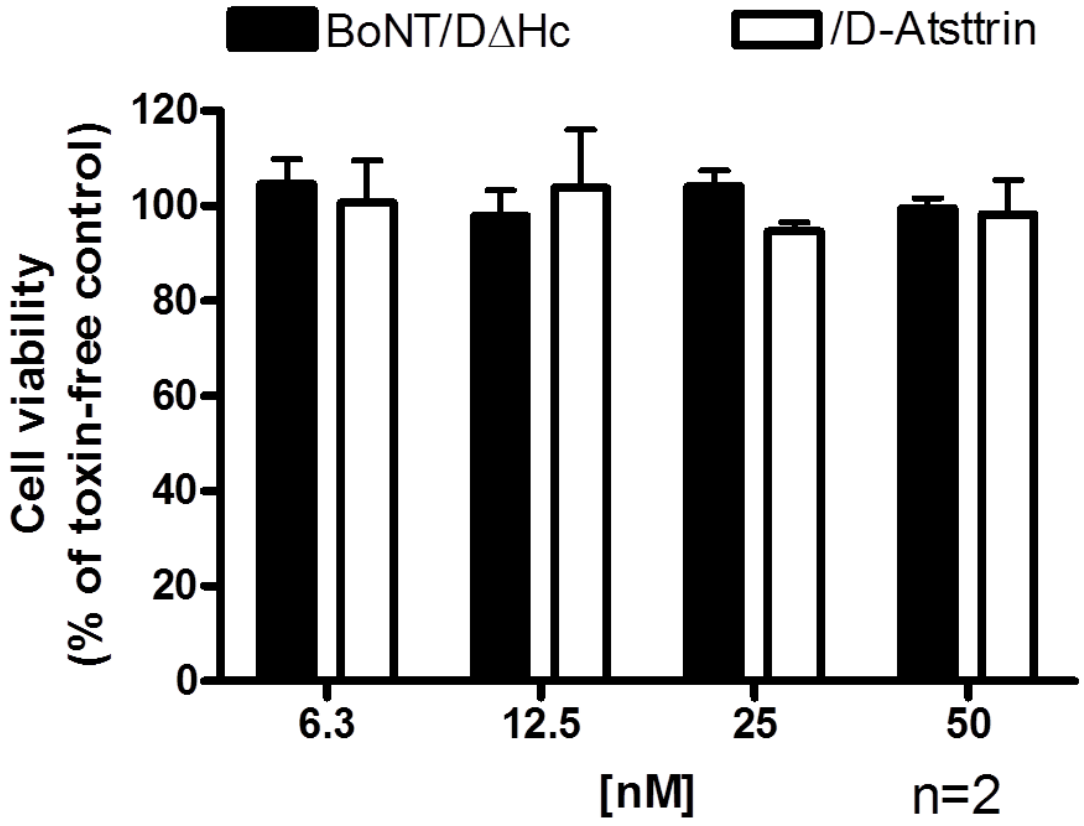

Figure 4.8. Effect of the retargeted therapeutic (/D-Atsttrin) on RAW cells viability. RAW cells were incubated with various doses of /D-Atsttrin or control protein BoNT/DΔH_C for 44 h, followed by 4 h incubation with alamar blue contained culture medium, avoiding light. Finally, macrophages were read at absorbance 570 nm by plate reader. Cell viability was quantified by expressing the above ratio as a % of the toxin free control samples. Data are mean ± S.E.M. (n=2).

4.2.5 /D-Atsttrin entered into cultured primary mouse peritoneal macrophages via binding to TNF receptor, cleaved VAMP-3 and inhibited evoked TNF-α and IL-6 release

It is necessary to verify the results obtained from RAW cells on primary macrophages, thus, we cultured primary mouse peritoneal macrophages and then exactly the same experiment carried on RAW cells was done on these primary mouse macrophages. Analysis by

Western blotting displayed significant cleavage of VAMP-3 by 25 nM and 50 nM of /D-Atsttrin (Figure 4.9A and B), whereas the non-targeted control protein treated samples only showed ~10% cleavage even at 50 nM concentration (Figure 4.9A and B). Similarly, IFNγ and LPS-evoked IL-6 and TNF-α release was significantly blocked by treatment with 25 nM and 50 nM of /D-Atsttrin. Under 50 nM concentration, approximately 70% of IL-6 and 80% of TNF-α release were attenuated (Figure 4.10). There is only < 25% inhibitions of IL-6 and TNF-α release treatment with similar concentrations of the control protein (Figure 4.10), thus, confirming there is significant targeted uptake of /D-Atsttrin by mouse macrophages.

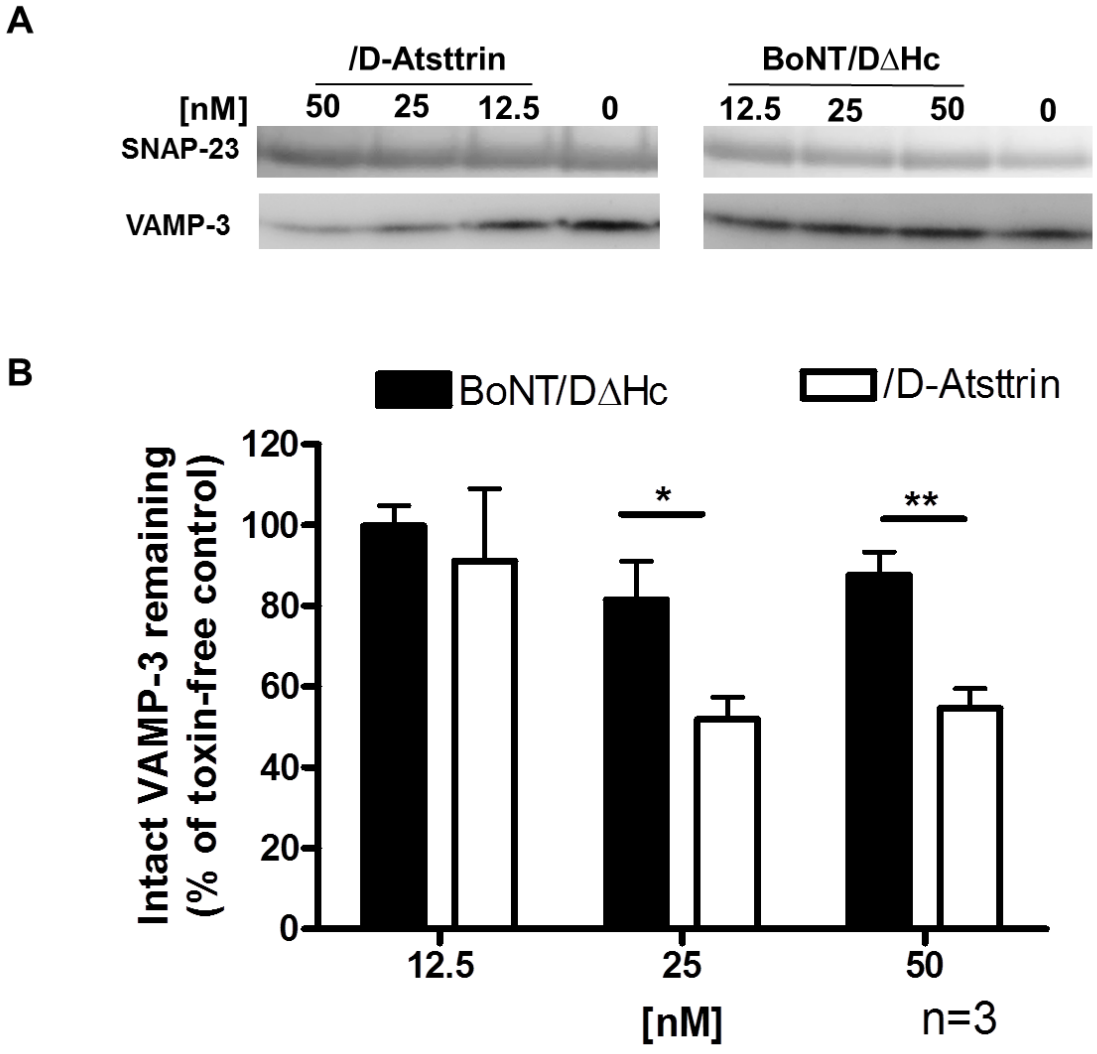

Figure 4.9. /D-Atsttrin and control protein on the cleaving ability of VAMP-3 in

primary macrophages.

A. Primary mouse peritoneal macrophages were treated with various doses of /D-Atsttrin or BoNT/DΔH_C for 6 h, followed by stimulation with IFNγ and LPS for 42 h. The cells were then lysed in LDS buffer and analysed by Western blotting to probe VAMP-3 cleavage as before. **B.** The amount of VAMP-3 remaining relative to the SNAP-23 internal loading control was calculated as before. Data plotted in panel B is mean ± S.E.M. (n=3). Statistical analysis was carried out using the Students unpaired T-test *: P<0.05 and **: P<0.01.

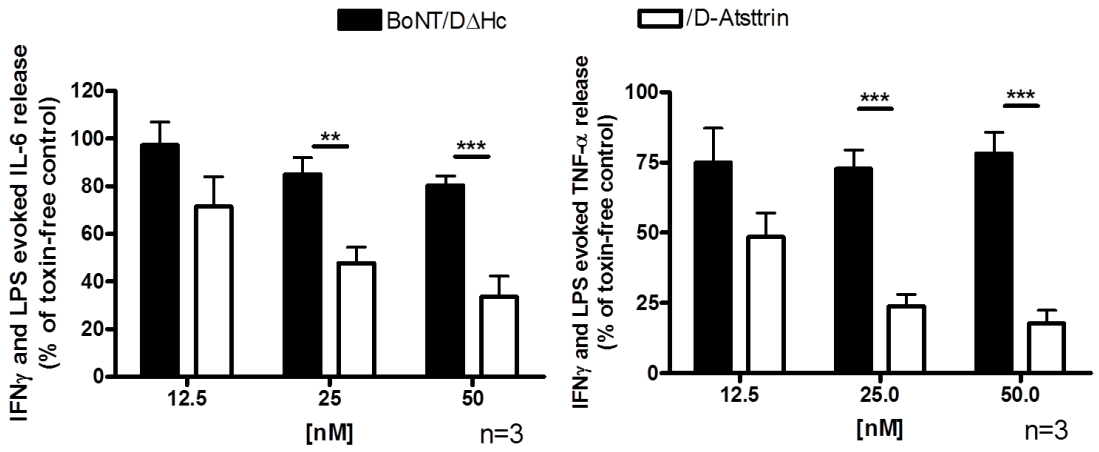

Figure 4.10. The ability of /D-Atsttrin to attenuate IL-6 and TNF-α release from mouse peritoneal primary macrophages.

After 6 h treatment with /D-Atsttrin or control protein, cells were stimulated with IFNγ and LPS for another 42 h. Then collected supernatants were used to measure evoked IL-6 and TNF-α release by ELISA. Data plotted in panel are mean ±S.E.M. (n=3). Students unpaired T-test was chosen for statistical analysis **: P<0.01 and ***: P<0.001.

4.2.6 HFLS cells express SNAP-23 and VAMP-3 and release IL-6 upon stimulation.

To confirm that HFLS cells express SNARE proteins and release IL- 6, HFLS cells were incubated with serum free culture medium for 44 h and stimulated with IL-1β for 4 h before harvesting. After Western blotting analysis, blots showed that SNAP-23 and

VAMP-3 were present in HFLS cells (Figure 4.11A) and the secretion of IL-6 was significantly increased upon stimulation (Figure 4.11B).

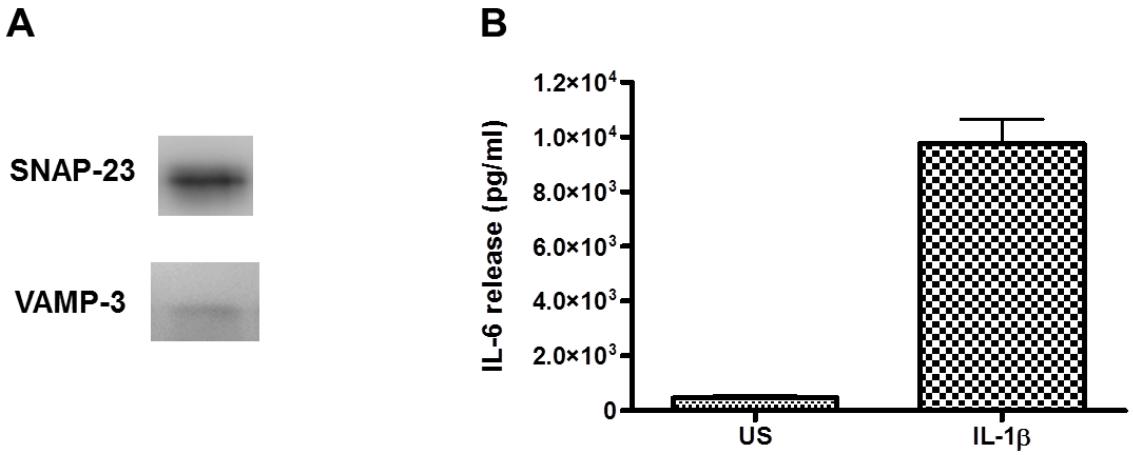

Figure 4.11. The verification of different SNARE proteins and evoked IL-6 release in HFLS cells.

A. Harvested HFLS cells were lysed in 2×LDS sample buffer and probed by Western blotting using anti-SNAP-23 and VAMP-3 antibodies. (B) IL-6 release during 4 h incubation with IL-1β (25 ng/ml) (stimulated) or medium only [unstimulated (US)] cells were analyzed by ELISA. Data plotted are mean ±S.E.M. (n=3).

4.2.7 BoNT/D protease in /D-Atsttrin was redirected into HFLS cells via binding to TNFR, resulting in cleavage of VAMP-3 and reduction of IL-6 release

At the beginning of this chapter, TNFR has been confirmed to be expressed on HFLS cells. Thus, HFLS cells were treated with various doses of /D-Atsttrin for 44 h followed by stimulation with IL-1β for 4 h, cells were harvested and analysed by Western blotting. Western blots exhibited VAMP-3 was cleaved by /D-Atsttrin at doses ≥ 100 nM. In contrast, the non-targeted control protein treated samples only showed minor cleavage of VAMP-3 at highest concentration (Figure 4.12 A). Similarly, IL-1β evoked IL-6 release was attenuated dose dependently; especially in the highest concentration, approximately 55% of IL-6 release was inhibited. In contrast, only 10% of reduction of IL-6 release was exhibited in ≥200 nM of control protein treated samples (Figure 4.12B).

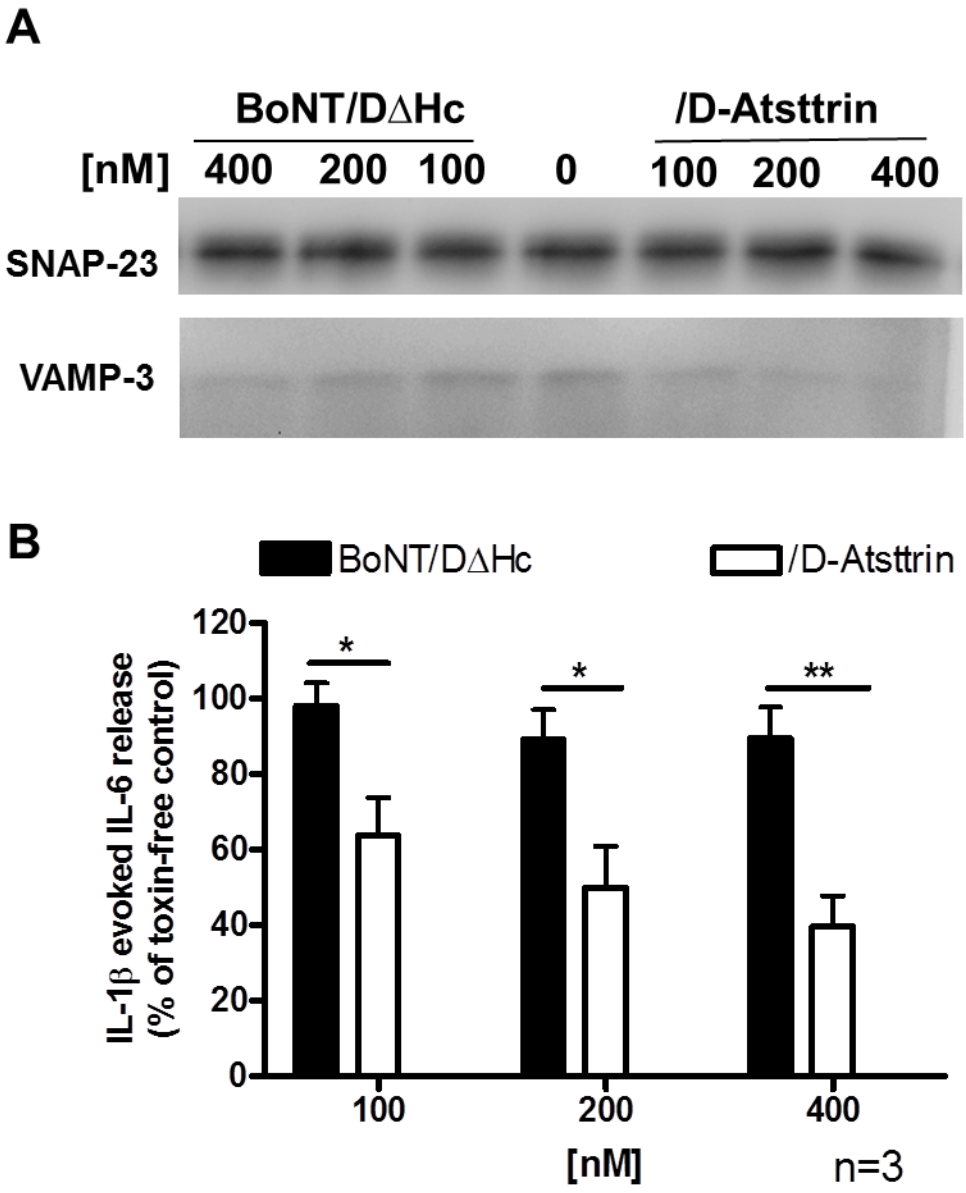

Figure 4.12 Effect of /D-Atsttrin and non-targeted control protein on cleavage of VAMP-3 and inhibition of IL-6 release in HFLS cells.

A. After incubation with various doses of /D-Atsttrin for 44 h, HFLS cells were stimulated with IL-1β (25ng/ml) for 4 h and then harvested for Western blotting analysis. The cleavage of VAMP-3 was probed with anti-VAMP-3 antibody and SNAP-23 was detected by anti-SNAP-23 antibody as an internal loading control. **B.** Collected supernatants were analysed by ELISA. The reduction of IL-6 was calculated as before. The Data plotted in panel B are mean ±S.E.M. (n=3). Students unpaired T-test was chosen for statistical

analysis *: $P<0.05$ and **: $P<0.01$.

4.2.8 The Atsttrin ligand re-targeted BoNT/D protease into rDRGs to cleave VAMP-1 and reduce secretion of SP

The TNF receptor is known to be expressed on DRGs. Therefore, cultured rat DRGs were incubated with 100 or 200 nM of /D-Atsttrin for 24 h to estimate the ability of /D-Atsttrin to enter rDRGs and cleave its target substrate VAMP-1, hopefully resulting in inhibition of SP release. Before harvesting, treated rDRGs were stimulated with 60 mM KCl for 30 min. Western blots exhibited ~ 50% of VAMP-1 was cleaved by 200 nM of /D-Atsttrin, however no significant cleavage was detected in control protein treated samples (Figure 4.13A and B). rDRGs pre-treated with /D-Atsttrin showed a significant reduction in potassium evoked SP release which correlated with the ability of /D-Atsttrin to cleave VAMP-1, 40% of SP was blocked by 100 nM (Figure 4.13 C). This result re-affirms the targeted internalization of the toxin via the TNFR to reduce the release of SP from sensory neurons, highlighting its therapeutic potential for treating chronic pain.

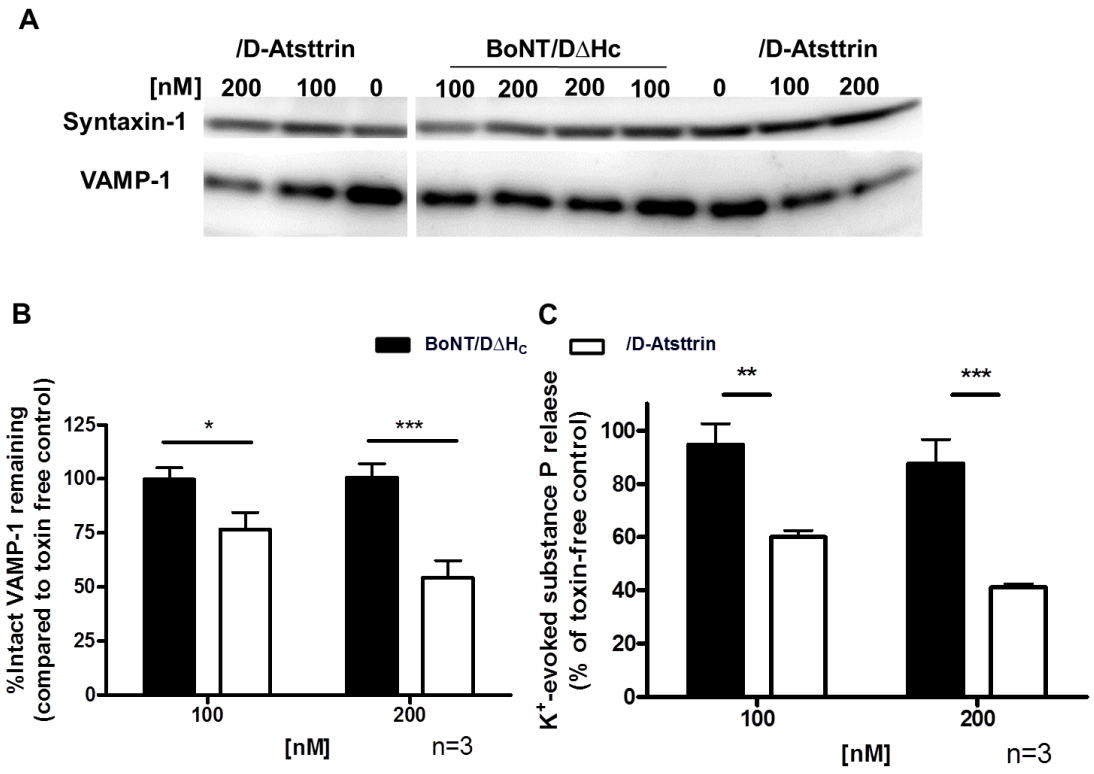

Figure 4.13. The effects of /D-Atsttrin on rDRGs.

A. rDRGs were treated with toxin for 24 h before stimulation with high potassium for 30 min. The cells were then harvested for Western blotting. Syntaxin-1 was blotted as a loading control and VAMP-1 to measure the uptake of /D-Atsttrin. **B**. VAMP-1 remaining after incubating with either biotherapeutic or control was calculated by expressing the ratio (intensity of VAMP-1 / the corresponding internal loading control (Syntaxin-1) as a % of the toxin free control sample. **C**. SP release was quantified using an ELISA kit. Data plotted in panel B. and C. are mean ±S.E.M. (n=3). Statistical analysis was carried out using the Students unpaired T-test *: $P<0.05$, **: $P<0.01$ and ***: $P<0.001$.

4.3 Discussion

All results reported in this chapter provide evidence that the novel therapeutic prevented pro-inflammatory cytokine and pain peptide release from specific target cells and sensory neurons, potentially acting as a painkiller to treat chronic pain. This achievement harnesses

the potent SNARE cleaving ability of BoNT which, by using a specific targeting ligand (Atsttrin) for selective TNFR binding, was successfully redirected into both immune cells and peripheral sensory neurons, two cell types important for both the transmission of pain as well as the induction of inflammation.

The targeted biotherapeutic was successfully engineered and produced in *E.coli* by directly using the recombinant strategy. We replaced the binding (H_c) domain of BoNT/D with our desired targeting ligand Atsttrin. The deletion of the binding domain and insertion of the targeting ligand did not affect the proper expression and purification of the BoNT/D based proteinase nor did it have an effect on the intrinsic ability of toxin to reach, enter the target cell and finally successfully cleave its target substrate, VAMP. TNFR is expressed on both macrophages and DRGs, confirmed via immunostaining of macrophages and DRGs with the specific anti-TNFR antibody. The recombinant method was chosen to generate this novel biotherapeutic in this project, because it can easily be scaled up and carried out under good manufacture production (GMP) conditions to produce large quantities of product with high quality in a short period of time.

We report, for the first time, dual targeting of the BoNT/D protease into both immune cells and sensory neurons via targeting to IL-1R or TNFR. As discussed previously cytokines are known to be important mediators in both inflammatory and neuropathic pain, they are involved in a feed forward loop inflammatory signalling which leads to persistent activation of immune cells and peripheral nociceptors. Our novel biotherapeutics cleaved the BoNT/D target substrate, VAMP-3 and attenuated the TNF-α and IL-6 release from a murine macrophage cell line (RAW264.7) and primary mouse macrophages. This result confirmed the successful re-targeting but also highlighted VAMP-3 is necessary for the release of pro-inflammatory cytokines from macrophages. We know from current clinically available therapeutics such as anti-TNF-α (TNF-α inhibitors) and IL-6 inhibitor based drugs that targeting TNF-α or IL-6 is confirmed in improving clinical symptoms. Atsttrin alone has been reported to control inflammation in mouse model of chronic pain by Jian et al(Jian et al., 2013). Tang, Liu et al. also reported Atsttrin alone is more efficacious in preclinical models of inflammatory arthritis than currently available clinical

therapies. Therefore we predict our targeted therapeutic will present similar if not greater anti-inflammatory effects than current therapeutics *in vivo*.

Similar to the immune cells, treatment of sensory neurons (DRGs) with the targeted biotherapeutic resulted in cleaving VAMP-1 which correlated nicely with an inhibition in the K^+ envoked substance P (SP) release, an important pain peptide. We found that the level of SP release was significantly reduced at the high concentrations. A similar study was carried out by Duggan et al. They coupled an *Erythrina cristagalli* lectin, which can recognize and bind to carbohydrates, to LC-HN/A to form LC-HN/A-ECL conjugates. The latter conjugates reduce SP release (Duggan et al., 2002). To add to the above advantages, this re-targeted biotherapeutic can also enter into sensory neurons, reduce the SP release which correlated with the cleavage of VAMP-1. As mentioned in the Introduction, SP is secreted from primary sensory nerves located at peripheral endings. SP is an important pain peptide and sensory neuronal transmitter which has also been implicated as having a role in stimulation and transduction of pain. In 1997, Brain also reported SP can improve microvascular permeability resulting in immune cell infiltration and inflammatory swelling (Brain, 1997). Taken together these results highlight SP as a hotspot target for pain relief therapeutics and leads to the hypothesis that the ability of /D-Atsttrin to attenuate SP release will have potential to treat pain, in addition to its anti-inflammation benefit.

Chapter 5 Novel secretion inhibitors of cytokines/neuropeptides targeted to macrophages or sensory neurons with potential for relieving chronic pain

5.1 Overview

Chronic pain, including rheumatoid arthritis (RA), is still a major medical challenge, with a high number of people suffering from persistent pain worldwide. Currently, three main types of medicine are widely used to treat chronic pain, including nonsteroidal anti-inflammatory drugs (NSAIDs), opioids and an adjuvant such as antidepressants and anticonvulsants. However, the short half-lives and various unacceptable adverse side effects such as addiction are continually reported (Volkow and McLellan, 2016). Thus, a pressing unmet need exists for persistently-acting and non-addictive medication for chronic pain.

Toward this end, botulinum neurotoxins have been proposed to have significant potential as local treatments for chronic pain. Clinical research demonstrated after treatment with botulinum toxin A complex (BOTOX) to migraine patients, their headache pain symptoms were significantly alleviated and, the frequency and duration of migraines were also reduced (Binder et al., 2000). There are 7 serotypes of BoNTs (/A-/G) with molecular weight ~150k. They consist of a ~50k N-terminal protease light chain domain (LC) and a ~100k C-terminal heavy chain domain (HC), linked via a disulphide bond. Most of BoNTs target neurons by binding to gangliosides and the synaptic vesicle protein 2 (serotypes: /A, /D-/F) or synaptotagmin (/B and /G) via the C-terminal half of HC (H_C) (Reviewed in (Meng and Wang, 2015)). Once BoNTs get internalised into the neurons, the N-terminal half of HC (H_N) forms a channel on the limited endosomal membrane and translocates the attached LC to the cytosol (Montal, 2010), in this way, it inactivates soluble N-ethylmaleimide-sensitive factor attachment protein receptors (SNAREs). Synaptosomal-associated protein 25k (SNAP-25) is cleaved by LC/A, /C1 and /E whereas synaptobrevin, also known as vesicle associated membrane protein (VAMP) isoform 1, 2 and 3 are truncated by LC/B, /D, /F and /G. BoNT/C1 additionally cleaves syntaxin. Cleavage of these SNAREs results in the disruption of the vesicle fusion and blockade of transmitter release (reviewed in (Meng and Wang, 2015)). Because of this unique property, BoNT serotypes /A and /B complex forms have been widely used for treating hyper-excitability disorders of cholinergically innervated muscles or glands. In 2010, BOTOX® was

approved by the FDA to treat chronic migraines (Boudreau et al., 2015). As a painkiller, it has the advantages of being non-addictive and having a long-lasting action by persistently cleaving SNAP-25 (Boudreau et al., 2015, Wang et al., 2011).

To avoid the unwanted muscle paralysis side effect, improvement of BoNT is desired so that it will selectively and specifically target BoNT SNARE-cleaving protease into inflammatory cells and/or sensory neurons rather than motor neurons for treating chronic inflammatory pain (e.g. RA) and neuropathic pain. RA is a common autoimmune chronic inflammatory joint disease and macrophages are critically involved in the pathogenesis of RA. They secrete various pro-inflammatory cytokines and chemokines, and contribute to the cartilage and bone destruction in RA (Ma and Pope, 2005). The most important pro-inflammatory cytokines which play an essential role in the development of RA are tumor necrosis factor-α (TNFα), Interleukin 1β (IL-1β) and IL-6 (Scheller et al., 2011, Muller-Ladner et al., 2005, Ji et al., 2002). TNFα and IL-6 sensitize joint nociceptors to mechanical stimulation and, thus, directly contribute to mechanical hyperalgesia (Schaible, 2014). It is known that macrophages require VAMP3 to secrete cytokines (Murray and Stow, 2014, Murray et al., 2005). Thus, targeted delivery of VAMP-cleaving protease into macrophages could offer a novel means for potential treatment of RA disease. Hence a site-specific, robust, reliable and efficient strategy for modification of BoNTs is highly desirable for generating retargeted BoNTs' proteases. In order to meet this demand, we exploited the sortase-mediated protein ligation technique to make functional targeted BoNT based fusion proteins by stitching BoNT protease to the cell-specific targeting ligands. *Staphylococcus aureus sortase* A, a thiol transpeptidase exists in many Gram-positive bacteria responsible for covalent anchoring of cell surface proteins to bacterial cell walls (Mao et al., 2004). Protein with an exposed LPXTG motif can be specifically ligated by sortase A to an aminoglycine protein/peptide via an amide bond in the physiological reaction conditions.

Using general molecular biology techniques, a short non-structural linker followed by LPETG motif was attached to the C-terminal of BoNT/D core-therapeutic consisting of LC and H_N domains lacking the neuronal binding domain H_C (BoNT/DΔH_C). The resultant

protein BoNT/DΔH_C-CS was expressed in *E .coli* and purified with retention of its full VAMP cleaving protease activity. This protein was ligated to a recombinantly produced interleukin 1β (IL-1β) or a synthesized calcitonin gene-related peptide (CGRP) receptor antagonist ($CGRP_{8-37}$) within minutes via a sortase-catalyzed reaction to produce the retargeted BoNT/D based therapeutic candidates: /DIL-1β and /D-$CGRP_{8-37,}$ respectively. As macrophages express the IL-1 receptor (Chizzonite et al., 1989, Dinarello, 1991) and dorsal root ganglion neurons (DRGs) express the CGRP receptor (Segond von Banchet et al., 2002), the above mentioned ligated ligands successfully delivered the BoNT/D core-therapeutic into either cultured macrophages or DRGs. This results in inhibiting the release of inflammatory cytokines or pain transmitter peptides (substance P). Our results highlight their potential as anti-inflammatory and/or anti-nociceptive therapeutics. Our strategy also demonstrates the potentially broad applicability for generating botulinum neurotoxin derived targeting therapeutics.

5.1.1 Aim and objectives

The primary aim of this chapter was to develop the sortase-mediated protein ligation technique to attach different ligands to the BoNT/DΔH_C-CS protease, thus generating novel BoNT/D based bio-therapeutics. Specifically, we used sortase A mediated conjugation to generate biotherapeutics /DIL-1β and /D-CGRP8-37, by ligating IL-1β or $CGRP_{8-37}$ to BoNT/DΔHC-CS. To confirm successful retargeting of the BoNT/D protease into macrophages or sensory neurons (rDRGs), VAMP3 or VAMP1 cleavage post intoxication was measured. Furthermore, functional effects of these therapeutics on the target cells was measured by the blockade of evoked cytokine (TNF-α and IL-6) and pain peptide (SP) release.

5.2 Results

5.2.1 BoNT/D core-therapeutic with sortase A recognition motif was expressed and purified with good yield and purity.

Dr. Jiafu Wang selected the sortase A mediated conjugation strategy to target BoNT/D core-therapeutic into selective cells because this method allows us to efficiently ligate targeting ligand (peptides or proteins with or without modification) to the core-therapeutic (Fig. 5.1A). Accordingly, he constructed the relevant plasmids. Briefly, the synthetic gene fragment encoding LC.H_N of BoNT/D with codon optimized for *E. coli* expression was inserted into the pET29a vector. Note that this synthetic gene contains a thrombin recognition consensus site at the loop region between the LC and H_N domains for precise nicking. Subsequently, a short nucleotide sequence encoding a non-structural linker and a sortase A recognition motif (LPETG) followed by a thrombin recognition sequence was inserted between the 3'end of H_N/D gene and nucleotides encoding a C-terminal His_6 tag. This generated a construct, encoding BoNT/DΔH_C-CS (abbreviated as /DΔH_C-CS, Fig. 5.1B). After transformation of the resultant plasmid into *E. coli* BL21.DE3, /DΔH_C-CS was expressed in *E. coli* using an auto-induction medium and successfully purified by immobilised metal ion affinity chromatography (IMAC) with a yield of (~4 mg/litre of culture). /DΔH_C-CS was expressed and purified as the single-chain (SC) form with the predicted *Mr* r100k (Fig. 5.1C). The purified /DΔH_C-CS SC was then nicked into the di-chain (DC) form by thrombin. This was confirmed by SDS-PAGE in the presence or absence of a reducing agent, dithiothreitol (DTT). The nicked sample remained a single band in the absence of the reducing agent and its constituents (LC and H_N-CS) were only separated in the presence of DTT, confirming that the interchain of disulphide was formed in the *E .coli* (Fig. 5.1D).

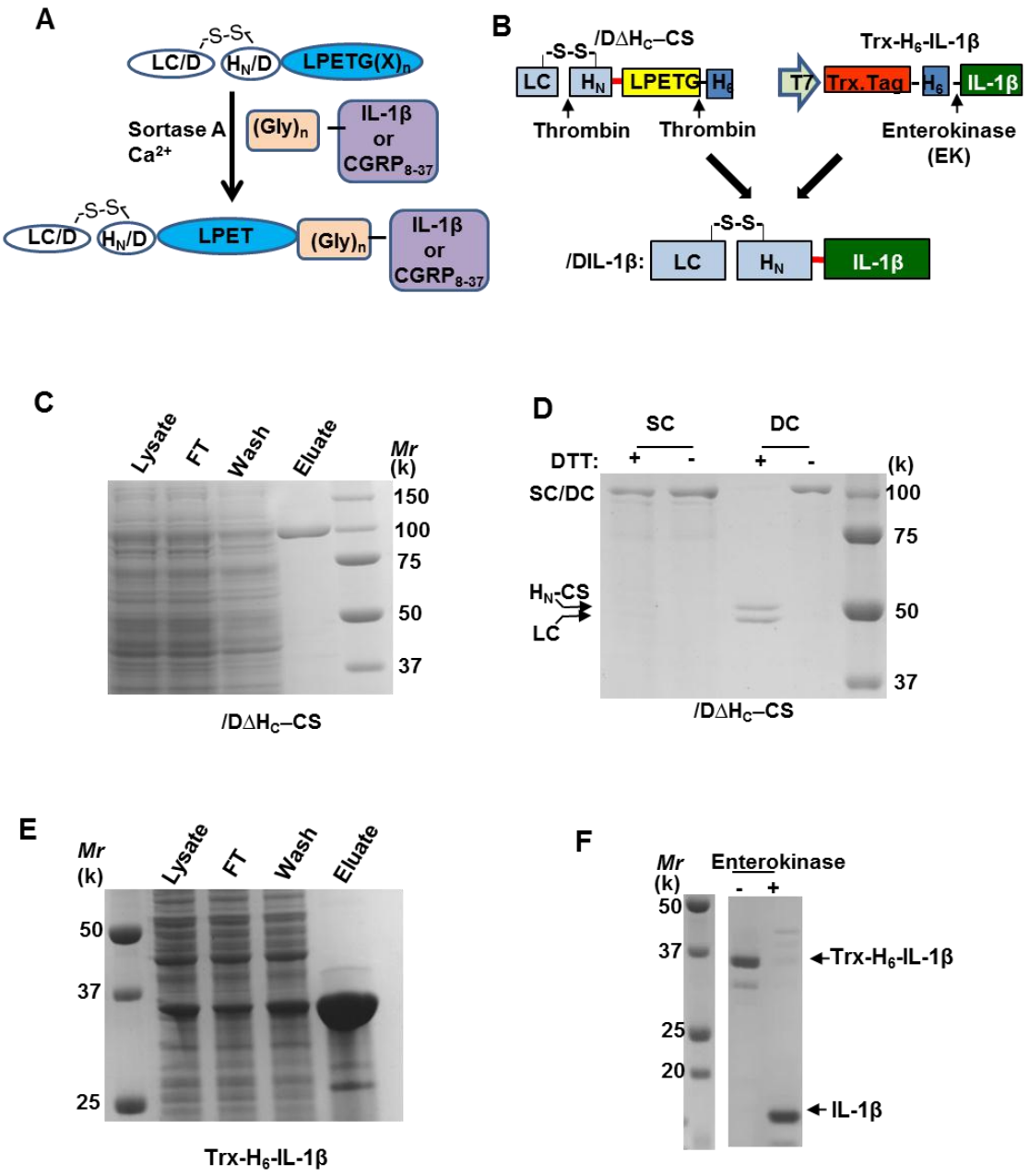

Figure 5.1. Protein engineering BoNT/D core-therapeutic and targeting ligand.

A. Schematic of the sortase A mediated conjugation strategy. Sortase A can recognize the LPETG motif at the C-terminal of LC.H_N/D and the bond between T and G to form a thioest intermediate. Glycine residues, which are linked to the N-terminal of IL-1β or synthesized $CGRP_{8-37}$ can attack that intermediate to result in a fusion protein. **B.** Illustration of protein engineering /DIL-1β via ligating Gly_5-IL-1β to /DH_C-CS by sortase A. It is not necessary to purify the Gly_5-IL-1β after cleavage by enterokinase. **C.** /DΔH_C-

CS was expressed in *E .coli* and purified by IMAC. Aliquots from IMAC were analyzed by SDS-PAGE followed by Coomassie staining. **D.** /DΔH_C-CS SC and thrombin nicked DC were subjected to SDS-PAGE. **E.** Purification of Trx-H_6-IL-1β fusion protein by IMAC. **F.** SDS-PAGE analysis of Trx-H_6-IL-1β protein with or without enterokinase treatment.

5.2.2 Protein engineering inflammatory cell targeting ligand and its efficient conjugation to BoNT/D core therapeutic via sortase enzyme

To target BoNT/D core-therapeutic into inflammatory cells, we selected the IL-1β as a targeting ligand because IL-1 receptors were expressed on certain inflammatory cells including macrophages, synoviocytes etc (Chizzonite et al., 1989, Dinarello, 1991). We inserted the synthetic gene encoding Gly_5-IL-1β protein into a bacterial expression vector pET32b immediately after the enterokinase cleavage site to create a construct, encoding Trx-His_6-Gly_5-IL-1β protein (Fig.5.1B, abbreviated as Trx-H_6-IL-1β). This allows enterokinase to remove the Trx-His_6 tags from the Gly_5-IL-1β for subsequent ligation to BoNT/D core-therapeutic (Fig. 5.1B). Similarly, Trx-H_6-Gly_5-IL-1β fusion protein was expressed in BL21.DE3 and purified by IMAC with a yield of (~60 mg/liter of culture). Purified fusion protein was visualized on the Coomassie stained SDS-PAGE gel with *Mr* ~28k (Fig.5.1E). Incubation of fusion protein with enterokinase released Gly_5-IL-1β from Trx-His_6 tags, yielding the predicted size of *Mr* 17k, yielding the predicted size of rote-His_6 tag (Fig. 5.1F).

Incubation of enterokinase cleaved product mixture with /DΔH_C-CS in the optimized reaction condition, sortase A rapidly ligated IL-1β to /DΔH_C-CS within 10 min to yield BoNT/DΔH_C-IL-1β (/DIL-1β) conjugated protein. Further incubation did not yield more conjugated protein (Fig. 5.2A). /DIL-1β product was further purified by anion-exchange chromatography (AEX) to remove any unbound IL-1β substrate and contaminant present (Fig. 5.2B). The final product was analyzed by SDS-PAGE in the absence or presence of DTT. The LC/D and H_N/D-IL-1β were only separated in the presence of DTT (Fig. 5.2C), confirming that the inter-chain disulphide bond was not affected by the reaction.

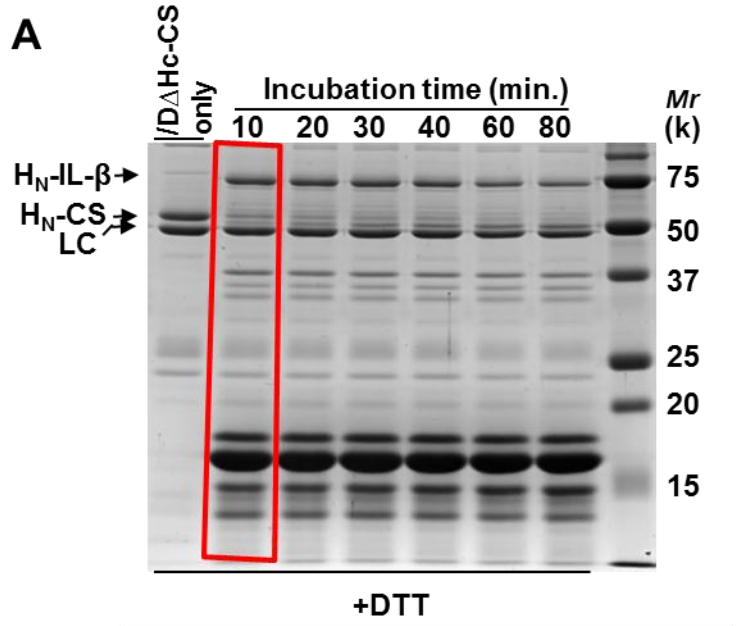
A
/DΔHc-CS only
Incubation time (min.)
10 20 30 40 60 80
Mr (k)
H_N-IL-β
H_N-CS
LC
75
50
37
25
20
15
+DTT

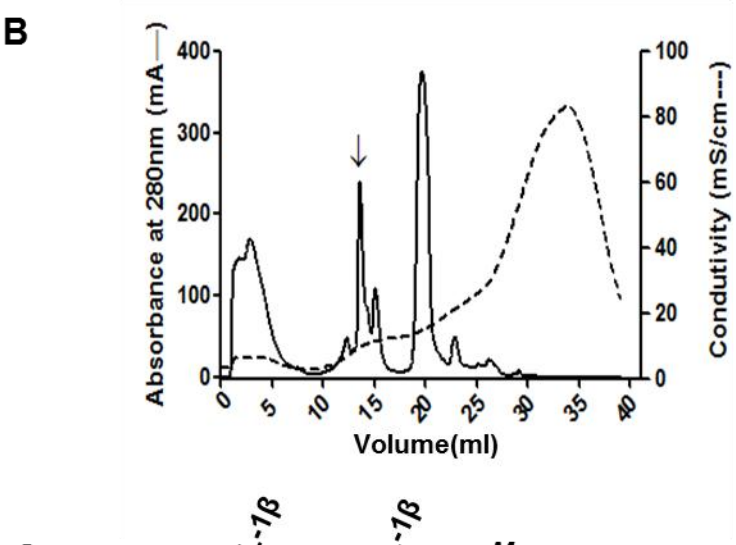
B
Absorbance at 280nm (mA—)
Condutivity (mS/cm---)
Volume(ml)

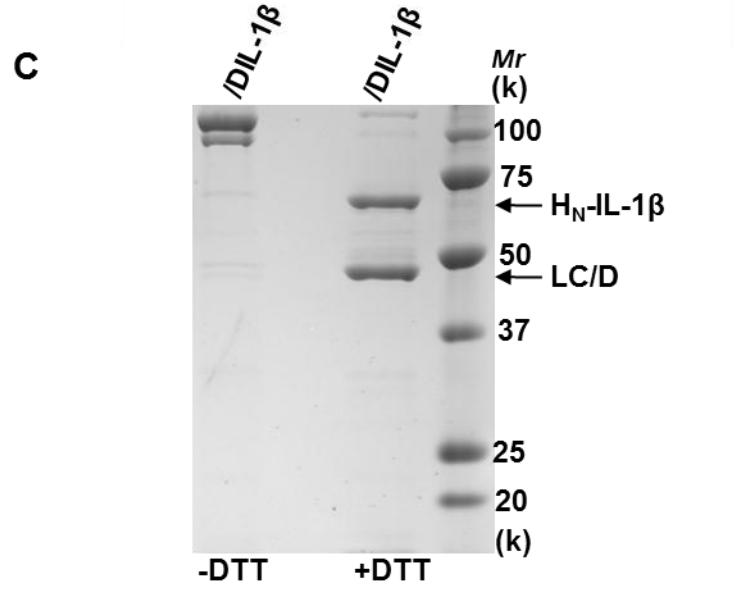
C
/DIL-1β
/DIL-1β
Mr (k)
100
75
H_N-IL-1β
50
LC/D
37
25
20
(k)
-DTT
+DTT

Figure 5.2. Production of /DIL-1β.

A. DΔH_C-CS was incubated with sortase A and enterokinase cleaved Trx-H_6-IL-1β mixture at 37ºC. Samples were taken at different time points and subjected to SDS-PAGE in the presence of 50 mM DTT followed by Coomassie staining. **B.** Anion-exchange chromatography was used to separate /DIL-1β conjugate from the unconjugated product and contaminants. Arrow indicates the eluted peak for /DIL-1β. **C.** Pooled /DIL-1β product from AEX was subjected to SDS-PAGE followed by Coomassie staining.

5.2.3 /DIL-1β conjugate exerts receptor binding and SNARE-cleaving biological activities

Next, it is important to confirm that recombinant IL-1β retains the desired targeting activity after ligating to /DΔH_C-CS. We used a cell proliferation method to assess its activity in RAW 264.7 macrophage cells. /DIL-1β displayed only a slight but not significant decrease of its activity compared to the commercial human IL-1β (Fig. 5.3A). This confirms that the ligated product retains the desired bio-activity of its ligand. As expected, /DΔH_C-CS (the control protein) did not show any effect on cell proliferation (Fig. 5.3A). Using a recombinant model substrate GFP-VAMP2$_{(2\text{-}94)}$-His_6, we proved that /DIL-1β conjugate has similar protease activity as the non-targeted control protein (/DΔH_C-CS) (Fig. 5.3B). Thus, ligating the desired targeting ligand into /DΔH_C-CS did not substantially affect the biological activities of its protease and its ligand.

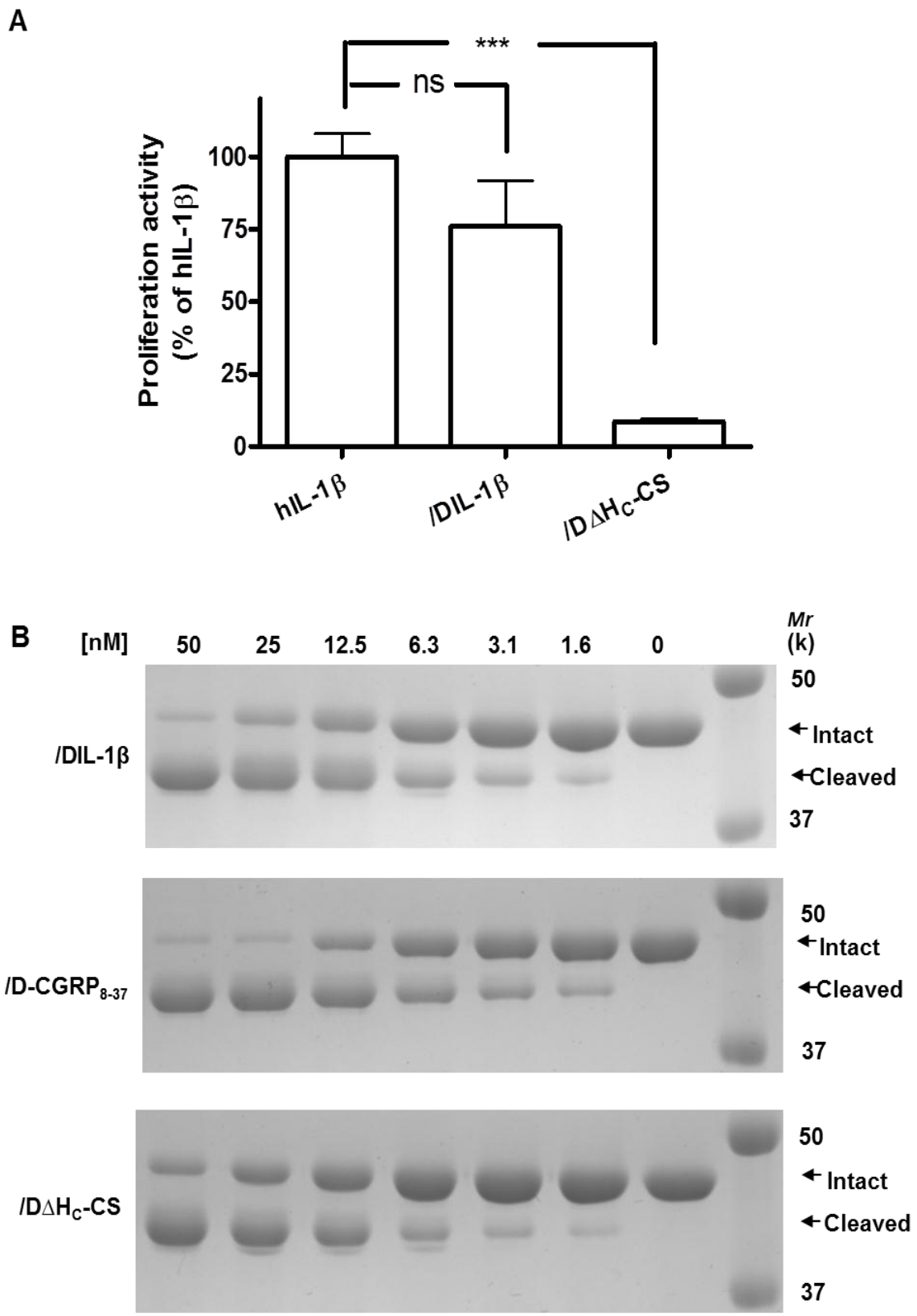
A
***
ns
Proliferation activity
(% of hIL-1β)
100
75
50
25
0
hIL-1β
/DIL-1β
/DΔHC-CS
B
[nM]
50
25
12.5
6.3
3.1
1.6
0
Mr
(k)
/DIL-1β
/D-CGRP8-37
/DΔHC-CS
50
Intact
Cleaved
37

Figure 5.3. /DIL-1β retains biological activities of its ligand and protease.

A. Bar chart showing proliferation activity of IL-1β ligand contained in /DIL-1β. RAW cells were treated with serial diluted /DIL-1β, /DΔH_C-CS or commercial human IL-1β for 48 h and the % of cell proliferation quantified by measuring newly synthesized DNA during cell division using Click-iT® EdU microplate assay kit. The values obtained for /DIL-1β or /DΔH_C-CS treated cells were converted to the corresponding commercial IL-1β concentration. Data plotted are mean ± S.E.M. (n=3). ns: non-significant, ***: P<0.001. **B**. /DIL-1β, /D-CGRP$_{8-37}$ and /DΔH_C-CS have similar protease activity in cleaving a recombinant GFP-VAMP2$_{2-94}$-His$_6$ substrate.

5.2.4 IL-1β successful delivered BoNT/D VAMP-cleaving protease into RAW264.7 cells and primary peritoneal macrophages resulting in inhibition of IL-6 release

As mentioned in the Introduction, macrophages play an important role in pathogenesis of chronic inflammatory diseases including RA. Macrophages express IL-1 receptor and certain SNARE proteins, especially SNAP-23 and VAMP3 (Boddul et al., 2014). Cultured RAW264.7 macrophages were treated with or without /DIL-1β for 6 h before stimulation of cytokine release with interferon gamma (IFNγ) and lipopolysaccharides (LPS) for 42 h. Upon stimulation with IFNγ and LPS, cultured macrophages secreted a large quantity of the pro-inflammatory cytokine IL-6 (Fig.5.4A). Treatment with /DIL-1β resulted in the cleavage of VAMP3 especially on high concentration treated samples (Fig. 4B) and inhibition of IL-6 release (Fig. 5.4C). In contrast, the non-targeted control protein /DΔH_C-CS only gave little cleavage and inhibition of IL-6 release even if at the highest concentration tested (Fig. 5.4B and C). We repeated this experiment on primary macrophages isolated from mouse peritoneal cavity. Cultured primary macrophages released IL-6 upon stimulation with IFNγ and LPS to similar extents as RAW264.7 macrophages (Fig. 5.4D). Reassuringly, /DIL-1β entered primary macrophages, truncated VAMP3 and attenuated IL-6 release, unlike the control protein (Fig. 5.4E, F). Note that, neither the targeted nor non-targeted control toxin had an effect on cell viability (Fig. 5.5). Thus, our results confirm that fused IL-1β can deliver BoNT/D protease specifically into macrophages.

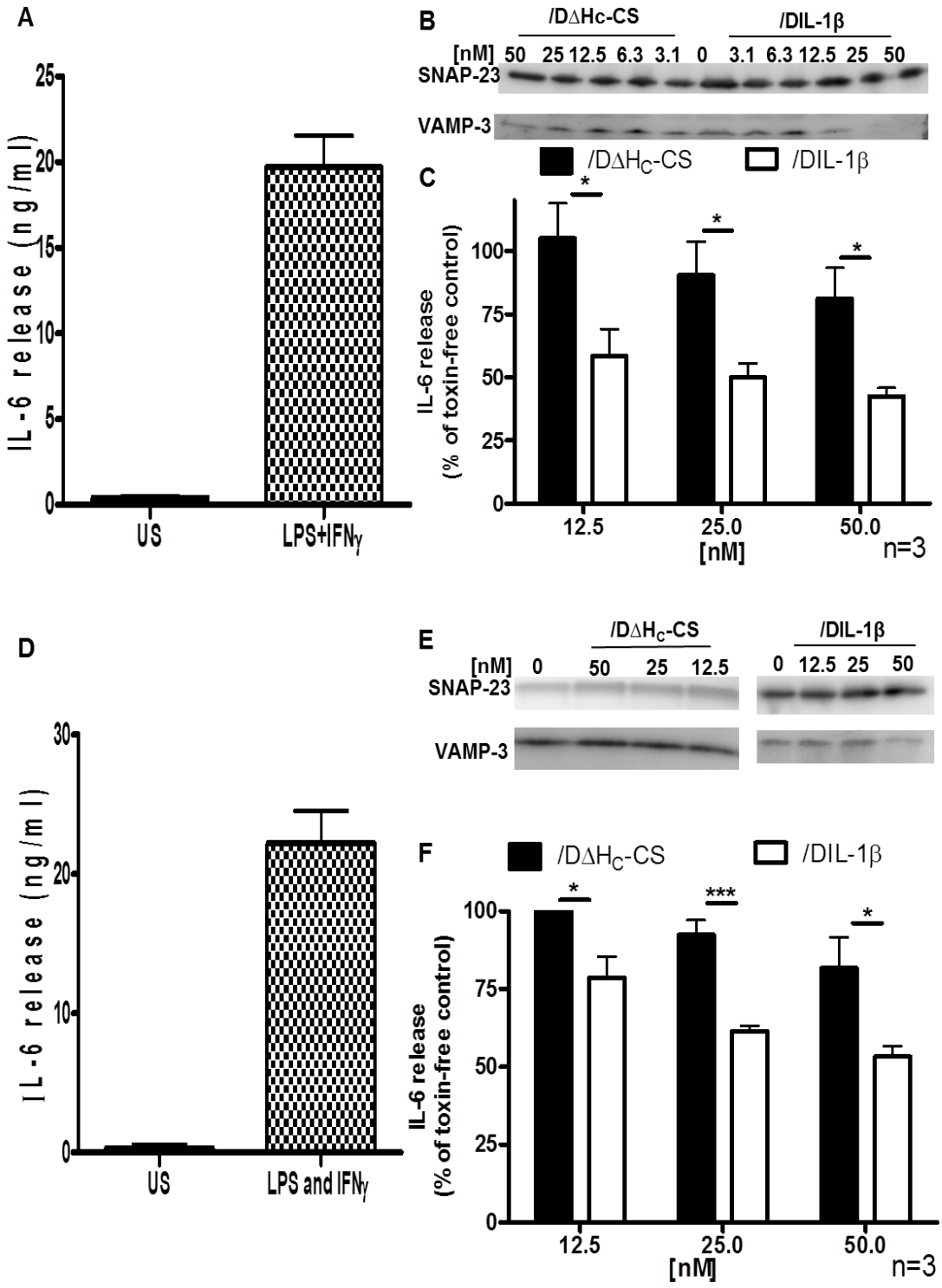

Figure 5.4. /DIL-1β entered the cultured macrophages, cleaved VAMP3 and inhibited evoked IL-6 release, unlike the untargeted control.

A-C. RAW 264.7 cells or **(D-F).** primary mouse macrophage were incubated with medium or various doses of /DIL-1β or /DΔH_C-CS for 6 h. Toxins were then removed and cells were cultured in medium with LPS (100 ng/ml) and IFNγ (500 pg/ml) for 42 h. LPS and IFNγ stimulate similar extents of IL-6 release from RAW 264.7 cells **(A)** and primary mouse macrophage (**D)** compared to US, unstimulated. **B.** Cleavage of VAMP3 in RAW 264.7 cells or (E) primary mouse macrophages by treated proteins was probed by Western blotting. SNAP-23 was probed as an internal loading control. The intensity of VAMP3 was divided by the corresponding internal loading control (SNAP-23) to normalize any variation in loading/protein concentration between wells. VAMP3 remaining after treatment with protein samples was calculated by expressing the above ratio as a % of the toxin free control sample **(C)**. **F.** Inhibition of IL-6 release from cultured primary mouse macrophages by /DIL-1β or /DΔH_C-CS were analyzed as for panels B and C. Data plotted are mean ± S.E.M. (n=3). *: P<0.05, ***: P<0.001.

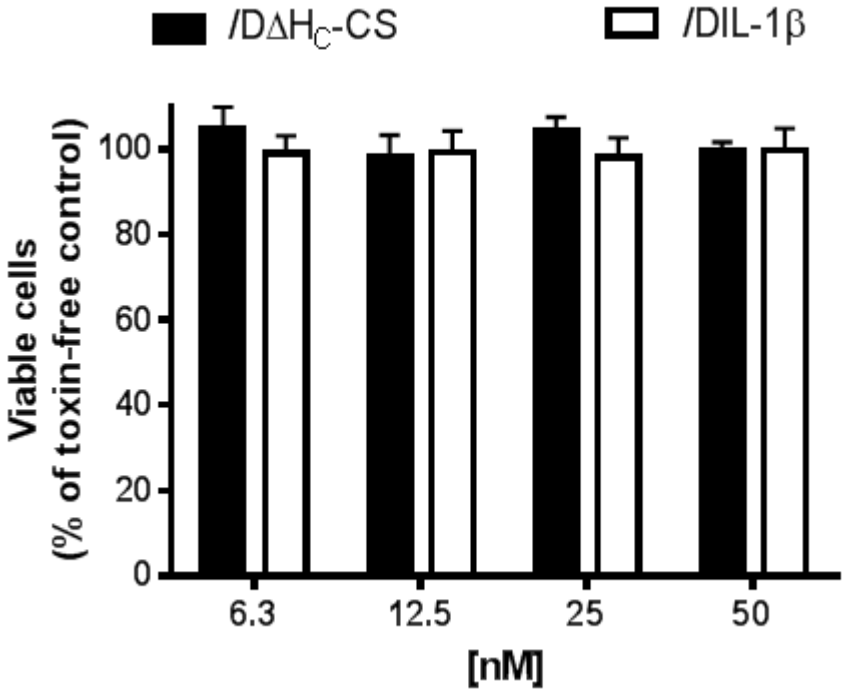

Figure 5.5. Effect of /DIL-1β and /DΔH_C-CS on RAW cell viability.

RAW cells were plated into a 96 well plate with ~ 0.4×10^5 cells/well and cultured for 24 h at 37°C, 5% CO_2. On the following day, the cells were incubated with various doses of

/DIL-1β or /DΔH_C-CS for 44 h, followed by 4 h incubation with alamar blue contained culture medium before reading at absorbance 570 nm. Viable cells after treatment was quantified as a % of the toxin free control sample (vehicle) treated cells. Data graphed are mean ± S.E.M. from 2 independent experiments.

5.2.5 Conjugating a CGRP antagonist to /DΔH_C-CS targets sensory neurons and inhibits pain-peptide release

Our results have confirmed that sortase A enzyme can efficiently ligate the small recombinant protein to the BoNT/D core therapeutic with retention of the biological activities of ligand and SNARE-cleaving protease. To target /DΔH_C-CS into sensory neurons for potential pain relief, we exploited a CGRP antagonist as a targeting ligand because sensory neurons are known to express CGRP receptors (Segond von Banchet et al., 2002). A truncated CGRP peptide, $CGRP_{8-37}$, can bind to CGRP receptor and antagonize CGRP activity (Durham, 2004). After 30 min incubation of a synthesized Gly_3-$CGRP_{8-37}$ peptide with /DΔH_C-CS and sortase A, nearly all of /DΔH_C-CS was ligated to $CGRP_{8-37}$, yielding /D-$CGRP_{8-37}$ conjugate as demonstrated by a shift towards higher molecular size in the SDS-PAGE gel (Fig. 5.6A and B). Anti-CGRP antibody recognized the /D-$CGRP_{8-37}$ sample but not the /DΔH_C-CS (Fig.5.6C), further confirming $CGRP_{8-37}$ successfully conjugated to /DΔH_C-CS. Cultured rat DRGs were incubated with or without /D-$CGRP_{8-37}$ for 24 h before stimulation with 60 mM KCl for 30 min. Depolarization of DRGs stimulated the release of substance P approximately 5-fold over basal release (Fig. 5.6D). Treatment with /D-$CGRP_{8-37}$ led to a significant cleavage of VAMP1 especially at 200 nM (Fig. 5.6E and F) resulting in a substantial reduction of potassium evoked substance P release (Fig. 5.6G). In contrast, non-targeted control protein failed to cleave VAMP1 and inhibit substance P release (Fig.5.6E-G). Thus, our data confirmed that $CGRP_{8-37}$ specifically delivered BoNT/D protease into sensory neurons.

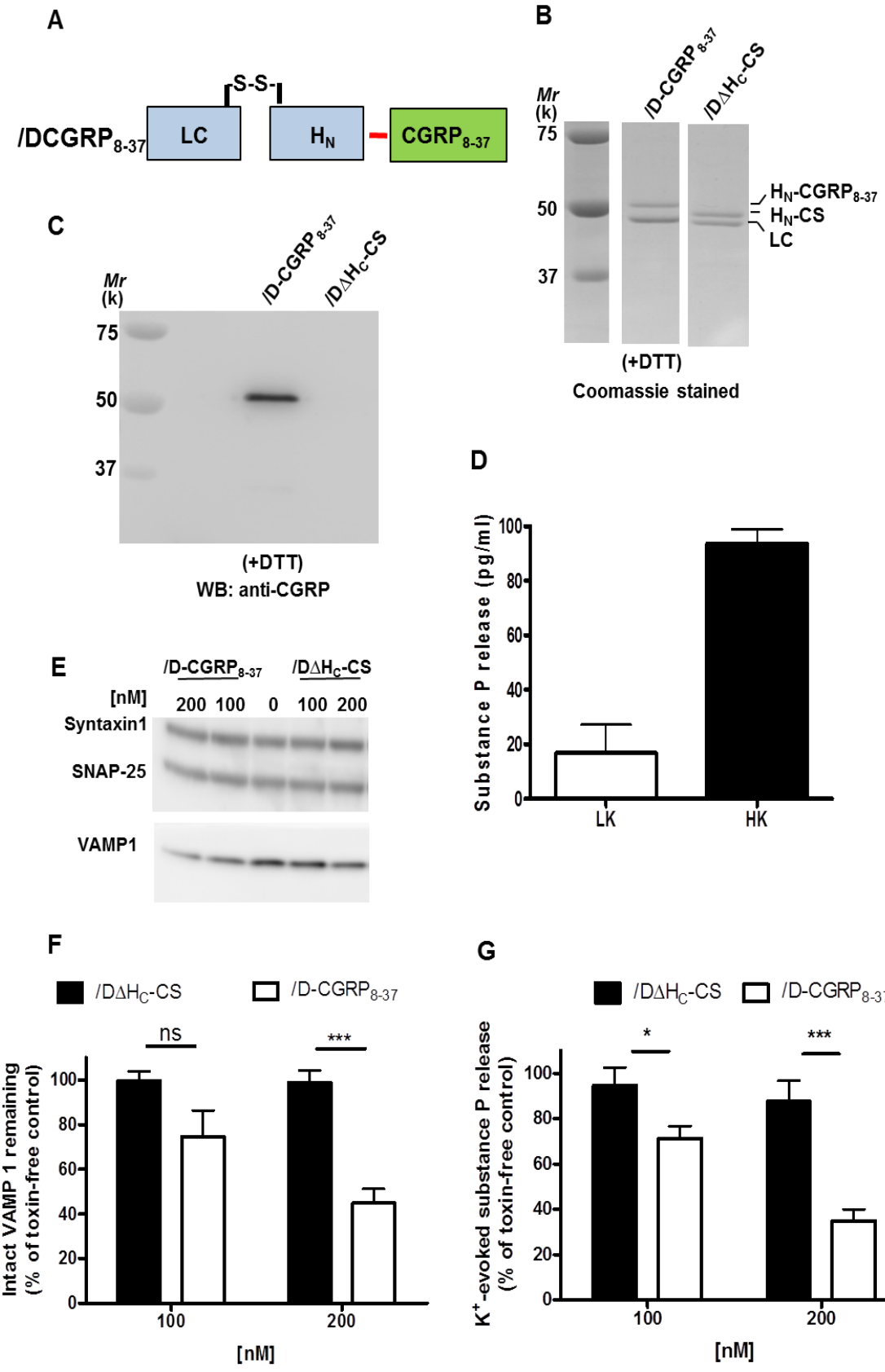
A
S-S
/DCGRP8-37
LC
HN
CGRP8-37
B
Mr
(k)
75
50
37
/D-CGRP8-37
/DΔHC-CS
HN-CGRP8-37
HN-CS
LC
(+DTT)
Coomassie stained
C
Mr
(k)
75
50
37
/D-CGRP8-37
/DΔHC-CS
(+DTT)
WB: anti-CGRP
D
Substance P release (pg/ml)
100
80
60
40
20
0
LK
HK
E
/D-CGRP8-37
/DΔHC-CS
[nM]
200 100 0 100 200
Syntaxin1
SNAP-25
VAMP1
F
/DΔHC-CS
/D-CGRP8-37
ns
***
Intact VAMP 1 remaining
(% of toxin-free control)
100
80
60
40
20
0
100
200
[nM]
G
/DΔHC-CS
/D-CGRP8-37
*
***
K+-evoked substance P release
(% of toxin-free control)
100
80
60
40
20
0
100
200
[nM]

Figure 5.6. Conjugation of $CGRP_{8-37}$ to /DΔH_C-CS yielded /D-$CGRP_{8-37}$ which cleaved VAMP1 and inhibited depolarization evoked substance P release from cultured DRGs.

A. Schematic of /D-$CGRP_{8-37}$. **(B,C)** DTT reduced /D-$CGRP_{8-37}$ and /DΔH_C-CS samples were analyzed by SDS-PAGE followed by Coomassie staining **(B)** or by Western blotting with a rabbit anti-CGRP antibody (1:10,000) **(C)**. **(D-G)** Cultured rat DRGs were incubated with medium and /D-$CGRP_{8-37}$ or control protein for 24 h before stimulation with ~60 mM KCl for 30 min at 37ºC. **D.** Depolarization of DRGs stimulated the release of substance P approximately 5-fold over basal release (LK, low potassium; HK, high potassium). **E.** Representative Western blot showing the cleavage of VAMP1 by /D-$CGRP_{8-37}$ compared to control protein. Syntaxin1 and SNAP-25 were probed as loading control. **D.** Intact VAMP1 remaining after incubating with 100 nM or 200 nM of either protein was calculated by expressing the ratio (intensity of VAMP1/the corresponding internal loading control (Syntaxin1)) as a % of the toxin free control sample. **G.** /D-$CGRP_{8-37}$ but not the control protein attenuated the K^+-evoked substance P release when compared to the toxin-free sample. Data plotted in panel (D), (F) and (G) are mean ± S.E.M. (n=3). ns: non-significant, *: $P<0.05$, and ***: $P<0.001$.

5.3 Discussion

Here we have demonstrated an efficient and robust method for site-specifically ligating recombinantly produced BoNT core-therapeutics to ligands (either recombinant protein or synthesized peptide) for targeted delivery of SNARE-cleaving protease into specific cell types. This strategy is based on the modular structure arrangement of BoNT by replacing the neuronal receptor binding domain with a linker and SrtA motif, and retention of the essential therapeutic domains: SNARE protease and its associated translocation domain. The resultant core-therapeutic is readily ligated to the ligands. Functional tests proved that the engineered targeting BoNT proteases have anti-inflammatory and/or anti-nociceptive potential: bind and enter rodent macrophages or sensory neurons, cleave SNAREs and block evoked release of cytokines or pain peptides.

Production of active botulinum neurotoxins requires strict safety containment not just for the process itself but also for the staff and the laboratory environment. Very few laboratories have the authority to produce these exceptionally potent molecules. This could be achieved by separately expressing two inactive BoNT segments followed by their assembly in reaction tubes in the presence of sortase A. This technology could also be useful for preparing other toxin molecules, such as ricin, diphtheria toxin or Pseudomonas exotoxin. Thus, sortase A mediated ligation technology for producing therapeutic molecules or research tools may offer multiple advantages in addition to no chemical manipulation or activation of the N-peptides and C-peptides: (i) to overcome the safety issues due to toxicity of expressed protein in host (Vazquez-Cintron et al., 2017, Masuyer et al., 2014, Ferrari et al., 2011). Vazquez-Cintron et al. reported a novel type of BoNT/C1 called atoxic derivative (ad) of BoNT/C1 with much lower toxicity compared with wild type BoNT/C1. Atoxic derivative (ad) of BoNT/C1 was recombinantly generated by mutating three amino acid located in the metalloprotease domain of original BoNT/C1. It was then tested on primary cortical neurons and mice and found the toxicity was reduced dramatically (Vazquez-Cintron et al., 2017). (ii) to attach active targeting proteins which require post-modification (Tao et al., 2017, Ferrari et al., 2011).; Natural BoNT/B has lower ability to bind to human synaptotagmin II (h-Syt II) receptor than ~~ability of binding~~ to mouse synaptotagmin II (m-Syt II) receptor (Tao et al., 2017). Dong and his colleagues identified three key amino acids in h-Syt II for assisting BoNT/B binding. After mutating one or two of these amino acids, binding affinity to synaptotagmin II (h-Syt II) was enhanced. This may increase the efficacy of BoNT/ B and reduce side effects (Tao et al., 2017). (iii) to incorporate non-native peptides and/or non-peptidic molecules into proteins (Foster, 2009, Ferrari et al., 2011); In this chapter, we demonstrated synthesised N-terminal Glycine linked $CGRP_{8-37}$ with C-terminal amidation (non-native peptide) successfully ligated to BoNT/DΔH_C-CS (protein) using sortase A mediated ligation technology. (iv) to attach small fluorescent probes to the targeting peptides during synthesis to track the molecules in the targeted cells.

We chose sortase A mediated technology to engineer BoNT based targeted therapeutic candidates as potential for treating RA and/or neuropathic pain. RA poses a major health and economic burden. The pathogenesis of arthritis is not yet fully understood. Nevertheless, the abundance and activation of macrophages in the inflamed synovial membrane/pannus significantly correlate with the severity of RA (Kinne et al., 2000). No arthritis cure exists at present. The advent of the biotherapeutics has now radically changed the approach to treatment, because these can relieve pain in some patients by blocking the effects of endogenous pain mediators, thereby, exerting analgesic and anti-inflammatory actions. Administering monoclonal antibodies against TNFα or IL-6 or their receptors has proved beneficial in clinical therapy of patients with RA (Feldmann, 2002, Ternant et al., 2015). Although these bio-therapeutics have yielded encouraging results, their high price, numerous adverse reactions and diminishing efficacy over time emphasize the urgent need for improved versions. Yeh et al adopted the antibody-mediated delivery method to target BoNT/B protease into macrophages via the Fc and complement receptor-mediated endocytosis pathway. A BoNT/B and an anti-BoNT/B antibody mixture entered macrophages and blocked the release of cytokines (Yeh et al., 2011). Herein, exploiting the presence of IL-1R on the macrophage, we produced the recombinant IL-1β and used it as a targeting ligand to deliver the BoNT/D protease into macrophages. Our results clearly demonstrate that the IL-1β-fused BoNT/D core-therapeutic molecule can enter cultured macrophage cell lines as well as murine primary macrophages because of the observed cleavage of its intracellular targets and eventual blockade of cytokine exocytosis, in contrast to non-targeted control. The current study is also in accord with our earlier findings and other groups' data that VAMP3 is required for IL-6 release from macrophages (Boddul et al., 2014, Manderson et al., 2007).

Substance P and CGRP are well-known pain-peptides which are released from primary nociceptive afferents after peripheral nerve injury and involved in nociception in both the peripheral and the central nervous system (Dubin and Patapoutian, 2010). Peripheral released neuropeptides can regulate various functions of cells, including macrophages, synoviocytes and T cells and augment the production of pro-inflammatory cytokines, prostaglandin E2 or collagenase (Lotz et al., 1987, Delgado et al., 2003, Yaraee et al.,

2003). Thus, developing new therapeutics either inhibiting the release of these two neuropeptides or blocking their receptor activation is fully warranted. $CGRP_{8–37}$ has been demonstrated to inhibit vasodilation and neurogenic inflammation in animal models due to blocking binding of endogenous CGRP to CGRP receptors. However, its clinical effectiveness is limited due to its short half-life (Durham, 2004). Interestingly, Dragon's blood, which is a traditional Chinese medicine, can control inflammation and relieve pain symptoms by inhibiting the secretion of substance P (Li et al., 2012). Moreover, local injection of BoNT/A complexes or recombinantly engineered BoNTs attenuated the neuropathic pain in rodent models (Wang et al., 2017a, Park et al., 2006, Mangione et al., 2016), perhaps by blocking pain-peptide release from peripheral nociceptive fibers. In this study, we select $CGRP_{8-37}$ as a targeting ligand for selectively delivery of BoNT/D protease into sensory neurons with aim to attenuate pain-peptide release. /D-$CGRP_{8-37}$ gave much more pronounced cleavage of VAMP1 and inhibition of depolarization-evoked substance P release from cultured mouse DRGs than non-targeted control proteins, highlighting the specific uptake of BoNT/D protease through the ligated $CGRP_{8-37}$ ligand. Although inhibition of substance P release by /D-$CGRP_{8-37}$ is incomplete, this might be due to only a subpopulation of DRGs expressing CGRP receptor (Segond von Banchet et al., 2002).We also produced $CGRP_{8-37}$ fused BoNT/D core therapeutic fusion protein in *E .coli* which proved lack of significant improvement in SNARE cleavage and inhibition of neuropeptides release from DRGs when compared to non-targeted control protein. It seems that C-terminal amidation of $CGRP_{8-37}$ is essential for targeting efficacy. This hypothesis accords with an earlier finding that replacement of the C-terminal amide in CGRP peptide with a carboxyl results in substantial reduction in human CGRP receptor 1 affinity (Carpenter et al., 2001). This also approves the advantages of using sortase A mediated strategy by independently producing two active therapeutic components. An earlier study reported that incubation of a chemically conjugated substance P-LC/A with cultured neuronal cells cleaved SNAREs and an intracisternal injection of this conjugate decreased thermal hyperalgesia in a mouse model of Taxol induced neuropathic pain (Mustafa et al., 2013). We also tried to use synthesized substance P (Fig.5.7A and B) as targeting ligand and found substance P is slightly less effective than $CGRP_{8-37}$ in delivering BoNT/D protease into DRGs as reflected by the extent of VAMP1 cleavage (Fig. 5.7C).

Overall, in order to deliver SNARE protease into specific neuronal types or non-neuronal cells as relatively new approaches for pain relief, we introduced a new method for protein engineering BoNT-derived targeting molecules as potential therapeutic candidates for treating RA or neuropathic pain. Inhibiting the release of pro-inflammatory cytokines or major pain neuropeptides by these reagents encourages further studies on effects of these candidates on animal models of inflammatory and neuropathic pain.

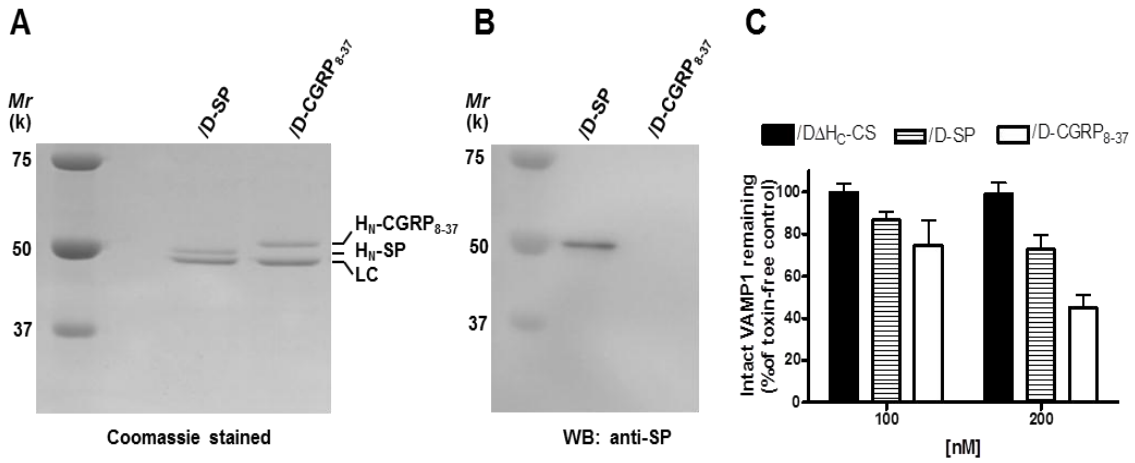

Figure 5.7. Effect of /D-SP conjugate on VAMP1 cleavage in cultured DRGs.

/D-SP conjugate was produced as for /D-CGRP$_{8-37}$. DTT reduced conjugate samples were subjected to SDS-PAGE followed by Coomassie staining (A) or Western blotting using an antibody against substance P (1:2500) (B). (C) Rat DRGs were incubated with /D-SP conjugate for 24 h at 37°C. The cells were then harvested in LDS-sample buffer for Western blotting. Intact VAMP1 remaining after overnight treatment was plotted as % of toxin-free control. SP: substance P. Data are mean ± SEM from two independent experiments. Data for /D-CGRP$_{8-37}$ conjugate and control protein from Fig. 5.6 were replotted here for comparison.

Chapter 6 Conclusion and future work

6.1 Conclusion

6.1.1 Successful production of novel dual targeting BoNT/D based bio-therapeutics with the potential for treating chronic pain

In conclusion, this research project (Chapter 3 and 4) reports that fusion proteins (/DIL-1β, /DRA and /D-Atsttrin) were successfully produced using a recombinant strategy. It reveals that IL-1RA and Atsttrin can be used as targeting ligands to successfully direct the SNARE inactivating protease domain of BoNT into non-neuronal cell types previously resistant to toxin. Both Macrophages and DRGs contain IL-1 and TNF receptor; herein, /DIL-1β, /DRA and /D-Atsttrin for the first time reported are dual targeting therapeutics resulting in blockade of both pro-inflammatory cytokines (TNF-α and IL-6) and neuropeptide (SP) release, enhancing potential therapeutic effects. Therefore, they exhibit therapeutic potential in the area of treatment of chronic inflammatory and neuropathic pain. They will be further confirmed on animal study using proper animal models. If we could obtain desired results, we may do clinical trials on human via local injection.

6.1.2 Developed a protein ligation strategy for conjugating BoNT-core therapeutic domains to cell-specific targeting ligand for re-directing SNARE protease into over-secretory cells.

Many ligands are inactive after production in *E. coli*, as post-translation modification is required. Moreover, some ligands require chemical modification after synthesis. Thus, in this project (Chapter 5), we took /DIL-1β as an example to explore the sortase-mediated protein ligation method as its functional activity has been confirmed in the Chapter 3. Finally, we successfully developed this protein ligation strategy and established a platform for efficiently ligating BoNT-core therapeutic domains (LC-H_N) to the active ligand. This allows us to assess the suitability of an array of ligands for targeting BoNT protease into specific cells to normalise exocytosis of transmitters for potential treatment of hyper-secretory diseases. During the development, two BoNT/D based prototype therapeutic

candidates [/DIL-1β (conjugate) and /D-CGRP$_{8-37}$] have been generated using this method. They demonstrated the ability of cleaving their SNARE substrates and reducing the pro-inflammatory cytokine (IL-6) or substance P release.

6.2 Future work

6.2.1 Animal study

Our *in vitro* studies have confirmed that /DIL-1β, /DRA, /D-Atsttrin and /D-CGRP$_{8-37}$ have therapeutic potential for relieving chronic pain. Their anti-arthritic and –nociceptive activities will be measured in future in rat models of arthritis and neuropathic pain (elaborated below).

6.2.1.1 Investigating the efficacy of engineered candidates in attenuating inflammation and pain in rat chronic monoarthritic pain model

Our initial aim is to generate novel non-toxic, long lasting dual targeting biotherapeutics to treat chronic inflammatory and neuropathic pain. Monoarthritis in the rat is the model used to closely mimic inflammatory pain (Coulthard et al., 2002). It has been used by researchers to study pain transduction and pain relief (Coulthard et al., 2002). Therefore, we plan to use the rat monoarthritis pain model to investigate the ability of potential candidates for controlling chronic inflammatory pain. To achieve this goal, we will use adult male Sprague Dawley rats weighting 150-200 g to build up chronic monoarthritic pain model by injecting complete Freund's adjuvant (CFA) into the unilateral ankle articular cavity (Wang et al., 2017b). After confirming this chronic pain model successfully set up, /DIL-1β, /DRA, /D-Atsttrin, /D-CGRP$_{8-37}$ or saline will be injected into the inflamed ankle. On 7d and 14d after injection, pain behaviour, including infrared thermal imaging, Von Frey hair, transverse diameter ankle joints and ankle perimeter will be tested and measured to assess the effectiveness of /DIL-1β, /DRA, /D-Atsttrin and /D-

$CGRP_{8-37}$. In micro level, spinal cord and DRGs will be dissected from rats used for pain behaviour assessment and then analysed to explore the mechanism of /DIL-1β, /DRA, /D-Atsttrin, and /D-$CGRP_{8-37}$ on analgesia and anti-inflammation using immunofluorescence staining.

6.2.1.2 Using rat OA model to measure the effects of potential candidates on treating chronic inflammatory pain

Beside monoarthritic pain model, animal model of OA is also the useful mean to investigate chronic pain-related behaviour, process and analgesics. Surgeon, chemical inducing and normally occurring are three common methods to build up the OA. We will induce OA in rats by intra-articularly injection of monosodium iodoacetate (MIA) (0.3mg). MIA disrupts the homeostasis in the joint, resulting in damaging joint structures and inducing OA within 3 days after injection (Lampropoulou-Adamidou et al., 2014). Intra-articularly injection of our potential candidates is to be performed and its anti-inflammatory and –nociceptive activities will be assessed using the von Frey hair algesiometry method and immunohistochemical staining of several markers of osteoarthritis (Goudarzi et al., 2018).

6.2.1.3 Spared nerve injury (SNI) model will be used for measuring the efficacy of therapeutics on attenuating chronic neuropathic pain.

Rat SNI model is the model used to closely mimic human neuropathic pain elicited by peripheral nerve injury via a simple surgical procedure (Pertin et al., 2012). Briefly, this surgical procedure stich the tibial nerve and the common peroneal nerve together and keep the sural nerve as intact (Richner et al., 2011). The hind paw of the surgical side appears marked hypersensitivity due to the transduction of pain sensations via the sural nerve only (Richner et al., 2011). The SNI model established in 2000, up to date, it has been developed to a robust, reliable and persisting neuropathic pain model and widely used in anti-hyperalgesic, allodynia and anti-nociception study (Pertin et al., 2012, Wang et al.,

2017a). Our engineered four potential candidates will be tested in the rat SNI model using cold plate, hot plate and Von Frey assays to exam the ability of anti-nociception (Miranda et al., 2017).

References

AMIN, K. 2012. The role of mast cells in allergic inflammation. *Respir Med,* 106**,** 9-14.

ANOLIK, J. H., RAVIKUMAR, R., BARNARD, J., OWEN, T., ALMUDEVAR, A., MILNER, E. C., MILLER, C. H., DUTCHER, P. O., HADLEY, J. A. & SANZ, I. 2008. Cutting edge: anti-tumor necrosis factor therapy in rheumatoid arthritis inhibits memory B lymphocytes via effects on lymphoid germinal centers and follicular dendritic cell networks. *J Immunol,* 180**,** 688-92.

AREND, W. P. 1991. Interleukin 1 receptor antagonist. A new member of the interleukin 1 family. *J Clin Invest,* 88**,** 1445-51.

BARKIN, R. L., BARKIN, S. J. & BARKIN, D. S. 2005. Perception, assessment, treatment, and management of pain in the elderly. *Clin Geriatr Med,* 21**,** 465-90, v.

BARTOK, B. & FIRESTEIN, G. S. 2010. Fibroblast-like synoviocytes: key effector cells in rheumatoid arthritis. *Immunol Rev,* 233**,** 233-55.

BATEMAN, A. & BENNETT, H. P. 2009. The granulin gene family: from cancer to dementia. *Bioessays,* 31**,** 1245-54.

BENDSZUS, M. & STOLL, G. 2003. Caught in the act: in vivo mapping of macrophage infiltration in nerve injury by magnetic resonance imaging. *J Neurosci,* 23**,** 10892-6.

BENEMEI, S., NICOLETTI, P., CAPONE, J. G. & GEPPETTI, P. 2009. CGRP receptors in the control of pain and inflammation. *Curr Opin Pharmacol,* 9**,** 9-14.

BENYAMIN, R., TRESCOT, A. M., DATTA, S., BUENAVENTURA, R., ADLAKA, R., SEHGAL, N., GLASER, S. E. & VALLEJO, R. 2008. Opioid complications and side effects. *Pain Physician,* 11**,** S105-20.

BESSON, J. M. 1999. The neurobiology of pain. *Lancet,* 353**,** 1610-5.

BINDER, W. J., BRIN, M. F., BLITZER, A., SCHOENROCK, L. D. & POGODA, J. M. 2000. Botulinum toxin type A (BOTOX) for treatment of migraine headaches: an open-label study. *Otolaryngol Head Neck Surg,* 123**,** 669-76.

BINZ, T., SIKORRA, S. & MAHRHOLD, S. 2010. Clostridial neurotoxins: mechanism of SNARE cleavage and outlook on potential substrate specificity reengineering. *Toxins (Basel),* 2**,** 665-82.

BLACK, R. A., RAUCH, C. T., KOZLOSKY, C. J., PESCHON, J. J., SLACK, J. L., WOLFSON, M. F., CASTNER, B. J., STOCKING, K. L., REDDY, P., SRINIVASAN, S., NELSON, N., BOIANI, N., SCHOOLEY, K. A., GERHART, M., DAVIS, R., FITZNER, J. N., JOHNSON, R. S., PAXTON, R. J., MARCH, C. J. & CERRETTI, D. P. 1997. A metalloproteinase disintegrin that releases tumour-necrosis factor-alpha from cells. *Nature,* 385**,** 729-33.

BODDUL, S. V., MENG, J., DOLLY, J. O. & WANG, J. 2014. SNAP-23 and VAMP-3 contribute to the release of IL-6 and TNFalpha from a human synovial sarcoma cell line. *FEBS J,* 281**,** 750-65.

BOUDREAU, G. P., GROSBERG, B. M., MCALLISTER, P. J., LIPTON, R. B. & BUSE, D. C. 2015. Prophylactic onabotulinumtoxinA in patients with chronic migraine and comorbid depression: An open-label, multicenter, pilot study of efficacy, safety and effect on headache-related disability, depression, and anxiety. *Int J Gen Med,* 8**,** 79-86.

BRAIN, S. D. 1997. Sensory neuropeptides: their role in inflammation and wound healing. *Immunopharmacology,* 37**,** 133-52.

BREIVIK, H., COLLETT, B., VENTAFRIDDA, V., COHEN, R. & GALLACHER, D. 2006. Survey of chronic pain in Europe: prevalence, impact on daily life, and treatment. *Eur J Pain,* 10**,** 287-333.

BREMER, E. 2013. Targeting of the tumor necrosis factor receptor superfamily for cancer immunotherapy. *ISRN Oncol,* 2013**,** 371854.

BRENNAN, F., CARR, D. B. & COUSINS, M. 2007. Pain management: a fundamental human right. *Anesth Analg,* 105**,** 205-21.

BRUCK, W. 1997. The role of macrophages in Wallerian degeneration. *Brain Pathol,* 7**,** 741-52.

BUHLMANN, N., LEUTHAUSER, K., MUFF, R., FISCHER, J. A. & BORN, W. 1999. A receptor activity modifying protein (RAMP)2-dependent adrenomedullin

receptor is a calcitonin gene-related peptide receptor when coexpressed with human RAMP1. *Endocrinology,* 140**,** 2883-90.

CARE, S. C. O. T. A. I. H. 2006. Methods of treating chronic pain. *Methods of Treating Chronic Pain: A Systematic Review*. 177,1771-2.

CARPENTER, K. A., SCHMIDT, R., VON MENTZER, B., HAGLUND, U., ROBERTS, E. & WALPOLE, C. 2001. Turn structures in CGRP C-terminal analogues promote stable arrangements of key residue side chains. *Biochemistry,* 40**,** 8317-25.

CARR, C. M. & MUNSON, M. 2007. Tag team action at the synapse. *EMBO Rep,* 8**,** 834-8.

CAYMAN 2013. Substance P EIA Kit Item No. 583751.

CHADDOCK, J. A., PURKISS, J. R., DUGGAN, M. J., QUINN, C. P., SHONE, C. C. & FOSTER, K. A. 2000. A conjugate composed of nerve growth factor coupled to a non-toxic derivative of Clostridium botulinum neurotoxin type A can inhibit neurotransmitter release in vitro. *Growth Factors,* 18**,** 147-55.

CHANG, J. H., LEE, K. J., KIM, S. K., YOO, D. H. & KANG, T. Y. 2014. Validity of SW982 synovial cell line for studying the drugs against rheumatoid arthritis in fluvastatin-induced apoptosis signaling model. *Indian J Med Res,* 139**,** 117-24.

CHANG, S. K., GU, Z. & BRENNER, M. B. 2010. Fibroblast-like synoviocytes in inflammatory arthritis pathology: the emerging role of cadherin-11. *Immunol Rev,* 233**,** 256-66.

CHERYL L. STUCKY, M. S. G., AND XU ZHANG 2001. Mechanisms of pain. *PNAS,* 98**,** 11845-11846.

CHIZZONITE, R., TRUITT, T., KILIAN, P. L., STERN, A. S., NUNES, P., PARKER, K. P., KAFFKA, K. L., CHUA, A. O., LUGG, D. K. & GUBLER, U. 1989. Two high-affinity interleukin 1 receptors represent separate gene products. *Proc. Natl. Acad. Sci. U.S.A.,* 86**,** 8029-8033.

CLARK, I. A. 2007. How TNF was recognized as a key mechanism of disease. *Cytokine Growth Factor Rev,* 18**,** 335-43.

CONDON, D. 2010. Chronic pain services severely lacking. [Online] Aailable http://www.irishhealth.com/article.html?id=18139 Last accessed: 7th September, 2018.

CORREALE, J. & VILLA, A. 2004. The neuroprotective role of inflammation in nervous system injuries. *J Neurol,* 251**,** 1304-16.

COULTHARD, P., PLEUVRY, B. J., BREWSTER, M., WILSON, K. L. & MACFARLANE, T. V. 2002. Gait analysis as an objective measure in a chronic pain model. *J Neurosci Methods,* 116**,** 197-213.

DAVID J. DRIPPS, B. J. B., ROBERT C. THOMPSON, AND STEPHEN P. EISENBERG 1991. Interleukin- 1 (IL-1) Receptor Antagonist Binds to the 80-kDa IL-1 Receptor but Does Not Initiate IL-1 Signal Transduction. *The Journal of Biological Chemistry* 266**,** 10331-10336.

DE JONGH, R. F., VISSERS, K. C., MEERT, T. F., BOOIJ, L. H., DE DEYNE, C. S. & HEYLEN, R. J. 2003. The role of interleukin-6 in nociception and pain. *Anesth Analg,* 96**,** 1096-103.

DELGADO, A. V., MCMANUS, A. T. & CHAMBERS, J. P. 2003. Production of tumor necrosis factor-alpha, interleukin 1-beta, interleukin 2, and interleukin 6 by rat leukocyte subpopulations after exposure to substance P. *Neuropeptides,* 37**,** 355-61.

DINARELLO, C. A. 1991. Interleukin-1 and interleukin-1 antagonism. *Blood,* 77**,** 1627-52.

DINARELLO, C. A. 1999. Overview of inflammatory cytokines and their role in pain. *In: Watkins, L.R., Maier, S.F. (Eds.), Cytokines and Pain.***,** 1–19.

DIONNE, R. A., MAX, M. B., GORDON, S. M., PARADA, S., SANG, C., GRACELY, R. H., SETHNA, N. F. & MACLEAN, D. B. 1998. The substance P receptor antagonist CP-99,994 reduces acute postoperative pain. *Clin Pharmacol Ther,* 64**,** 562-8.

DOLLY, J. O., LAWRENCE, G. W., MENG, J., WANG, J. & OVSEPIAN, S. V. 2009. Neuro-exocytosis: botulinum toxins as inhibitory probes and versatile therapeutics. *Curr Opin Pharmacol,* 9**,** 326-35.

DOLLY, J. O., WANG, J., ZURAWSKI, T. H. & MENG, J. 2011. Novel therapeutics based on recombinant botulinum neurotoxins to normalize the release of transmitters and pain mediators. *FEBS J,* 278**,** 4454-66.

DUBIN, A. E. & PATAPOUTIAN, A. 2010. Nociceptors: the sensors of the pain pathway. *J Clin Invest,* 120**,** 3760-72.

DUGGAN, M. J., QUINN, C. P., CHADDOCK, J. A., PURKISS, J. R., ALEXANDER, F. C., DOWARD, S., FOOKS, S. J., FRIIS, L. M., HALL, Y. H., KIRBY, E. R., LEEDS, N., MOULSDALE, H. J., DICKENSON, A., GREEN, G. M., RAHMAN, W., SUZUKI, R., SHONE, C. C. & FOSTER, K. A. 2002. Inhibition of release of neurotransmitters from rat dorsal root ganglia by a novel conjugate of a Clostridium botulinum toxin A endopeptidase fragment and Erythrina cristagalli lectin. *J Biol Chem,* 277**,** 34846-52.

DURHAM, P. L. 2004. CGRP-receptor antagonists--a fresh approach to migraine therapy? *N Engl J Med,* 350**,** 1073-5.

DURHAM, P. L. 2006. Calcitonin gene-related peptide (CGRP) and migraine. *Headache,* 46 Suppl 1**,** S3-8.

FELDMANN, M. 2002. Development of anti-TNF therapy for rheumatoid arthritis. *Nat Rev Immunol,* 2**,** 364-71.

FENG, J. Q., GUO, F. J., JIANG, B. C., ZHANG, Y., FRENKEL, S., WANG, D. W., TANG, W., XIE, Y. & LIU, C. J. 2010. Granulin epithelin precursor: a bone morphogenic protein 2-inducible growth factor that activates Erk1/2 signaling and JunB transcription factor in chondrogenesis. *FASEB J,* 24**,** 1879-92.

FERRARI, E., MAYWOOD, E. S., RESTANI, L., CALEO, M., PIRAZZINI, M., ROSSETTO, O., HASTINGS, M. H., NIRANJAN, D., SCHIAVO, G. & DAVLETOV, B. 2011. Re-assembled botulinum neurotoxin inhibits CNS functions without systemic toxicity. *Toxins (Basel),* 3**,** 345-55.

FERREIRA, S. H., LORENZETTI, B. B., BRISTOW, A. F. & POOLE, S. 1988. Interleukin-1 beta as a potent hyperalgesic agent antagonized by a tripeptide analogue. *Nature,* 334**,** 698-700.

FOLLENFANT, R. L., NAKAMURA-CRAIG, M., HENDERSON, B. & HIGGS, G. A. 1989. Inhibition by neuropeptides of interleukin-1 beta-induced, prostaglandin-independent hyperalgesia. *Br J Pharmacol,* 98**,** 41-3.

FOSTER, K. A. 2009. Engineered toxins: new therapeutics. *Toxicon,* 54**,** 587-92.

FOX, D. A., GIZINSKI, A., MORGAN, R. & LUNDY, S. K. 2010. Cell-cell interactions in rheumatoid arthritis synovium. *Rheum Dis Clin North Am,* 36**,** 311-23.

FRYMOYER, J. W. 1988. Back Pain and Sciatica. *N Engl J Med* 318**,** 291-300.

FU, Z., CHEN, C., BARBIERI, J. T., KIM, J. J. & BALDWIN, M. R. 2009. Glycosylated SV2 and gangliosides as dual receptors for botulinum neurotoxin serotype F. *Biochemistry,* 48**,** 5631-41.

FUKUOKA, H., KAWATANI, M., HISAMITSU, T. & TAKESHIGE, C. 1994. Cutaneous hyperalgesia induced by peripheral injection of interleukin-1 beta in the rat. *Brain Res,* 657**,** 133-40.

GOUDARZI, R., REID, A. & MCDOUGALL, J. J. 2018. Evaluation of the novel avocado/soybean unsaponifiable Arthrocen to alter joint pain and inflammation in a rat model of osteoarthritis. *PLoS One,* 13**,** e0191906.

GRAZIOTTIN, A., SKAPER, S. D. & FUSCO, M. 2014. Mast cells in chronic inflammation, pelvic pain and depression in women. *Gynecol Endocrinol,* 30**,** 472-7.

GROTHE, C., HEESE, K., MEISINGER, C., WEWETZER, K., KUNZ, D., CATTINI, P. & OTTEN, U. 2000. Expression of interleukin-6 and its receptor in the sciatic nerve and cultured Schwann cells: relation to 18-kD fibroblast growth factor-2. *Brain Res,* 885**,** 172-81.

HALDEMAN, S. D. A. S. 2012. Adjunctive Analgesics. *Evidence-based Management of Low Back Pain*.

HANAHAN, D., JESSEE, J. & BLOOM, F. R. 1991. Plasmid transformation of Escherichia coli and other bacteria. *Methods Enzymol,* 204**,** 63-113.

HARRISON, S. & GEPPETTI, P. 2001. Substance p. *Int J Biochem Cell Biol,* 33**,** 555-76.

HRABAL, R., CHEN, Z., JAMES, S., BENNETT, H. P. & NI, F. 1996. The hairpin stack fold, a novel protein architecture for a new family of protein growth factors. *Nat Struct Biol,* 3**,** 747-52.

HU, P. & MCLACHLAN, E. M. 2002. Macrophage and lymphocyte invasion of dorsal root ganglia after peripheral nerve lesions in the rat. *Neuroscience,* 112**,** 23-38.

IDRISS, H. T. & NAISMITH, J. H. 2000. TNF alpha and the TNF receptor superfamily: structure-function relationship(s). *Microsc Res Tech,* 50**,** 184-95.

INVITROGEN™ 2008. Click-iT® EdU Microplate Assay Catalog no. C10214.

JI, H., PETTIT, A., OHMURA, K., ORTIZ-LOPEZ, A., DUCHATELLE, V., DEGOTT, C., GRAVALLESE, E., MATHIS, D. & BENOIST, C. 2002. Critical roles for

interleukin 1 and tumor necrosis factor alpha in antibody-induced arthritis. *J Exp Med,* 196**,** 77-85.

JI, R. R. 2004. Peripheral and central mechanisms of inflammatory pain, with emphasis on MAP kinases. *Curr Drug Targets Inflamm Allergy,* 3**,** 299-303.

JIAN, J., KONOPKA, J. & LIU, C. 2013. Insights into the role of progranulin in immunity, infection, and inflammation. *J Leukoc Biol,* 93**,** 199-208.

JIN, R., RUMMEL, A., BINZ, T. & BRUNGER, A. T. 2006. Botulinum neurotoxin B recognizes its protein receptor with high affinity and specificity. *Nature,* 444**,** 1092-5.

JONES, R. 2001. Nonsteroidal anti-inflammatory drug prescribing: past, present, and future. *Am J Med,* 110**,** 4S-7S.

KAWABATA, A., KAWAO, N., KURODA, R., TANAKA, A., ITOH, H. & NISHIKAWA, H. 2001. Peripheral PAR-2 triggers thermal hyperalgesia and nociceptive responses in rats. *Neuroreport,* 12**,** 715-9.

KIDD, B. L. & URBAN, L. A. 2001. Mechanisms of inflammatory pain. *Br J Anaesth,* 87**,** 3-11.

KINNE, R. W., BRAUER, R., STUHLMULLER, B., PALOMBO-KINNE, E. & BURMESTER, G. R. 2000. Macrophages in rheumatoid arthritis. *Arthritis Res,* 2**,** 189-202.

KREMER, J. M., BLANCO, R., BRZOSKO, M., BURGOS-VARGAS, R., HALLAND, A. M., VERNON, E., AMBS, P. & FLEISCHMANN, R. 2011. Tocilizumab inhibits structural joint damage in rheumatoid arthritis patients with inadequate responses to methotrexate: results from the double-blind treatment phase of a randomized placebo-controlled trial of tocilizumab safety and prevention of structural joint damage at one year. *Arthritis Rheum,* 63**,** 609-21.

KULKA, M., SHEEN, C. H., TANCOWNY, B. P., GRAMMER, L. C. & SCHLEIMER, R. P. 2008. Neuropeptides activate human mast cell degranulation and chemokine production. *Immunology,* 123**,** 398-410.

LACY, D. B., TEPP, W., COHEN, A. C., DASGUPTA, B. R. & STEVENS, R. C. 1998. Crystal structure of botulinum neurotoxin type A and implications for toxicity. *Nat Struct Biol,* 5**,** 898-902.

LAMPROPOULOU-ADAMIDOU, K., LELOVAS, P., KARADIMAS, E. V., LIAKOU, C., TRIANTAFILLOPOULOS, I. K., DONTAS, I. & PAPAIOANNOU, N. A. 2014. Useful animal models for the research of osteoarthritis. *Eur J Orthop Surg Traumatol,* 24**,** 263-71.

LAWRENCE, G., WANG, J., CHION, C. K., AOKI, K. R. & DOLLY, J. O. 2007. Two protein trafficking processes at motor nerve endings unveiled by botulinum neurotoxin E. *J Pharmacol Exp Ther,* 320**,** 410-8.

LAZARCZYK, M., MATYJA, E. & LIPKOWSKI, A. 2007. Substance P and its receptors -- a potential target for novel medicines in malignant brain tumour therapies (mini-review). *Folia Neuropathol,* 45**,** 99-107.

LEE, H. L., LEE, K. M., SON, S. J., HWANG, S. H. & CHO, H. J. 2004. Temporal expression of cytokines and their receptors mRNAs in a neuropathic pain model. *Neuroreport,* 15**,** 2807-11.

LI, M., SHI, J., TANG, J. R., CHEN, D., AI, B., CHEN, J., WANG, L. N., CAO, F. Y., LI, L. L., LIN, C. Y. & GUAN, X. M. 2005. Effects of complete Freund's adjuvant on immunohistochemical distribution of IL-1beta and IL-1R I in neurons and glia cells of dorsal root ganglion. *Acta Pharmacol Sin,* 26**,** 192-8.

LI, Y. S., WANG, J. X., JIA, M. M., LIU, M., LI, X. J. & TANG, H. B. 2012. Dragon's blood inhibits chronic inflammatory and neuropathic pain responses by blocking the synthesis and release of substance P in rats. *J Pharmacol Sci,* 118**,** 43-54.

LIU, C. J. 2011. Progranulin: a promising therapeutic target for rheumatoid arthritis. *FEBS Lett,* 585**,** 3675-80.

LIU, T., VAN ROOIJEN, N. & TRACEY, D. J. 2000. Depletion of macrophages reduces axonal degeneration and hyperalgesia following nerve injury. *Pain,* 86**,** 25-32.

LOCKSLEY, R. M., KILLEEN, N. & LENARDO, M. J. 2001. The TNF and TNF receptor superfamilies: integrating mammalian biology. *Cell,* 104**,** 487-501.

LORENTZ, A., SELLGE, G. & BISCHOFF, S. C. 2015. Isolation and characterization of human intestinal mast cells. *Methods Mol Biol,* 1220**,** 163-77.

LOTZ, M., CARSON, D. A. & VAUGHAN, J. H. 1987. Substance P activation of rheumatoid synoviocytes: neural pathway in pathogenesis of arthritis. *Science,* 235**,** 893-5.

MA, H., MENG, J., WANG, J., HEARTY, S., DOLLY, J. O. & O'KENNEDY, R. 2014. Targeted delivery of a SNARE protease to sensory neurons using a single chain antibody (scFv) against the extracellular domain of P2X(3) inhibits the release of a pain mediator. *Biochem J,* 462**,** 247-56.

MA, Y. & POPE, R. M. 2005. The role of macrophages in rheumatoid arthritis. *Curr Pharm Des,* 11**,** 569-80.

MANDERSON, A. P., KAY, J. G., HAMMOND, L. A., BROWN, D. L. & STOW, J. L. 2007. Subcompartments of the macrophage recycling endosome direct the differential secretion of IL-6 and TNFalpha. *J Cell Biol,* 178**,** 57-69.

MANGIONE, A. S., OBARA, I., MAIARU, M., GERANTON, S. M., TASSORELLI, C., FERRARI, E., LEESE, C., DAVLETOV, B. & HUNT, S. P. 2016. Nonparalytic botulinum molecules for the control of pain. *Pain,* 157**,** 1045-55.

MAO, H., HART, S. A., SCHINK, A. & POLLOK, B. A. 2004. Sortase-mediated protein ligation: a new method for protein engineering. *J Am Chem Soc,* 126**,** 2670-1.

MARCHAND, F., PERRETTI, M. & MCMAHON, S. B. 2005. Role of the immune system in chronic pain. *Nat Rev Neurosci,* 6**,** 521-32.

MASUYER, G., CHADDOCK, J. A., FOSTER, K. A. & ACHARYA, K. R. 2014. Engineered botulinum neurotoxins as new therapeutics. *Annu Rev Pharmacol Toxicol,* 54**,** 27-51.

MAXWELL, L. J., ZOCHLING, J., BOONEN, A., SINGH, J. A., VERAS, M. M., TANJONG GHOGOMU, E., BENKHALTI JANDU, M., TUGWELL, P. & WELLS, G. A. 2015. TNF-alpha inhibitors for ankylosing spondylitis. *Cochrane Database Syst Rev***,** CD005468.

MCINNES, I. B. & SCHETT, G. 2011. The pathogenesis of rheumatoid arthritis. *N Engl J Med,* 365**,** 2205-19.

MENG, J., OVSEPIAN, S. V., WANG, J., PICKERING, M., SASSE, A., AOKI, K. R., LAWRENCE, G. W. & DOLLY, J. O. 2009. Activation of TRPV1 mediates calcitonin gene-related peptide release, which excites trigeminal sensory neurons and is attenuated by a retargeted botulinum toxin with anti-nociceptive potential. *J Neurosci,* 29**,** 4981-92.

MENG, J. & WANG, J. 2015. Role of SNARE proteins in tumourigenesis and their potential as targets for novel anti-cancer therapeutics. *Biochim Biophys Acta,* 1856**,** 1-12.

MENG, J., WANG, J., LAWRENCE, G. & DOLLY, J. O. 2007. Synaptobrevin I mediates exocytosis of CGRP from sensory neurons and inhibition by botulinum toxins reflects their anti-nociceptive potential. *J Cell Sci,* 120**,** 2864-74.

MENG, J., WANG, J., STEINHOFF, M. & DOLLY, J. O. 2016. TNFalpha induces co-trafficking of TRPV1/TRPA1 in VAMP1-containing vesicles to the plasmalemma via Munc18-1/syntaxin1/SNAP-25 mediated fusion. *Sci Rep,* 6**,** 21226.

MICHEAU, O. & TSCHOPP, J. 2003. Induction of TNF receptor I-mediated apoptosis via two sequential signaling complexes. *Cell,* 114**,** 181-90.

MIRANDA, H. F., SIERRALTA, F., ARANDA, N., POBLETE, P., CASTILLO, R. L., NORIEGA, V. & PRIETO, J. C. 2017. Antinociception induced by rosuvastatin in murine neuropathic pain. *Pharmacol Rep,* 70**,** 503-508.

MOALEM, G. & TRACEY, D. J. 2006. Immune and inflammatory mechanisms in neuropathic pain. *Brain Res Rev,* 51**,** 240-64.

MONTAL, M. 2010. Botulinum neurotoxin: a marvel of protein design. *Annu Rev Biochem,* 79**,** 591-617.

MULLER-LADNER, U., PAP, T., GAY, R. E., NEIDHART, M. & GAY, S. 2005. Mechanisms of disease: the molecular and cellular basis of joint destruction in rheumatoid arthritis. *Nat Clin Pract Rheumatol,* 1**,** 102-10.

MURRAY, R. Z., KAY, J. G., SANGERMANI, D. G. & STOW, J. L. 2005. A role for the phagosome in cytokine secretion. *Science,* 310**,** 1492-5.

MURRAY, R. Z. & STOW, J. L. 2014. Cytokine Secretion in Macrophages: SNAREs, Rabs, and Membrane Trafficking. *Front Immunol,* 5**,** 538.

MUSTAFA, G., ANDERSON, E. M., BOKRAND-DONATELLI, Y., NEUBERT, J. K. & CAUDLE, R. M. 2013. Anti-nociceptive effect of a conjugate of substance P and light chain of botulinum neurotoxin type A. *Pain,* 154**,** 2547-53.

NATHAN, C. F. 1987. Secretory products of macrophages. *J Clin Invest,* 79**,** 319-26.

NEY, J. P. & JOSEPH, K. R. 2007. Neurologic uses of botulinum neurotoxin type A. *Neuropsychiatr Dis Treat,* 3**,** 785-98.

NOSS, E. H. & BRENNER, M. B. 2008. The role and therapeutic implications of fibroblast-like synoviocytes in inflammation and cartilage erosion in rheumatoid arthritis. *Immunol Rev,* 223**,** 252-70.

O'CALLAGHAN, J. P. & MILLER, D. B. 2010. Spinal glia and chronic pain. *Metabolism,* 59 Suppl 1**,** S21-6.

O'CONNOR, T. M., O'CONNELL, J., O'BRIEN, D. I., GOODE, T., BREDIN, C. P. & SHANAHAN, F. 2004. The role of substance P in inflammatory disease. *J Cell Physiol,* 201**,** 167-80.

OH, H. M. & CHUNG, M. E. 2015. Botulinum Toxin for Neuropathic Pain: A Review of the Literature. *Toxins (Basel),* 7**,** 3127-54.

OLSSON, Y. 1968. Mast cells in the nervous system. *Int Rev Cytol,* 24**,** 27-70.

PARK, H. J., LEE, Y., LEE, J., PARK, C. & MOON, D. E. 2006. The effects of botulinum toxin A on mechanical and cold allodynia in a rat model of neuropathic pain. *Can J Anaesth,* 53**,** 470-7.

PENG, L., TEPP, W. H., JOHNSON, E. A. & DONG, M. 2011. Botulinum neurotoxin D uses synaptic vesicle protein SV2 and gangliosides as receptors. *PLoS Pathog,* 7**,** e1002008.

PENNEFATHER, J. N., LECCI, A., CANDENAS, M. L., PATAK, E., PINTO, F. M. & MAGGI, C. A. 2004. Tachykinins and tachykinin receptors: a growing family. *Life Sci,* 74**,** 1445-63.

PERKINS, N. M. & TRACEY, D. J. 2000. Hyperalgesia due to nerve injury: role of neutrophils. *Neuroscience,* 101**,** 745-57.

PERTIN, M., GOSSELIN, R. D. & DECOSTERD, I. 2012. The spared nerve injury model of neuropathic pain. *Methods Mol Biol,* 851**,** 205-12.

PHILLIPS, C. J. 2009 The cost and burden of chronic pain *British Journal of pain* 3**,** 2-5.

RAO, P. & KNAUS, E. E. 2008. Evolution of nonsteroidal anti-inflammatory drugs (NSAIDs): cyclooxygenase (COX) inhibition and beyond. *J Pharm Pharm Sci,* 11**,** 81s-110s.

REN, K. & TORRES, R. 2009. Role of interleukin-1beta during pain and inflammation. *Brain Res Rev,* 60**,** 57-64.

RICHNER, M., BJERRUM, O. J., NYKJAER, A. & VAEGTER, C. B. 2011. The spared nerve injury (SNI) model of induced mechanical allodynia in mice. *J Vis Exp*.

SACHA A MALIN, B. M. D., DEREK C MOLLIVER 2007. Production of dissociated sensory neuron cultures and considerations for their use in studying neuronal function and plasticity. *Nature Protocols,* 2**,** 152 - 160.

SAPUNAR, D., KOSTIC, S., BANOZIC, A. & PULJAK, L. 2012. Dorsal root ganglion - a potential new therapeutic target for neuropathic pain. *J Pain Res,* 5**,** 31-8.

SCHAFERS, M., BRINKHOFF, J., NEUKIRCHEN, S., MARZINIAK, M. & SOMMER, C. 2001. Combined epineurial therapy with neutralizing antibodies to tumor necrosis factor-alpha and interleukin-1 receptor has an additive effect in reducing neuropathic pain in mice. *Neurosci Lett,* 310**,** 113-6.

SCHAFERS, M., LEE, D. H., BRORS, D., YAKSH, T. L. & SORKIN, L. S. 2003a. Increased sensitivity of injured and adjacent uninjured rat primary sensory neurons to exogenous tumor necrosis factor-alpha after spinal nerve ligation. *J Neurosci,* 23**,** 3028-38.

SCHAFERS, M., SVENSSON, C. I., SOMMER, C. & SORKIN, L. S. 2003b. Tumor necrosis factor-alpha induces mechanical allodynia after spinal nerve ligation by activation of p38 MAPK in primary sensory neurons. *J Neurosci,* 23**,** 2517-21.

SCHAIBLE, H.-G. 2014. Nociceptive neurons detect cytokines in arthritis. *Arthritis Research & Therapy,* 16**,** 470.

SCHELLER, J., CHALARIS, A., SCHMIDT-ARRAS, D. & ROSE-JOHN, S. 2011. The pro- and anti-inflammatory properties of the cytokine interleukin-6. *Biochim Biophys Acta,* 1813**,** 878-88.

SCIMECA, M. M., SAVAGE, S. R., PORTENOY, R. & LOWINSON, J. 2000. Treatment of pain in methadone-maintained patients. *Mt Sinai J Med,* 67**,** 412-22.

SEGOND VON BANCHET, G., PASTOR, A., BISKUP, C., SCHLEGEL, C., BENNDORF, K. & SCHAIBLE, H. G. 2002. Localization of functional calcitonin gene-related peptide binding sites in a subpopulation of cultured dorsal root ganglion neurons. *Neuroscience,* 110**,** 131-45.

SHAO, Z., BROWNING, J. L., LEE, X., SCOTT, M. L., SHULGA-MORSKAYA, S., ALLAIRE, N., THILL, G., LEVESQUE, M., SAH, D., MCCOY, J. M.,

MURRAY, B., JUNG, V., PEPINSKY, R. B. & MI, S. 2005. TAJ/TROY, an orphan TNF receptor family member, binds Nogo-66 receptor 1 and regulates axonal regeneration. *Neuron,* 45**,** 353-9.

SHERRY, J. 2018. OVERVIEW OF LOWER BACK PAIN. *Somerton Physiotherapy*.

SOMMER, C. & KRESS, M. 2004. Recent findings on how proinflammatory cytokines cause pain: peripheral mechanisms in inflammatory and neuropathic hyperalgesia. *Neurosci Lett,* 361**,** 184-7.

SOMMER, C., MARZINIAK, M. & MYERS, R. R. 1998a. The effect of thalidomide treatment on vascular pathology and hyperalgesia caused by chronic constriction injury of rat nerve. *Pain,* 74**,** 83-91.

SOMMER, C., PETRAUSCH, S., LINDENLAUB, T. & TOYKA, K. V. 1999. Neutralizing antibodies to interleukin 1-receptor reduce pain associated behavior in mice with experimental neuropathy. *Neurosci Lett,* 270**,** 25-8.

SOMMER, C., SCHMIDT, C. & GEORGE, A. 1998b. Hyperalgesia in experimental neuropathy is dependent on the TNF receptor 1. *Exp Neurol,* 151**,** 138-42.

TANAKA, T., NARAZAKI, M. & KISHIMOTO, T. 2014. IL-6 in inflammation, immunity, and disease. *Cold Spring Harb Perspect Biol,* 6**,** a016295.

TANG, W., LU, Y., TIAN, Q. Y., ZHANG, Y., GUO, F. J., LIU, G. Y., SYED, N. M., LAI, Y., LIN, E. A., KONG, L., SU, J., YIN, F., DING, A. H., ZANIN-ZHOROV, A., DUSTIN, M. L., TAO, J., CRAFT, J., YIN, Z., FENG, J. Q., ABRAMSON, S. B., YU, X. P. & LIU, C. J. 2011. The growth factor progranulin binds to TNF receptors and is therapeutic against inflammatory arthritis in mice. *Science,* 332**,** 478-84.

TAO, L., PENG, L., BERNTSSON, R. P., LIU, S. M., PARK, S., YU, F., BOONE, C., PALAN, S., BEARD, M., CHABRIER, P. E., STENMARK, P., KRUPP, J. & DONG, M. 2017. Engineered botulinum neurotoxin B with improved efficacy for targeting human receptors. *Nat Commun,* 8**,** 53.

TERNANT, D., BEJAN-ANGOULVANT, T., PASSOT, C., MULLEMAN, D. & PAINTAUD, G. 2015. Clinical Pharmacokinetics and Pharmacodynamics of Monoclonal Antibodies Approved to Treat Rheumatoid Arthritis. *Clin Pharmacokinet,* 54**,** 1107-23.

THACKER, M. A., CLARK, A. K., MARCHAND, F. & MCMAHON, S. B. 2007. Pathophysiology of peripheral neuropathic pain: immune cells and molecules. *Anesth Analg,* 105**,** 838-47.

THEOHARIDES, T. C. & COCHRANE, D. E. 2004. Critical role of mast cells in inflammatory diseases and the effect of acute stress. *J Neuroimmunol,* 146**,** 1-12.

VALLEJO, R., DE LEON-CASASOLA, O. & BENYAMIN, R. 2004. Opioid therapy and immunosuppression: a review. *Am J Ther,* 11**,** 354-65.

VAN DEN BERG, T. K., DOPP, E. A. & DIJKSTRA, C. D. 2001. Rat macrophages: membrane glycoproteins in differentiation and function. *Immunol Rev,* 184**,** 45-57.

VAZQUEZ-CINTRON, E. J., BESKE, P. H., TENEZACA, L., TRAN, B. Q., OYLER, J. M., GLOTFELTY, E. J., ANGELES, C. A., SYNGKON, A., MUKHERJEE, J., KALB, S. R., BAND, P. A., MCNUTT, P. M., SHOEMAKER, C. B. & ICHTCHENKO, K. 2017. Engineering Botulinum Neurotoxin C1 as a Molecular Vehicle for Intra-Neuronal Drug Delivery. *Sci Rep,* 7**,** 42923.

VERGNOLLE, N., BUNNETT, N. W., SHARKEY, K. A., BRUSSEE, V., COMPTON, S. J., GRADY, E. F., CIRINO, G., GERARD, N., BASBAUM, A. I., ANDRADE-GORDON, P., HOLLENBERG, M. D. & WALLACE, J. L. 2001. Proteinase-activated receptor-2 and hyperalgesia: A novel pain pathway. *Nat Med,* 7**,** 821-6.

VOLKOW, N. D. & MCLELLAN, A. T. 2016. Opioid Abuse in Chronic Pain--Misconceptions and Mitigation Strategies. *N Engl J Med,* 374**,** 1253-63.

WANG, D., ZHANG, S., LI, L., LIU, X., MEI, K. & WANG, X. 2010. Structural insights into the assembly and activation of IL-1beta with its receptors. *Nat Immunol,* 11**,** 905-11.

WANG, J., CASALS-DIAZ, L., ZURAWSKI, T., MENG, J., MORIARTY, O., NEALON, J., EDUPUGANTI, O. P. & DOLLY, O. 2017a. A novel therapeutic with two SNAP-25 inactivating proteases shows long-lasting anti-hyperalgesic activity in a rat model of neuropathic pain. *Neuropharmacology,* 118**,** 223-232.

WANG, J., MENG, J., LAWRENCE, G. W., ZURAWSKI, T. H., SASSE, A., BODEKER, M. O., GILMORE, M. A., FERNANDEZ-SALAS, E., FRANCIS, J., STEWARD, L. E., AOKI, K. R. & DOLLY, J. O. 2008. Novel chimeras of botulinum

neurotoxins A and E unveil contributions from the binding, translocation, and protease domains to their functional characteristics. *J Biol Chem,* 283**,** 16993-7002.

WANG, J., ZURAWSKI, T. H., MENG, J., LAWRENCE, G., OLANGO, W. M., FINN, D. P., WHEELER, L. & DOLLY, J. O. 2011. A dileucine in the protease of botulinum toxin A underlies its long-lived neuroparalysis: transfer of longevity to a novel potential therapeutic. *J Biol Chem,* 286**,** 6375-85.

WANG, L., WANG, K., CHU, X., LI, T., SHEN, N., FAN, C., NIU, Z., ZHANG, X. & HU, L. 2017b. Intra-articular injection of Botulinum toxin A reduces neurogenic inflammation in CFA-induced arthritic rat model. *Toxicon,* 126**,** 70-78.

WAUGH, J. & PERRY, C. M. 2005. Anakinra: a review of its use in the management of rheumatoid arthritis. *BioDrugs,* 19**,** 189-202.

WEBER, A., WASILIEW, P. & KRACHT, M. 2010. Interleukin-1 (IL-1) pathway. *Sci Signal,* 3**,** cm1.

WIJELATH, E. S., CARLSEN, B., COLE, T., CHEN, J., KOTHARI, S. & HAMMOND, W. P. 1997. Oncostatin M induces basic fibroblast growth factor expression in endothelial cells and promotes endothelial cell proliferation, migration and spindle morphology. *J Cell Sci,* 110 (Pt 7)**,** 871-9.

WOOLF, C. J., AMERICAN COLLEGE OF, P. & AMERICAN PHYSIOLOGICAL, S. 2004. Pain: moving from symptom control toward mechanism-specific pharmacologic management. *Ann Intern Med,* 140**,** 441-51.

WOOLF, J. S. A. C. J. 2002. Can we conquer pain? *Natureneuroscience.*

YAMAKI, K., THORLACIUS, H., XIE, X., LINDBOM, L., HEDQVIST, P. & RAUD, J. 1998. Characteristics of histamine-induced leukocyte rolling in the undisturbed microcirculation of the rat mesentery. *Br J Pharmacol,* 123**,** 390-9.

YAMAZAKI, T., YOKOYAMA, T., AKATSU, H., TUKIYAMA, T. & TOKIWA, T. 2003. Phenotypic characterization of a human synovial sarcoma cell line, SW982, and its response to dexamethasone. *In Vitro Cell Dev Biol Anim,* 39**,** 337-9.

YARAEE, R., EBTEKAR, M., AHMADIANI, A. & SABAHI, F. 2003. Neuropeptides (SP and CGRP) augment pro-inflammatory cytokine production in HSV-infected macrophages. *Int Immunopharmacol,* 3**,** 1883-7.

YEH, F. L., ZHU, Y., TEPP, W. H., JOHNSON, E. A., BERTICS, P. J. & CHAPMAN, E. R. 2011. Retargeted clostridial neurotoxins as novel agents for treating chronic diseases. *Biochemistry,* 50**,** 10419-21.

YU, L. C., HOU, J. F., FU, F. H. & ZHANG, Y. X. 2009. Roles of calcitonin gene-related peptide and its receptors in pain-related behavioral responses in the central nervous system. *Neurosci Biobehav Rev,* 33**,** 1185-91.

ZHANG, X., GONCALVES, R. & MOSSER, D. M. 2008. The isolation and characterization of murine macrophages. *Curr Protoc Immunol,* Chapter 14**,** Unit 14 1.

ZHOU, L., DE PAIVA, A., LIU, D., AOKI, R. & DOLLY, J. O. 1995. Expression and purification of the light chain of botulinum neurotoxin A: a single mutation abolishes its cleavage of SNAP-25 and neurotoxicity after reconstitution with the heavy chain. *Biochemistry,* 34**,** 15175-81.

ZUO, Y., PERKINS, N. M., TRACEY, D. J. & GECZY, C. L. 2003. Inflammation and hyperalgesia induced by nerve injury in the rat: a key role of mast cells. *Pain,* 105**,** 467-79.